SINGLE AND MULTIPLE ELECTROMAGNETIC SCATTERING BY DIELECTRIC OBSTACLES FROM A RESONANCE PERSPECTIVE

by

Douglas J. Riley

Dissertation submitted to the Faculty of the
Virginia Polytechnic Institute and State University
in partial fulfillment of the requirements for the degree of

DOCTOR OF PHILOSOPHY

in

Electrical Engineering

APPROVED:

William A. Davis, Chairman

I. M. Besieris

D. A. de Wolf

W. E. Kohler

W. L. Stutzman

December, 1986

Blacksburg, Virginia

SINGLE AND MULTIPLE ELECTROMAGNETIC SCATTERING BY DIELECTRIC OBSTACLES FROM A RESONANCE PERSPECTIVE

by

Douglas J. Riley

Committee Chairman: William A. Davis
Electrical Engineering

(ABSTRACT)

A new application of the singularity expansion method (SEM) is explored. This application combines the classical theory of wave propagation through a multiple scattering environment and the SEM. Since the SEM is generally considered a theory for surface currents on conducting scatterers, extensions are made which permit, under certain conditions, a singularity expansion representation of the electromagnetic field scattered by a dielectric scatterer. Application of this expansion is then made to the multiple scattering case using both single and multiple interactions. A resonance scattering tensor form is used for the SEM description which leads to an associated tensor form of the solution to the multiple scattering problem with each SEM pole effect appearing explicitly. The coherent field is determined for both spatial and SEM parameter random variations.

A numerical example for the case of an ensemble of lossy dielectric spheres is made. Accurate resonance expansions for the single scattering problem are derived, and resonance trajectories based on the Debye relaxation model for the refractive index are introduced. Application of the resonance expansions to the multiple scattering

results for a slab containing a distribution of spheres with varying radii is made. Conditions are discussed for when the hybrid theory is appropriate.

ACKNOWLEDGMENTS

Appreciation is given to Dr. W. A. Davis for suggesting this problem and encouraging its development. Appreciation is also given to Drs. I. M. Besieris, D. A. de Wolf, W. E. Kohler, and W. L. Stutzman for their many useful suggestions to improve the focus and scope of this work.

TABLE OF CONTENTS

LIST OF FIGURES

LIST OF TABLES

CHAPTER I

INTRODUCTION

It is well known that an electromagnetic wave propagating through the atmosphere at a frequency which is at or near a molecular resonance of oxygen or water vapor can be severely attenuated. This attenuation is due to absorption and reradiation at other frequencies by these molecules. The location of the resonances, and the extent of attenuation that can be expected in a neighborhood around them, are quite well understood. Indeed, several analytical models to characterize the spectroscopy of the atmosphere have been proposed to quantitatively determine the attenuation, although, in general, the models are non-rigorous in that they are empirically derived to give a proper fit with experimental data (Straiton, 1975; Liebe and Gimmestad, 1978). In Figure 1.1 is shown curves which depict typical frequency-dependent attenuation attributed to oxygen and water vapor. Though molecular in nature, the figure clearly illustrates the existence of strong resonances within a multiple scattering environment.

The possible presence of visible resonances associated with an ensemble of electromagnetic scatterers provided the stimulus for undertaking the present investigation. As opposed to molecular resonances, the focus of this study is on the existence and implications of resonances associated with ensembles composed of macroscopic or microscopic *particles*. A rigorous theory which directly correlates the

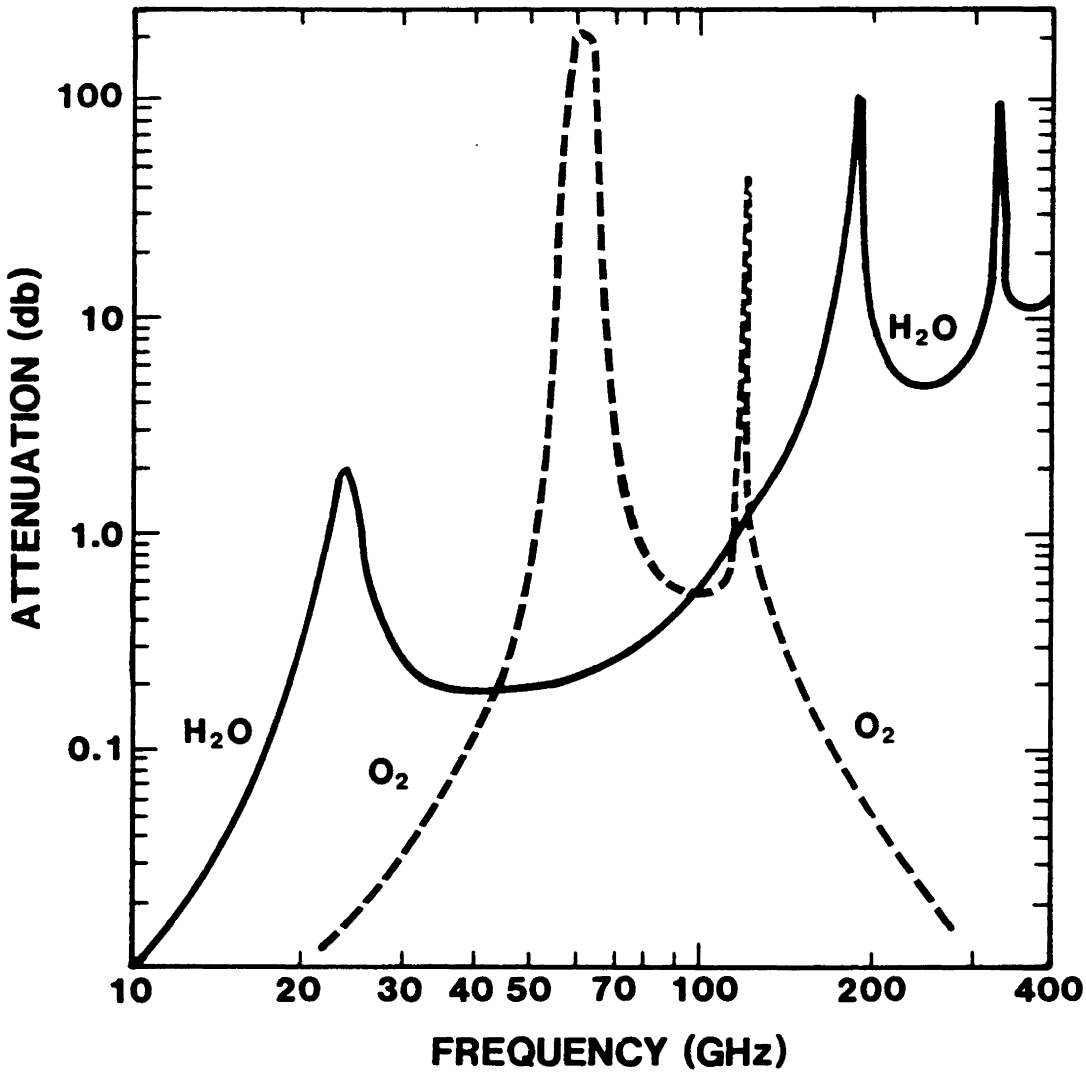

Figure 1.1: Oxygen and water vapor attenuation vertically from sea level for a standard atmosphere. The attenuation is for a wave passing through the *entire* atmosphere (Straiton, 1975).

extent to which non-molecular "ensemble resonances" will attenuate and depolarize an electromagnetic wave previously has not existed.

In addition to filling a theoretical gap, a resonance theory can be of practical utility when strong resonance features are clearly visible, as suggested by the following. By ascertaining knowledge of the precise location of a particular resonance in the complex plane, and its corresponding strength (or residue), it is possible under certain conditions to completely specify the response of the ensemble in a concise form -- a form which may be valid over a large, broadband spectrum neighboring the center of the resonance. Thus, from a computational viewpoint this alternative form could be desirable.

As noted, strong attenuation peaks exist in the neighborhood of the molecular resonances of oxygen and water vapor. Similar strong resonance peaks may or may not be visible for ensembles composed of microscopic or macroscopic particles, however. As an example, consider the well known multiple scattering environments such as rain and atmospheric aerosols. These environments are generally composed of a variety of particles with differing shape and composition. These differences tend to obscure, and perhaps obliterate, strong resonance features. Thus, when strong resonances are *not* present, a resonance theory will inherently complicate the problem. In the special cases when resonance features are present, which generally requires that the particles in the ensemble are quite similar in shape and composition, a resonance theory is appropriate. The theory is therefore presented under the assumption that resonances are indeed clearly visible.

A general ensemble resonance theory is presented in this thesis

which is fundamentally based on two otherwise independent theories. Namely, a resonance theory for single scatterers known as the singularity expansion method (Baum, 1971), and a discrete multiple scattering theory based on the Twersky procedure (Twersky, 1978). The Twersky procedure for vector quantities lends itself quite naturally to the hybrid formulation. The singularity expansion method (SEM), however, requires fundamental extensions to be of utility. This is because the SEM was primarily developed to characterize surface currents which reside on perfectly conducting electromagnetic scatterers in terms of the scatterer's resonances. To be of utility in the present context, an extension of the basic theory which enables the field scattered by a dielectric obstacle to be represented in terms of the obstacle's natural resonance structure was necessary.

The basis for the singularity expansion method, and the closely related eigenmode expansion method, is essentially on the calculus of residues and the Mittag-Leffler expansion theorem. Thus, the SEM is fundamentally a frequency-domain approach to a scattering problem. Baum's contribution was to interpret how an incoming electromagnetic wave interacts with a scatterer to excite various natural modes of the obstacle. The term "coupling coefficient" was introduced to describe this interaction; the coupling coefficient mathematically corresponds to a residue. The "proper" form for this residue (proper in the sense that the correct time-domain response of the obstacle is generated when inverse transforms are taken) has been a topic of great debate over the past decade (Pearson, 1976; Morgan, 1984; Felsen, 1985). Further arbitration on this issue is not made in this thesis.

In the first part of the thesis, a singularity expansion is proposed for the current density throughout a single, penetrable electromagnetic scatterer based a volumetric Fredholm integral equation. The development represents the required extension, for a certain class of problems, of the surface integral equation technique for perfectly conducting obstacles initially presented by Baum (1971), and mathematically refined by Marin (1973). Resonance expansions are subsequently generated for the electromagnetic field scattered by the obstacle, and a *resonance scattering tensor* is introduced as an alternative to the standard "scattering matrix."

Multiple scattering by distributions of tenuous, uncorrelated scatterers based on Twersky's (1978) theory is presented in the second part of the thesis. Fundamental work on multiple scattering of scalar waves by an ensemble of scatterers has been made by Foldy (1945), Lax (1951), Twersky (1962), and de Wolf (1971). Ishimaru (1978) presented a concise treatment for scalar waves based on the Twersky procedure for the coherent field and the incoherent intensity. The development presented in this thesis is a vector extension of the scalar case for the coherent field. An extension of this type was made by Tsolakis and Stutzman (1982), and Tsolakis (1982). The emphasis of the development presented here, which differs from previous work, is on the use of the resonance scattering tensor as derived in the first part of the thesis.

An application of the hybrid theory to an ensemble of homogeneous spherical water droplets is made in the final part. The application is made relative to the millimeter frequency spectrum. Accurate resonance expansions for the electric field scattered by these droplets, and

resonance trajectories showing resonance locations as a function of a physically meaningful, frequency-dependent, complex refractive index are introduced. The expansions are subsequently used in the multiple scattering results of the second part to clearly depict the dominance of slab resonances on attenuating the wave propagating through an ensemble. Extensions are made which demonstrate how resonances are altered when the spheres in the ensemble possess varying radii; thereby giving rise to the concept of "average ensemble resonances."

The organization of the thesis is as follows. In Chapter II, a resonance expansion for the current density and scattered field for dielectric obstacles is developed. A resonance scattering tensor for the far-scattered field is subsequently presented. In Chapter III, a vector-valued multiple scattering theory based on the Twersky procedure and the resonance scattering tensor is presented. In Chapter IV, application of the hybrid theory is made to a slab containing a distribution of dielectric spheres. The application is divided into two parts: In Part I, a single dielectric sphere is rigorously analyzed to determine its natural resonance structure, and a resonance expansion is then generated. In Part II, an appropriate resonance scattering tensor is derived, and is then used to generate results for ensemble scattering. A summary of general results and contributions contained within the thesis, as well as applicability and limitations of the proposed theory, and recommendations for future study are made in Chapter V.

CHAPTER II

MATHEMATICAL DEVELOPMENT FOR OBTAINING A SINGULARITY EXPANSION REPRESENTATON FOR CONDUCTING AND NON-CONDUCTING ELECTROMAGNETIC SCATTERERS

In this chapter, a singularity expansion, or alternatively, a resonance expansion, is formally developed for the current density distributed throughout a penetrable electromagnetic scatterer under a strong set of constraints. The expansion for the current density is subsequently used to obtain a resonance expansion for the electromagnetic field scattered by the obstacle. An expansion for the far-scattered field, and a resonance scattering tensor are also presented.

Unfortunately, a rigorous mathematical theory does not exist which proves the existence and convergence, in the general case, of the expansions derived here. However, significant progress has been made in establishing fundamental mathematical results in the case of perfectly conducting obstacles (Marin, 1973, 1974; Ramm, 1982). The volume development presented in this chapter represents an extension, under certain restrictions, of previous results established for the perfectly conducting case.

2.1 Singularity Expansion for a Volume Current Distribution

The single scattering problem of interest is shown in Figure 2.1. An isotropic obstacle with permittivity $\hat{\epsilon}$, permeability μ_o, and

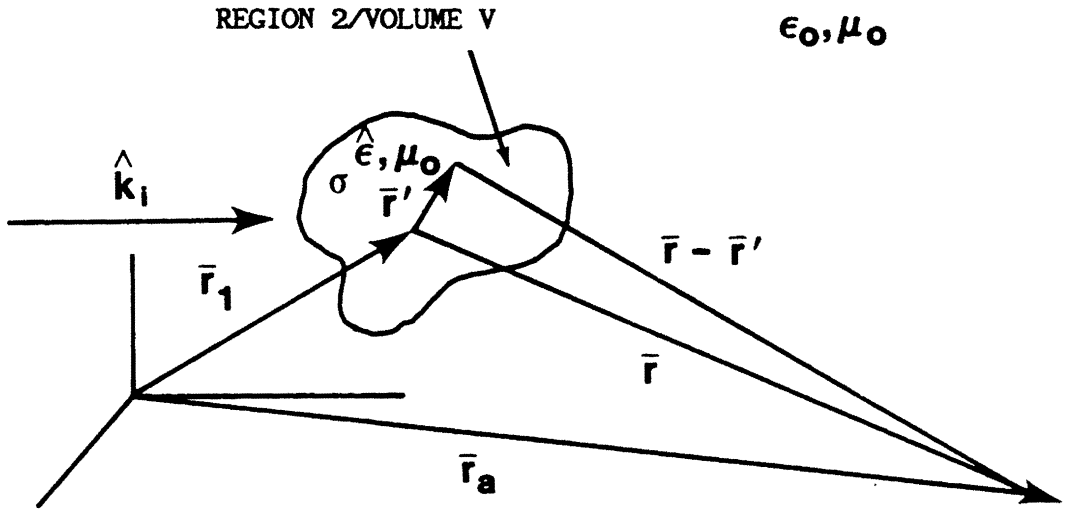

Figure 2.1: Geometry for scattering by a single obstacle.

conductivity σ is shown. The region external to the obstacle is assumed to be free-space with parameters ϵ_o, and μ_o. An $\exp(j\omega t)$ time-dependence is assumed and suppressed. The complex variable, s, corresponding to the two-sided Laplace transformation, is introduced such that $s=j\omega$. Note that this implies that the free-space wavenumber, k_o, is given by $k_o=-j(\frac{s}{c})$, where c denotes the speed of light in a vacuum.

The total electric field within the obstacle, region 2, obeys the following integral equation (Morse and Feshbach, 1953):

$$\bar{E}_2^t(\bar{r};s) = \bar{E}^i(\bar{r};s) + \tau^2\int_V d\bar{r}'[1-m_2^2(\bar{r}',s)]\ \bar{\bar{G}}_\infty(\bar{r}|\bar{r}';s) \cdot \bar{E}_2^t(\bar{r}';s),\ \bar{r} \in V \tag{2.1}$$

The variable τ is used to represent s/c, and m_2 represents the index of refraction which is related to the relative permittivity of region 2 by $m_2^2=\epsilon_{2r}$. The refractive index is given explicitly by

$$m_2(\bar{r};s) = \left[(\frac{\hat{\epsilon}}{\epsilon_o}) + (\frac{\sigma}{s\epsilon_o})\right]^{1/2}$$

where $\hat{\epsilon} \doteq \epsilon' - j\,\epsilon''$. The functions ϵ', ϵ'', and σ are assumed to be functions of s. A brief table of values for these parameters for several materials and frequencies can be found in Harrington (1961).

In equation (2.1), $\bar{\bar{G}}_\infty(\bar{r}|\bar{r}';s)$ represents the dyadic free-space Green's function given by (Morse and Feshbach, 1953)

$$\bar{\bar{G}}_\infty = (\bar{\bar{I}} - \frac{1}{\tau^2}\,\bar{\bar{\nabla}}\bar{\bar{\nabla}})\,\frac{e^{-\tau|\bar{r}-\bar{r}'|}}{4\pi\,|\bar{r}-\bar{r}'|} \tag{2.2}$$

where $\bar{\bar{I}}$ represents an identity dyadic. In light of the singularity of $\bar{\bar{G}}_\infty$ when $\bar{r}=\bar{r}'$, which is $O(|\bar{r}-\bar{r}'|^{-3})$ using the Landau big 'oh' notation (Landau, 1927), the validity and interpretation of (2.1) with (2.2) when $\bar{r}\epsilon V$ has been given by Van Bladel (1961).

An integral equation for the current density throughout region 2 is obtained by using $\bar{J} = s\epsilon_o(m_2^2 - 1)\ \bar{E}_2^t$ ($\bar{J}$ represents an effective current source, Van Bladel, 1964). The resulting expression for $\bar{J}$ is then

$$\bar{J}(\bar{r};s) = s\epsilon_o(m_2^2 -1)\ \bar{E}^i - \tau^2(m_2^2-1) \int_V d\bar{r}'\ \bar{\bar{G}}_\infty(\bar{r}|\bar{r}';s) \cdot \bar{J}(\bar{r}';s),\ \bar{r}\epsilon V$$

To simplify notation, the following substitutions are made: $c_1(\bar{r};s) \doteq s\epsilon_o[m_2^2 - 1]$ and $c_2(\bar{r};s) \doteq -\tau^2[m_2^2 - 1]$. The equation for $\bar{J}$ is then equivalently written as

$$\bar{J}(\bar{r};s) = c_1(\bar{r};s)\bar{E}^i + c_2(\bar{r};s)\int_V d\bar{r}'\ \bar{\bar{G}}_\infty(\bar{r}|\bar{r}';s) \cdot \bar{J}(\bar{r}';s),\ \bar{r} \in V \tag{2.3}$$

To explore possible solutions for (2.3), it is necessary to define an appropriate mathematical space. For this purpose, let $\mathcal{H}$ denote a Hilbert space with support V. For smooth bodies, $\bar{J}$ will be at least a square integrable function and therefore $\mathcal{H}$ is taken to be the space of complex square integrable functions defined on a finite volume V. This space is commonly written as $L_2(V)$ (Stakgold, 1979). The inner-product between two elements $\bar{u}$ and $\bar{v}$ of $\mathcal{H}$ is defined to be

$$\langle \bar{u}, \bar{v} \rangle \triangleq \int_V d\bar{r}' \; \bar{u}(\bar{r}') \cdot \bar{v}^*(\bar{r}'),$$

where "*" denotes complex conjugation. Using this bracket notation, (2.3) is written as

$$\bar{J} = c_1 \bar{E}^i + c_2 \langle \bar{G}_\infty(\bar{r}|\bar{r}';s), \bar{J}^*(\bar{r}';s) \rangle \tag{2.3a}$$

It is noted that although $\bar{G}_\infty$ is not in $L_2(V)$ (hence, not a *Hilbert-Schmidt kernel*), the inner product is well-defined in $\mathcal{H}$ as long as $(\bar{J}-c_1\bar{E}^i)/c_2 \in \mathcal{H}$.

In operator form (2.3a) becomes

$$(\bar{\bar{I}} - c_2 \bar{\bar{\mathcal{K}}}) \cdot \bar{J} = c_1 \bar{E}^i \tag{2.4}$$

where $\bar{\bar{\mathcal{K}}} \cdot \bar{u} \triangleq \langle \bar{G}_\infty(\bar{r}|\bar{r}';s), \bar{u}^*(\bar{r}') \rangle$, for every $\bar{u}$ in the *domain* of $\mathcal{K}$, which is written as $\bar{u} \in D_{\mathcal{K}}$. Observe that $D_{\mathcal{K}}$ is a subspace of $\mathcal{H}$.

A formal solution to (2.4) is given by

$$\bar{J} = (\bar{\bar{I}} - c_2 \bar{\bar{\mathcal{K}}})^{-1} \cdot c_1 \bar{E}^i$$

assuming the inversion operator is well-defined.

An explicit representation for $\bar{J}$ in terms of the singularities associated with the operator $(\bar{\bar{I}} - c_2 \bar{\bar{\mathcal{K}}})^{-1}$ is desired. For notational simplicity, $\bar{\bar{\mathcal{A}}}(\bar{r};s)$ will be used to represent $(\bar{\bar{I}} - c_2 \bar{\bar{\mathcal{K}}})$. The existence

of such an expansion for $\bar{\bar{\mathcal{A}}}^{-1}$ is not guaranteed, however, because $\bar{\bar{\mathcal{A}}}$ is not a self-adjoint operator. Specifically, for $\bar{u}$, $\bar{v} \in D_{\mathcal{A}}$, $\langle \bar{\bar{\mathcal{A}}} \cdot \bar{u}, \bar{v}^* \rangle = \langle \bar{u}, (\bar{\bar{\mathcal{A}}} \cdot \bar{v})^* \rangle$, which establishes that $\bar{\bar{\mathcal{A}}}$ only possesses *real* symmetry (for $\bar{\bar{\mathcal{A}}}$ to be self-adjoint it would have to satisfy $\langle \bar{\bar{\mathcal{A}}} \cdot \bar{u}, \bar{v} \rangle = \langle \bar{u}, \bar{\bar{\mathcal{A}}} \cdot \bar{v} \rangle$). As a consequence, the well-known spectral theorem of linear operator theory cannot be invoked to obtain the desired expansion (one form of the spectral theorem is given below[1]). Indeed, since $\bar{\bar{\mathcal{A}}}$ is not self-adjoint the eigenfunctions of $\bar{\bar{\mathcal{A}}}$ may not span the *range* of $\bar{\bar{\mathcal{A}}}$, and therefore it may not be possible to represent (exactly) an arbitrary element in the range of $\bar{\bar{\mathcal{A}}}$ as a Fourier decomposition[2]. Significant progress in the development of a spectral theory for non-self-adjoint operators in an infinite-dimensional space has been made by Ramm (1981, 1982).

Since the operator $\bar{\bar{\mathcal{A}}}$ does not fall within a class of operators for which sound results exist, basically two alternatives are available to obtain the desired spectral expansion for the solution of (2.4): (1) extend existing, or develop new, mathematical theories which address and overcome the complications associated with the spectral solution of (2.4); or (2) make assumptions about the spectrum of $\bar{\bar{\mathcal{A}}}$ which hopefully will be appropriate for a certain class of physical problems. In the

---

[1] **Spectral Theorem** (Hochstadt, 1973): The equation $(I-\lambda K)\varphi = f$, where λ is a constant and K is a compact, self-adjoint integral operator with eigenvalues $\{\alpha_n\}$ and orthonormal eigenfunctions $\{\varphi_n\}$, has the solution $\varphi = f + \sum_n \alpha_n \langle f, \varphi_n^* \rangle \varphi_n / (1-\lambda\alpha_n)$, if $1-\lambda\alpha_n \neq 0$ for all n.

[2] Consider a finite-dimensional complex matrix analog. Let P be an n by n non-Hermitian (non-self-adjoint) matrix. Since P is non-Hermitian it is not necessarily similar to a diagonal matrix, and therefore generalized, or "root", eigenvectors may exist. Thus, the eigenvectors may not span the n-space.

sequel, the latter approach is made.

With the caveat that a general theory does not exist which proves the existence and convergence of a resonance expansion for the general solution of (2.4), it is still possible to *formally* construct such an expansion which may be useful under certain conditions. The following development patterns the construction used by Marin (1973) for the solution of the magnetic field integral equation (MFIE) (Poggio and Miller, 1973) on a compact (i.e., closed and bounded) perfectly conducting surface. The proofs presented by Marin which establish that only pole singularities are associated with the integral operator for the MFIE do not carry over to the volume integral operator of interest. This is due to differences in their kernels (for the MFIE the singularity of the kernel is $O(|\bar{r}-\bar{r}'|^{-1})$ as $\bar{r}\to\bar{r}'$), and differences in the domains of support. Thus the *assumption* that only pole type singularities with an accumulation point at infinity exist for the inverse operator, $\bar{\bar{\mathcal{A}}}^{-1}$, is made. This is equivalent to assuming $\bar{\bar{\mathcal{A}}}^{-1}$ is a meromorphic operator-valued function[3] of s, with $s=s_\alpha$ defining the points of non-analyticity. In a strict sense this assumption is not correct even for compact dielectric obstacles due to possible occurrences of branch points in the refractive index. However, branch cut contributions may be negligibly small compared with the pole contributions. It is under this premise that the following development is presented.

Let $\bar{v}_\alpha$ and $\bar{\mu}_\alpha$ represent two unique (to within a multiplicative

---

[3] A meromorphic function is one which is analytic everywhere in the finite complex plane except for a possible collection of pole type singularities.

constant) non-trivial elements in $D_{\mathcal{A}}$ and $D_{\mathcal{A}^\dagger}$, respectively, with the properties that

$$\bar{\bar{\mathcal{A}}}(\bar{r};s_\alpha) \cdot \bar{v}_\alpha(\bar{r},s_\alpha) = 0 \; ; \quad \bar{\bar{\mathcal{A}}}^\dagger(\bar{r};s_\alpha) \cdot \bar{\mu}_\alpha(\bar{r};s_\alpha) = 0 \; ,$$

where $\bar{\bar{\mathcal{A}}}^\dagger$ denotes the adjoint of $\bar{\bar{\mathcal{A}}}$ given explicitly by

$$\bar{\bar{\mathcal{A}}}^\dagger \cdot \bar{v} = (\bar{\bar{I}} - c_2^* \bar{\bar{\mathcal{K}}}^\dagger) \cdot \bar{v} = \bar{v} - c_2^* \int_V d\bar{r}' \; \bar{\bar{G}}_\infty^*(\bar{r}'|\bar{r};s) \cdot \bar{v}(\bar{r}';s)$$

This follows because the adjoint is defined by the inner-product relationship $\langle \bar{\bar{\mathcal{A}}} \cdot \bar{u}, \bar{v} \rangle = \langle \bar{u}, \bar{\bar{\mathcal{A}}}^\dagger \cdot \bar{v} \rangle$, for every $\bar{u} \in D_{\mathcal{A}}$, $\bar{v} \in D_{\mathcal{A}^\dagger}$ (Stakgold, 1979).

An explicit representation for $\bar{J}$ is now constructed. From the basic operator equation (2.4), it follows that

$$\langle \bar{\bar{\mathcal{A}}}(\bar{r};s)\cdot\bar{J}(\bar{r};s), \bar{\mu}_\alpha^*(\bar{r};s_\alpha) \rangle = \langle c_1(\bar{r};s)\bar{E}^i(\bar{r};s), \bar{\mu}_\alpha^*(\bar{r};s_\alpha) \rangle$$

Also,

$$\langle \bar{\bar{\mathcal{A}}}(\bar{r};s_\alpha)\cdot\bar{J}(\bar{r};s), \bar{\mu}_\alpha^*(\bar{r};s_\alpha) \rangle = \langle \bar{J}(\bar{r};s), \bar{\bar{\mathcal{A}}}^\dagger(\bar{r};s_\alpha) \cdot \bar{\mu}_\alpha^*(\bar{r};s_\alpha) \rangle = 0$$

Combining these two relationships leads to

$$\langle [\bar{\bar{\mathcal{A}}}(s)-\bar{\bar{\mathcal{A}}}(s_\alpha)]\cdot\bar{J}(s), \bar{\mu}_\alpha^*(s_\alpha) \rangle = \langle c_1(s)\bar{E}^i(s), \bar{\mu}_\alpha^*(s_\alpha) \rangle \qquad (2.5)$$

where the explicit $\bar{r}$ dependence has been suppressed.

A Taylor series expansion for $\bar{\bar{\mathcal{A}}}(s)$ and $c_1(s)\bar{E}^i(s)$ about $s=s_\alpha$ is

now made:

$$\bar{\mathcal{A}}(s) = \bar{\mathcal{A}}(s_\alpha) + (s - s_\alpha)\left.\frac{d}{ds}\bar{\mathcal{A}}(s)\right|_{s=s_\alpha} + \cdots\cdots$$

$$c_1(s)\bar{E}^i(s) = c_1(s_\alpha)E^i(s_\alpha) + (s - s_\alpha)\left.\frac{d}{ds}[c_1(s)\bar{E}^i(s)]\right|_{s=s_\alpha} + \cdots\cdots , \tag{2.6}$$

where $\frac{d}{ds}\bar{\mathcal{A}}(s) = -\frac{d}{ds}[c_2(s)\bar{\mathcal{F}}(s)]$ with $\frac{d}{ds}\bar{\mathcal{F}}(s) = \langle \frac{d}{ds}\bar{G}_\infty(\bar{r}|\bar{r}';s), \cdot \rangle$.

In a neighborhood of the point $s=s_\alpha$, $\bar{J}$ may be represented in terms of the Laurent series

$$\bar{J}(\bar{r};s) = (s - s_\alpha)^{-1} a_\alpha(s_\alpha)\, \bar{v}_\alpha(\bar{r};s_\alpha) + \bar{\zeta}_\alpha(\bar{r};s) \tag{2.7}$$

where $\bar{\zeta}_\alpha(\bar{r};s)$ is the analytic portion of $\bar{J}$, a_α is a constant coefficient which depends on s_α, and a simple pole at $s=s_\alpha$ has been assumed. For perfectly conducting obstacles which do not possess generic degeneracies, only simple poles are believed to exist (Baum, 1976). However, certain impedance loaded bodies have been found to possess higher order poles (Baum, 1976). It is shown in Chapter IV that the poles are indeed simple for a lossy, homogeneous dielectric sphere.

From (2.5), (2.6), and (2.7) it follows that (Marin, 1973)

$$a_\alpha = \frac{\langle \bar{\mu}_\alpha(\bar{r};s_\alpha),\ [c_1(\bar{r};s_\alpha)\bar{E}^i(\bar{r};s_\alpha)]^* \rangle}{\langle \bar{\mu}_\alpha(\bar{r};s_\alpha),\ [\frac{d}{ds}\bar{\mathcal{A}}(\bar{r};s_\alpha)\cdot\bar{v}_\alpha(\bar{r};s_\alpha)]^* \rangle}$$

Therefore, locally around $s=s_\alpha$,

$$\bar{J}(\bar{r};s) = (s - s_\alpha)^{-1} \frac{\langle \bar{\mu}_\alpha(\bar{r};s_\alpha),\ [c_1(\bar{r};s_\alpha)\bar{E}^i(\bar{r};s_\alpha)]^* \rangle}{\langle \bar{\mu}_\alpha(\bar{r};s_\alpha),\ [\frac{d}{ds}\bar{\mathcal{A}}(\bar{r};s_\alpha)\cdot\bar{v}_\alpha(\bar{r};s_\alpha)]^* \rangle} \bar{v}_\alpha(\bar{r};s_\alpha) + \bar{\kappa}_\alpha(s)$$

where $\bar{\kappa}_\alpha$ is an analytic function of s, and $(d/ds)\bar{\mathcal{A}}(\bar{r};s_\alpha)$ is $(d/ds)\bar{\mathcal{A}}(\bar{r};s)$ evaluated at $s=s_\alpha$. The Mittag-Leffler expansion theorem of residue calculus[4] may now be invoked to *globally* obtain

$$\bar{J}(\bar{r};s) = \sum_{\alpha=1}^{\infty} \left\{ a_\alpha(s_\alpha)\ \bar{v}_\alpha(\bar{r};s_\alpha)\ (s - s_\alpha)^{-1} + \bar{\kappa}'_\alpha(s) \right\} + \bar{\chi}(s) \qquad (2.8)$$

where $\bar{\chi}(s)$ is an arbitrary entire function[5], and $\bar{\kappa}'_\alpha$ is an analytic function (polynomial). Observe that the validity of (2.8) requires that

---

[4]**Mittag-Leffler's Theorem For Simple Poles** (Markushevich, 1965): Let $s_1, s_2, \ldots, s_n, \ldots$ be an increasing sequence of distinct complex numbers converging to infinity, and let $G_1, G_2, \ldots, G_n, \ldots$ denote rational functions of the form $G_n = a_n/(s-s_n)$. Then there exists a meromorphic function f(s) whose poles coincide with the points $s_1, s_2, \ldots$, and whose principal part at the poles equals G_n, for each $n=1,2,\ldots$

Corollary (Markushevich, 1965): Let f(s) be a meromorphic function whose poles are given by the increasing sequence of distinct complex numbers $s_1, s_2, \ldots, s_n, \ldots$ with principal parts $G_1, G_2, \ldots, G_n, \ldots$ Then f(s) can be represented in the form $f(s)=g(s) + \sum_n [G_n(s) + P_n(s)]$, where g(s) is an entire function and $P_n(s)$ are polynomials.

[5]An entire function is one which is analytic everywhere in the finite complex plane. It has a Taylor series representation with an infinite radius of convergence. Functions such as exp(s), sin(s), s, and $(\sin\sqrt{s})/\sqrt{s}$, are examples of entire functions. Functions such as $\sqrt{s}$, $\sin\sqrt{s}$, and $1/s$ are not entire.

the incident waveform does not add additional poles to the system.

In deriving (2.8), it was assumed that $\bar{\mathcal{A}}^{-1}(s)$ is a meromorphic operator-valued function with only simple poles and therefore no branch points. The simple pole assumption need not be true in general because no formal proofs are known which establish this condition for the operator $\bar{\mathcal{A}}^{-1}$ considered here. As previously noted, the assumption that a branch cut is not present will generally not be true even for compact dielectric obstacles because of the occurrence of branch points in a frequency-dependent refractive index (the potential presence for the branch points appears when $d\bar{\mathcal{A}}(s)/ds$ is formed). However, the contribution due to the branch may be negligibly small compared to the pole contribution. A numerical example demonstrating when this is true for the case of a lossy dielectric sphere is given in Chapter IV.

Within the framework of the assumptions noted, expansion (2.8) represents a solution to (2.4). Though correct in form, the expression is of little practical utility due to the presence of the unknown functions $\bar{\kappa}_\alpha'$ and $\bar{\chi}$. If certain analytic properties about $\bar{J}$ are known *a priori*, appeal can be made to the theory of contour integration to obtain a simpler, and in some sense, more general, singularity expansion. The following two cases are of particular utility and interest (Pearson, 1981; Spiegel, 1964):

***Theorem* 1**: Let C denote a closed contour of radius R_o in the complex s plane which encircles either all or a subset of the simple poles associated with $\bar{J}$ (without passing through any poles). On this contour, let $|\bar{J}(s)| < M$, M a constant. In addition, let $\bar{J}$ be analytic at s=0 (a

condition which will be true for smooth, closed scatterers). An appropriate expansion for $\bar{J}(s)$ as $R_o \to \infty$ is then

$$\bar{J}(\bar{r};s) = \bar{J}(\bar{r};0) + \sum_{\alpha=1}^{\infty} a_\alpha(s_\alpha)\, \bar{v}_\alpha(\bar{r};s_\alpha) \left\{ \frac{1}{(s - s_\alpha)} + \frac{1}{s_\alpha} \right\} \tag{2.9}$$

When a frequency-independent unit vector, denoted by $\hat{e}_J$, is sufficient to characterize the eigenmodes of $\bar{J}$, the decomposition $\bar{J}(\bar{r};s) = [p(\bar{r};s)/q(\bar{r};s)]\, \hat{e}_J$, where $p(\bar{r};s)$ and $q(\bar{r};s)$ are entire functions of s with simple zeros, is possible. For this case, decomposition (2.9) can be equivalently written as

$$\bar{J}(\bar{r};s) = \bar{J}(\bar{r};0) + \sum_{\alpha=1}^{\infty} \hat{e}_J \frac{p(\bar{r};s_\alpha)}{\left.\frac{d}{ds} q(\bar{r};s)\right|_{s=s_\alpha}} \left\{ \frac{1}{(s - s_\alpha)} + \frac{1}{s_\alpha} \right\} \tag{2.10}$$

It is noted that, at least for the cases of the sphere and the circular loop, such an $\hat{e}_J$ exists.

Consistent with the theorem, a branch cut contribution, if present, can be added to the right hand side of (2.10). The specific form of the contribution is (cf. Spiegel, 1964)

$$\hat{e}_J \frac{s}{2\pi j} \int_{C_b} d\xi \, \frac{p(\bar{r};\xi)}{\xi\,(\xi - s)\, q(\bar{r};\xi)}$$

where C_b represents an appropriate path around the branch. Observe that

the implication here is that p and q can be more general functions than entire functions as long as the boundedness conditions and the simple poles assumptions are satisfied.

Theorem 2: Let C denote a closed contour of radius R_o in the complex s plane which encircles either all or a subset of the simple poles associated with $\bar{J}$ (without passing through any poles). On this contour, let $|s\ \bar{J}(s)| < M$, M a constant. An appropriate expansion for $\bar{J}(s)$ as $R_o \to \infty$ is then

$$\bar{J}(\bar{r};s) = \sum_{\alpha=1}^{\infty} a_\alpha(s_\alpha)\ \bar{v}_\alpha(\bar{r};s_\alpha)\ \frac{1}{(s - s_\alpha)} \tag{2.11}$$

As in Theorem 1, if $\bar{J}$ can be characterized by the unit vector $\hat{e}_J$ an appropriate representation is

$$\bar{J}(\bar{r};s) = \sum_{\alpha=1}^{\infty} \hat{e}_J\ \frac{p(\bar{r};s_\alpha)}{\frac{d}{ds}q(\bar{r};s)\Big|_{s=s_\alpha}}\ \frac{1}{(s - s_\alpha)} \tag{2.12}$$

A branch cut contribution, if present, can similarly be added to expansion (2.12); it is given by

$$\hat{e}_J\ \frac{1}{2\pi j} \int_{C_b} d\xi\ \frac{p(\bar{r};\xi)}{(\xi - s)\ q(\bar{r};\xi)}$$

It is emphasized that the subtle difference between the theorems is the rate of decay of $\bar{J}$ on the bounding contour.

Observe that if the hypotheses of Theorem 2 are satisfied, the hypotheses of Theorem 1 generally are as well, because for smooth bodies $\bar{J}$ will be analytic at s=0. The proofs for expansions (2.10) and (2.12) can be found, for example, in Arfken (1970), or Spiegel (1964). Extensions of Theorems 1 and 2 to accommodate various types of algebraic growth, and pole singularities with multiplicities higher than one are possible (Markushevich, 1965).

Because all parameters which appear in expansions (2.9)-(2.12) are completely specified, which was possible only by demanding stronger constraints on $\bar{J}$ then those used in deriving expansion (2.8), the expansions can be utilized in a practical sense. However, the expansions require a great deal of information about the obstacle which generally is not known (form of the natural modes, location of the natural resonances, and perhaps the static response). In the case of perfectly conducting obstacles of non-separable geometries, this information has been obtained using surface integral equation formulations in conjunction with a moment method numerical solution in the frequency-domain (Tesche, 1973; Marin, 1974; Pearson, 1976), and using finite-difference techniques in the time-domain (Cordaro and Davis, 1981; Davis and Riley, 1983). A moment method approach can also be used to obtain this information from the volume integral equations discussed here.

When an explicit separable solution for $\bar{J}$ is *not* available, expansions (2.9) and (2.11) have been conjectured to be the appropriate expansions for reconstructing $\bar{J}$ on perfectly conducting obstacles

(Pearson, *et al.*, 1982), although, in general, it is not known if the hypotheses of Theorems 1 and 2 are always satisfied by $\bar{J}$. When an explicit separation of variables solution for $\bar{J}$ is known, and $\bar{J}$ can be characterized by a frequency independent eigenvector, expansions (2.10) and (2.12) represent appropriate singularity expansions, because one can directly determine if the hypotheses of the theorems are satisfied.

2.2 Resonance Expansions for the Scattered Electric Field

The electric field scattered by an obstacle is given by (Van Bladel, 1964)

$$\bar{E}^{sc}(\bar{r};s) = -s\mu_o \langle \bar{\bar{G}}_\infty(\bar{r}|\bar{r}';s),\ \bar{J}^*(\bar{r}';s)\rangle \qquad \bar{r} \notin V \tag{2.13}$$

Replacing $\bar{J}$ by expansion (2.8) leads to

$$\bar{E}^{sc}(\bar{r};s) = -s\mu_o \left\{ \sum_{\alpha=1}^{\infty} \left[a_\alpha\ \bar{\delta}_\alpha(\bar{r},s,s_\alpha)\ (s - s_\alpha)^{-1} + \bar{\kappa}_\alpha'(\bar{r};s) \right] + \bar{\chi}'(\bar{r};s) \right\} \tag{2.14}$$

where $\bar{\chi}'$ is an entire function, $\bar{\delta}_\alpha \triangleq \langle \bar{\bar{G}}_\infty,\ \bar{v}^* \rangle$, and $\bar{\kappa}_\alpha' \triangleq \langle \bar{\bar{G}}_\infty,\ (\bar{\kappa}_\alpha')^* \rangle$ with $\bar{\kappa}_\alpha'$ being an analytic function of s.

If $\bar{J}$ satisfies the conditions of Theorem 1, then

$$\bar{E}^{sc}(\bar{r};s) = -s\mu_o \left\{ \sum_{\alpha=1}^{\infty} a_\alpha\ \bar{\delta}_\alpha(\bar{r},s,s_\alpha) \left[\frac{1}{s-s_\alpha} + \frac{1}{s_\alpha} \right] + \langle \bar{\bar{G}}_\infty(r|r';s), \bar{J}^*(\bar{r}',0) \rangle \right\} \tag{2.15}$$

If $\bar{J}$ satisfies the conditions of Theorem 2, then

$$\bar{E}^{sc}(\bar{r};s) = -s\mu_o \left\{ \sum_{\alpha=1}^{\infty} a_\alpha \, \bar{\delta}_\alpha(\bar{r},s,s_\alpha) \, (s - s_\alpha)^{-1} \right\} \tag{2.16}$$

Since $\bar{\delta}_\alpha$ is related to the Green's function $\bar{\bar{G}}_\infty$, $\bar{\delta}_\alpha$ is an entire function of s except for a finite order pole at s=0 (the field scattered by smooth finite bodies, however, is finite as s→0). The presence of this entire function, which will generally behave exponentially, implies that difficulty will be encountered if one attempts to expand the scattered field directly instead of initially expanding the current density. In particular, even when an explicit expression for the scattered field is known, one cannot directly apply Theorems 1 or 2 because, in general, the boundedness conditions will not be satisfied. In Chapter IV, the proper application of Theorems 1 and 2 to the separation of variable solution for the field scattered by the dielectric sphere is presented in detail.

2.3 Far-Scattered Field and the Resonance Scattering Tensor

In the radiation, or far-scattering zone considerable simplications in the form of the dyadic Green's function $\bar{\bar{G}}_\infty$ occurs. Specifically,

$$(\bar{\bar{I}} - \frac{1}{\tau^2} \bar{\bar{\nabla}}\bar{\bar{\nabla}}) \frac{e^{-\tau|\bar{r}-\bar{r}'|}}{4\pi\,|\bar{r}-\bar{r}'|} \sim (\bar{\bar{I}} - \hat{r}\hat{r}) \frac{e^{-\tau|\bar{r}-\bar{r}'|}}{4\pi\,|\bar{r}-\bar{r}'|} \sim (\bar{\bar{I}} - \hat{r}\hat{r}) \frac{e^{-\tau(r-\hat{k}_i\cdot\bar{r}')}}{4\pi\, r}$$

where $\hat{r} \doteq \bar{r}/|\bar{r}|$, $r \doteq |\bar{r}|$, and recalling $\tau = s/c$.

From (2.13) and the far-field dyadic Green's function, the far-scattered electric field is

$$\bar{E}^{sc} \sim s\mu_o \frac{e^{-\tau r}}{4\pi r} (\hat{r}\hat{r} - \bar{I}) \cdot \int_V d\bar{r}' \; \bar{J}(\bar{r}';s) \; e^{\tau \hat{k}_i \cdot \bar{r}'} \tag{2.18}$$

Replacing $\bar{J}$ by expansion (2.8) yields

$$\bar{E}^{sc} \sim \frac{e^{-\tau r}}{4\pi r} \sum_{\alpha=1}^{\infty} [a_\alpha(s_\alpha) \; \bar{\delta}_{\alpha f}(\hat{r},\hat{k}_i,s,s_\alpha) + \bar{\kappa}'_{\alpha f}(s,s_\alpha)] \; (s - s_\alpha)^{-1} + \bar{\chi}'_f(s) \tag{2.19}$$

where $\bar{\delta}_{\alpha f} \doteq s\mu_o \; (\hat{r}\hat{r}-\bar{I}) \cdot \langle e^{\tau \hat{k}_i \cdot \bar{r}'} \bar{I}, \; \bar{v}^*_\alpha(\bar{r}';s_\alpha) \rangle$, $\bar{\kappa}'_{\alpha f} \doteq s\mu_o \; (\hat{r}\hat{r}-\bar{I}) \cdot \langle e^{\tau \hat{k}_i \cdot \bar{r}'} \bar{I}, \; (\bar{\kappa}'_\alpha)^* \rangle$, and $\bar{\chi}'_f$ is an entire function.

A resonance scattering tensor, $\bar{\bar{r}}$, can be introduced as follows. Let $\bar{E}^i(\bar{r};s) \doteq \bar{E}^i(\bar{r}_1) \exp(-\tau \hat{k}_i \cdot \bar{r})$ (the incident wave is assumed to be a plane-wave locally to the scatterer). The coefficient a_α then becomes

$$a_\alpha = \langle \bar{\mu}_\alpha(\bar{r};s_\alpha), \; [\frac{d}{ds}\bar{\bar{d}}(\bar{r};s_\alpha) \cdot \bar{v}_\alpha(\bar{r};s_\alpha)]^* \rangle^{-1} \left\{ \int_V dr' \; e^{-\tau_\alpha \hat{k}_i \cdot \bar{r}'} \; c_1(\bar{r}';s_\alpha) * \right.$$

$$\left. * \; \bar{\mu}_\alpha(r';s_\alpha) \right\} \cdot \bar{E}^i(\bar{r}_1) \doteq \bar{R}_\alpha(s_\alpha) \cdot \bar{E}^i(\bar{r}_1)$$

where $\tau_\alpha \doteq s_\alpha/c$.

Expression (2.19) may now be written as

$$\bar{E}^{sc} \sim \frac{e^{-\tau r}}{4\pi r} \left\{ \sum_{\alpha=1}^{\infty} [\bar{\bar{\delta}}_{\alpha f}(\hat{r},\hat{k}_i,s,s_\alpha)\ \bar{R}_\alpha + \bar{\bar{\kappa}}'_{\alpha f}(s,s_\alpha)]\ (s - s_\alpha)^{-1} + \right.$$

$$\left. + \bar{\bar{\chi}}'_f(s) \right\} \cdot \bar{E}^i(\bar{r}_1) \qquad (2.20)$$

From (2.20), the resonance scattering tensor is defined to be

$$\bar{\bar{f}}(\hat{r},\hat{k}_i,s) \doteq \sum_{\alpha=1}^{\infty} [\bar{\bar{\delta}}_{\alpha f}(\hat{r},\hat{k}_i,s,s_\alpha)\ \bar{R}_\alpha(s_\alpha) + \bar{\bar{\kappa}}'_{\alpha f}(s,s_\alpha)]\ (s - s_\alpha)^{-1} + \bar{\bar{\chi}}'_f(s) \qquad (2.21)$$

where $\bar{\bar{\chi}}'_f$ is a tensor with components which are entire functions of s.

The scattering tensor as defined by (2.21) is the principal quantity of interest. The assumptions intrinsic to its validity are reviewed: (1) there exist non-trivial elements, $\bar{v}_\alpha(\bar{r};s) \in D_{\mathcal{A}}$, $\bar{\mu}_\alpha(\bar{r};s) \in D_{\mathcal{A}^\dagger}$, such that for $s=s_\alpha$, $\bar{\bar{\mathcal{A}}}(\bar{r};s_\alpha)\cdot\bar{v}_\alpha(\bar{r};s_\alpha) = \bar{\bar{\mathcal{A}}}^\dagger(\bar{r};s_\alpha)\cdot\bar{\mu}_\alpha(\bar{r};s_\alpha) = 0$, with $\bar{v}_\alpha$ and $\bar{\mu}_\alpha$ being unique (to within a multiplicative constant) for each s_α; (2) there exists only simple poles; and (3) the incident excitation is a plane-wave (this assumption can be relaxed).

From previous comments, when an explicit expression for the far-scattered field is known, it may be possible to expand a portion of the exact solution according to Theorems 1 or 2. In this case, the scattering tensor will take on a completely specified form. The specific form, however, will vary on a case by case basis. In Chapter IV, an appropriate form for the dielectric sphere is derived.

CHAPTER III

THE COHERENT ELECTRIC FIELD FOR AN ENSEMBLE OF SCATTERERS BASED ON TWERSKY'S MULTIPLE SCATTERING THEORY

The intent of this chapter is to derive a general vector expression for the coherent, or average, electric field for an ensemble of randomly distributed, non-correlated, tenuous scatterers. The development patterns the work of Tsolakis and Stutzman (1982) and Tsolakis (1982) which were vector extensions of the scalar case considered in detail by Ishimaru (1978). The resulting expression is commonly called the vector Foldy-Lax-Twersky equation.

The point of departure of this chapter with previous work on this subject is in the use of the resonance scattering tensor discussed in Chapter II. It is demonstrated how individual resonances associated with a distribution of scatterers in a slab configuration account for attenuation and depolarization of the propagating wave. Obviously, for this approach to be of utility strong resonance characteristics must be visible. For this to occur generally implies that the ensemble must be composed of very similar particles, for otherwise a "washing-out" of strong resonance features will occur.

Though only the coherent field for non-correlated scatterers is considered here, it is noted that it is possible to directly use the results of more sophisticated statistical analyses for ensemble scattering (for example, pair correlations, higher order moments, and incoherent intensity (cf. Tsolakis, *et al*, 1985)) by simply replacing the

standard scattering tensor used in each by an appropriately formed resonance scattering tensor.

The outline of the chapter is as follows. In Section 3.1, Twersky's multiple scattering theory for obtaining an integral equation for the coherent electric field is presented. In Section 3.2, this equation is specialized to a slab geometry containing a distribution of identical scatterers. A closed form solution for the coherent electric field for the case of a plane-wave incident at an oblique angle is derived; this represents a minor extension of the result for a normally incident plane-wave typically presented (Ishimaru, 1978; Tsolakis and Stutzman, 1982). In Section 3.2, the results of Section 3.1 are generalized to embody the case of a slab of particles with varying radii.

3.1 Mathematical Development

The most simple approximation for the field scattered by a distribution of, say, M scatterers is to assume that no multiple scattering (or interaction) between scatterers occurs. The total far-scattered field at a point $\bar{r}_a$ is then simply a superposition of (2.20) over all scatterers; namely,

$$\bar{E}^{sc}(\bar{r}_a;s) \simeq \sum_{m=1}^{M} \frac{e^{-\tau R_{am}}}{4\pi R_{am}} \bar{\bar{f}}(\hat{R}_{am},\hat{k}_{im};s) \cdot \bar{E}^{i}(\bar{r}_m) \qquad (3.1)$$

where $\bar{R}_{am} = \bar{r}_a - \bar{r}_m$, $R_{am} = |\bar{R}_{am}|$, $\hat{R}_{am} = \bar{R}_{am}/R_{am}$, $\hat{k}_{im}$ is $\hat{k}_i$ at $\bar{r}_m$, and $\tau = s/c$.

To account for partial wave interaction among scatterers,

Twersky's (1978) multiple scattering theory is used. Specifically, the total scattered field at $\bar{r}_a$ due to a distribution of M scatterers is given approximately by (retaining only first order interaction between two scatterers)

$$E^{sc}(\bar{r}_a;s) \simeq \sum_{m=1}^{M} \bar{\bar{u}}_m^a \cdot \bar{E}^i(\bar{r}_m) + \sum_{m=1}^{M} \sum_{\substack{t=1 \\ t\neq m}}^{M} \bar{\bar{u}}_m^a \cdot [\bar{\bar{u}}_t^m \cdot \bar{E}^i(\bar{r}_t)] + \sum_{m=1}^{M} \sum_{\substack{t=1 \\ t\neq m}}^{M} \sum_{\substack{\ell=1 \\ \ell\neq m,t}}^{M} \bar{\bar{u}}_m^a \cdot \{\bar{\bar{u}}_t^m \cdot [\bar{\bar{u}}_\ell^t \cdot \bar{E}^i(\bar{r}_\ell)]\} + \ldots\ldots \quad (3.2)$$

In this equation, the tensor $\bar{\bar{u}}_m^a$ is defined as

$$\bar{\bar{u}}_m^a(\hat{k}_{im};s) \doteq \frac{e^{-\tau R_{am}}}{4\pi R_{am}} \bar{\bar{f}}(\hat{R}_{am},\hat{k}_{im};s) \quad (3.3)$$

A close examination of (3.2) reveals how multiple interactions are accounted for. Figure 3.1 depicts the physical situation represented by the first term in (3.2) for M=2. The second and third terms are represented in Figures 3.2a,b, respectively.

Although (3.2) is theoretically valid, it is computationally impractical. By abandoning the desire for deterministic in favor of statistical information, this equation can be made tractable in a practical sense. Therefore, a representation for the coherent field at $\bar{r}_a$ is sought. Specifically, $\langle \bar{E}^{sc}(\bar{r}_a;s) \rangle$, with $\langle \cdot \rangle$ denoting the ensemble

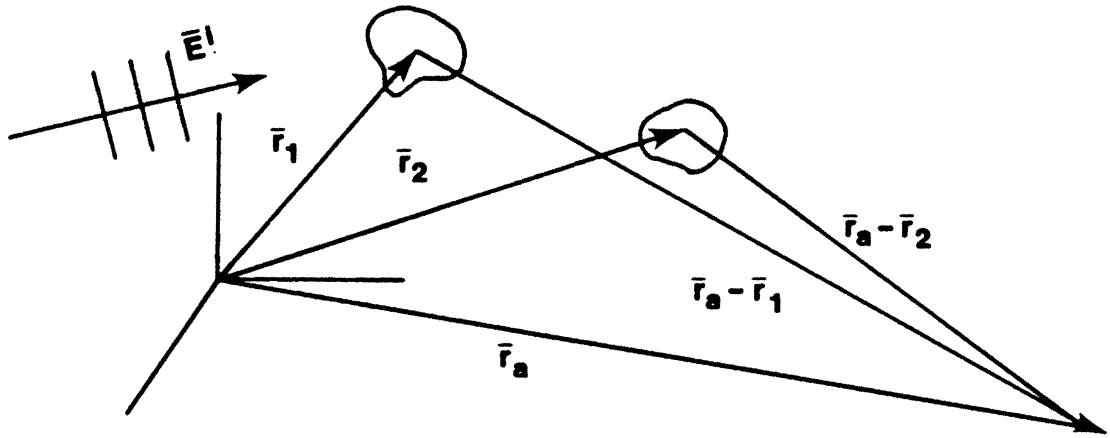

Figure 3.1: Two-scatterer geometry.

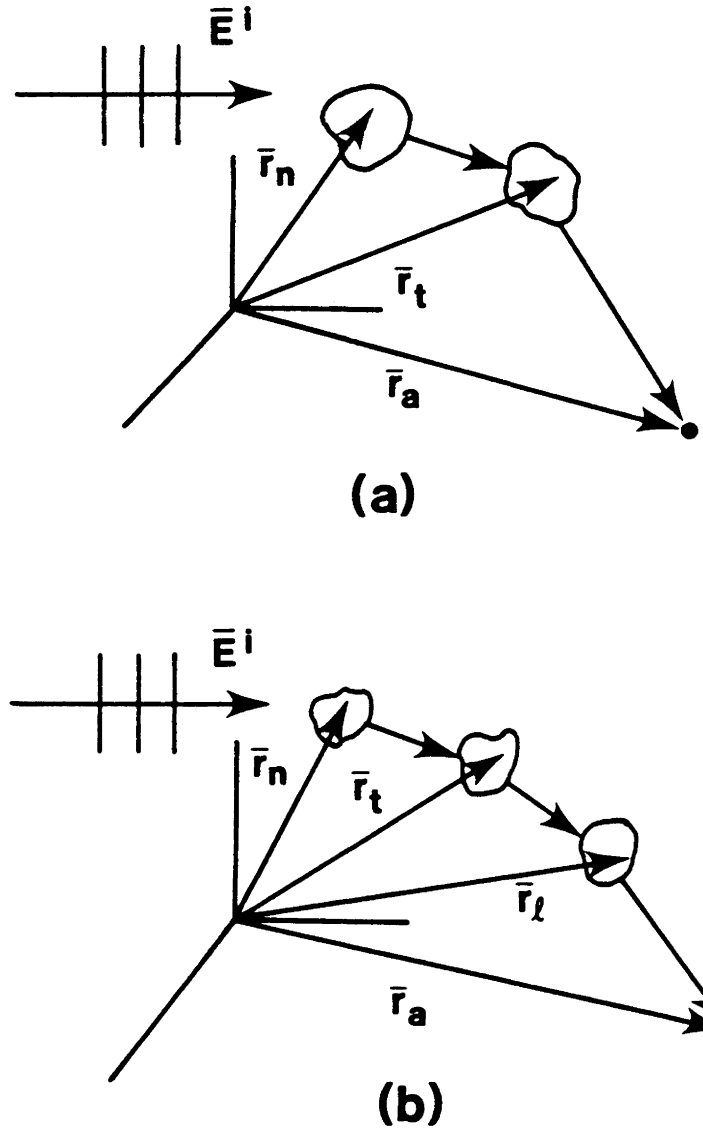

Figure 3.2: Multiple interactions: (a) 2; (b) 3.

average over position and other variations between particles (there will be no confusion with the inner-product definition of Chapter II, because the ensemble average will have only one element within the brackets). From (3.2), follows that

$$\langle \bar{E}^{sc}(\bar{r}_a;s)\rangle \simeq \sum_{m=1}^{M} \langle \bar{\bar{u}}_m^a \cdot \bar{E}^i(\bar{r}_m)\rangle + \sum_{m=1}^{M} \sum_{\substack{t=1 \\ t\neq m}}^{M} \langle \bar{\bar{u}}_m^a \cdot [\bar{\bar{u}}_t^m \cdot \bar{E}^i(\bar{r}_t)]\rangle + \ldots \tag{3.4}$$

It is assumed that the probability density for finding a scatterer within a volume $d\bar{r}$ is given by $\rho(\bar{r})/M$. Density functions can also be introduced which define particle variations such as shape, canting angle, and material composition. However, as previously mentioned, gross variations in the particles of the ensemble will tend, in general, to eliminate strong resonance features. As a consequence, only slight particle variations will be permitted; in particular, slight radius variations (this generally restricts the elements of the slab to be spherical). The probability density for the radial variations is defined to be $\eta(a_m)$ (which is assumed to be independent of the position density).

By taking the limit as M tends to infinity, the following equation averaged over position and radial variations is obtained (Ishimaru, 1978):

$$\langle \bar{E}^{sc}(\bar{r}_a;s)\rangle \simeq \int_{\bar{r}_m,a_m} d\bar{r}_m\, da_m\, \bar{\bar{u}}_m^a \cdot \bar{E}^i(\bar{r}_m)\, \rho(\bar{r}_m)\, \eta(a_m) + \\ + \int_{\bar{r}_m,a_m} d\bar{r}_m\, da_m \int_{\bar{r}_t} d\bar{r}_t\, \bar{\bar{u}}_m^a \cdot [\bar{\bar{u}}_t^m \cdot \bar{E}^i(\bar{r}_t)]\, \rho(\bar{r}_m)\, \rho(\bar{r}_t)\, \eta(a_m) + \ldots. \tag{3.5}$$

This expression is valid when the scatterer dimensions are much smaller than their spatial separations (tenuous distribution) and when each scatterer is assumed to be independent of all others. The former assumption is necessary due to the far-field constraint made in (3.3); the latter assumption is required since $\rho(\bar{r}_m,\bar{r}_t) = \rho(\bar{r}_m)\ \rho(\bar{r}_t)$ has been used. Both of these assumptions will break down as the density of particles becomes large with respect to the wavelength. Calculating the coherent field when scatterers are correlated is complicated. Contributors in this area have included: Twersky (1975); Tsang and Kong (1983); Varadan, *et al.* (1984); and Tsolakis, *et al.* (1985).

The coherent total electric field at $\bar{r}_a$ is given by

$$\langle \bar{E}^t(\bar{r}_a;s)\rangle = \bar{E}^i(\bar{r}_a) + \langle \bar{E}^{sc}(r_a;s)\rangle$$

Using (3.5), the following integral equation for $\langle \bar{E}^t\rangle$ results:

$$\langle \bar{E}^t(\bar{r}_a;s)\rangle \simeq \bar{E}^i(\bar{r}_a) + \int_{\bar{r}_m,a_m} d\bar{r}_m\, da_m\, \bar{\bar{u}}^a_m \cdot \langle \bar{E}^t(\bar{r}_m;s)\rangle\, \rho(\bar{r}_m)\, \eta(a_m) \quad (3.6)$$

Equation (3.6), commonly called the vector Foldy-Lax-Twersky equation, is the basic multiple scattering equation of interest here. In the derivation presented, the tensor $\bar{\bar{u}}^a_m$ is expressed in terms of the mth scatterer's resonance expansion (equation 3.2), and is therefore valid within the framework of the validity of the resonance scattering tensor, equation (2.21).

3.2 An Oblique Incident Plane-Wave on a Slab Containing a Distribution of Identical Scatterers

The geometry of interest is shown in Figure 3.3. An incident plane-wave given by

$$\bar{E}^i(x_a,z_a;s) = \bar{E}_o\, e^{-\tau[x_a \sin\theta_i + z_a \cos\theta_i]}$$

is assumed. The position density $\rho(\bar{r}_m)$ is assumed to be a constant, ρ_o, throughout the slab.

For this problem, integral equation (3.6) specializes to the following:

$$\langle \bar{E}^t(x_a,z_a;s)\rangle = \bar{E}_o\, e^{-\tau[x_a \sin\theta_i + z_a \cos\theta_i]} + \int_o^d dz_m \int_{-\infty}^{\infty} dx_m \int_{-\infty}^{\infty} dy_m\, \rho_o \frac{e^{-\tau|\bar{r}_a-\bar{r}_m|}}{4\pi|\bar{r}_a-\bar{r}_m|}\, \bar{f}(\hat{R}_{am},\hat{k}_{im};s) \cdot \langle \bar{E}^t(\bar{r}_m;s)\rangle \quad (3.7)$$

For general angle θ_i, the solution of (3.7) is quite difficult. This is because the ensemble of scatterers will behave similarly to a solid slab which is characterized by an effective complex refractive index which may be a tensor; thus, the wave transmitted into the slab generally will not propagate parallel to the incident wave (Tsang, 1983). To avoid this added complexity, only small angles of incidence (at most a few degrees) will be considered.

Under the small angle of incidence restriction, $\langle \bar{E}^t \rangle$ will behave as a plane-wave propagating nearly parallel to the incident wave. Thus,

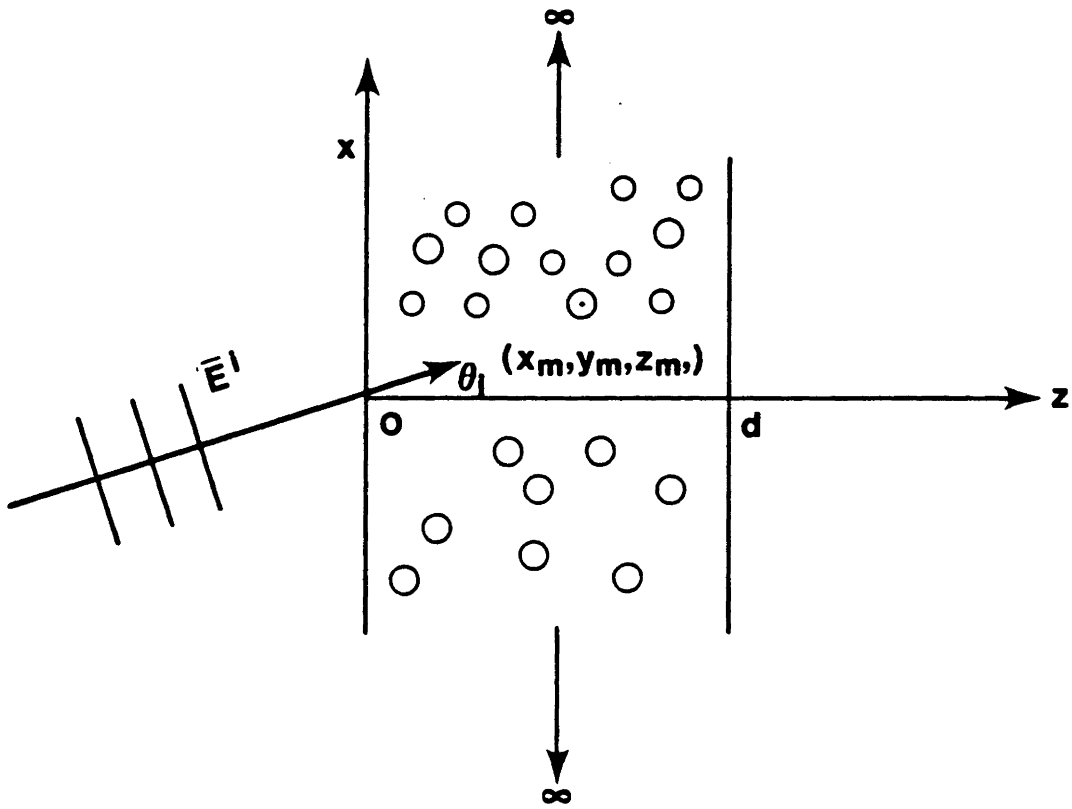

Figure 3.3: A slab containing a random distribution of scatterers.

$\langle \bar{E}^t \rangle$ will have the approximate form

$$\langle \bar{E}^t(x_a,z_a;s) \rangle = \bar{A}(x_a,z_a;s)\, e^{-\tau[x_a \sin\theta_i + z_a \cos\theta_i]}, \tag{3.8}$$

where $\bar{A}$ represents a slowly varying function of τ to be determined. Substituting (3.8) into equation (3.7) yields

$$\bar{A}(x_a,z_a;s) = \bar{E}_o + \rho_o\, e^{\tau[x_a \sin\theta_i + z_a \cos\theta_i]} \int_o^d dz_m\, e^{-\tau z_m \cos\theta_i} * \\ * \int_{-\infty}^{\infty} dy_m \int_{-\infty}^{\infty} dx_m \frac{e^{-\tau[|\bar{r}_a - \bar{r}_m| + x_m \sin\theta_i]}}{4\pi |\bar{r}_a - \bar{r}_m|} \bar{f}(\hat{R}_{am}, \hat{k}_{im};s) \cdot \bar{A}(x_m,z_m;s) \tag{3.9}$$

The integration over (x_m,y_m) is evaluated by the method of stationary phase (see Appendix A) to obtain

$$\int_{-\infty}^{\infty} dy_m \int_{-\infty}^{\infty} dx_m \frac{e^{-\tau[|\bar{r}_a - \bar{r}_m| + x_m \sin\theta_i]}}{4\pi |\bar{r} - \bar{r}_m|} \bar{f}(\hat{R}_{am}, \hat{k}_{im};s) \cdot \bar{A}(x_m,z_m;s) \sim$$

$$\sim \frac{\sec\theta_i}{2\tau} e^{-\tau[x_a \sin\theta_i + |z_a - z_m|]} \bar{f}(\hat{x} \sin\theta_i + \hat{z}\, \mathrm{sgn}(z_a - z_m) \cos\theta_i, \hat{k}_{im};s) \cdot$$

$$\cdot \bar{A}(x_a - |z_a - z_m| \tan\theta_i, z_m;s) + o(1/\tau) \tag{3.10}$$

Here, sgn(•) denotes the sign function, and o(•) represents the Landau little 'oh' notation (Landau, 1927).

Using result (3.10), equation (3.9) reduces to

$$\bar{A}(x_a,z_a;s) = \bar{E}_o + \frac{\sec\theta_i}{2\tau}\rho_o\, e^{\tau z_a\cos\theta_i} *$$

$$* \int_o^d dz_m\, e^{-\tau[z_m\cos\theta_i+|z_a-z_m|]}\, \bar{\bar{f}}(\hat{x}\sin\theta_i+\hat{z}\,\mathrm{sgn}(z_a-z_m)\cos\theta_i,\hat{k}_{im};s)\cdot$$

$$\cdot\, \bar{A}(x_a-|z_a-z_m|\tan\theta_i,z_m;s) \tag{3.11}$$

Equation (3.11) is a second kind Fredholm equation for $\bar{A}$ when $0 < z_a < d$. For $z_a > z_m$, $\bar{\bar{f}} = \bar{\bar{f}}(\hat{k}_{im},\hat{k}_{im};s)$. For $z_a < z_m$, $\bar{\bar{f}} = \bar{\bar{f}}(\hat{x}\sin\theta_i-\hat{z}\cos\theta_i, \hat{k}_{im};s)$. The former case corresponds to forward scattering. The latter case is predominently directed off the forward direction under the small angle of incidence restriction. For spherical scatterers of radius a, the forward scattered field is dominant over all other scattering directions for $k_o a > 1$, and this dominance progressively increases as the electrical size of the scatterer increases such that $k_o a >> 1$ (Bohren and Huffman, 1983). When there are several particles, the forward dominance is even greater due to phase cancellations in off-forward directions (Bohren and Huffman, 1983). Therefore, in general, the integral over $0 < z_m < z_a$ dominates the integral over $z_a < z_m < d$. Thus, it is approximately true that

$$\bar{A}(x_a,z_a;s) = \bar{E}_o + \frac{\sec\theta_i}{2\tau}\rho_o\, e^{\tau z_a(\cos\theta_i-1)}\, \bar{\bar{f}}(\hat{k}_{im},\hat{k}_{im};s)$$

$$\cdot \int_o^{z_a} dz_m\, e^{-\tau z_m[\cos\theta_i-1]}\, \bar{A}(x_a-(z_a-z_m)\tan\theta_i,z_m;s) \tag{3.12}$$

Equation (3.12) is valid for $0 \leq z_a \leq d$, and its accuracy improves as $\theta_i \to 0$.

For the case of a normally incident plane-wave ($\theta_i=0$), equation (3.12) becomes a Volterra equation of the second kind with a degenerate kernel[6], and may therefore be solved exactly (Hochstadt, 1973). For $\theta_i \neq 0$, the factor $x_a-(z_a-z_m)\tan\theta_i$, which appears as the first argument of $\bar{A}$, implies an exact solution is not obtainable. A special case of practical interest does exist, however, which permits one to obtain an exact solution; namely, when the observation position is along the propagation direction $\hat{k}_{im}$. The configuration is as shown in Figure 3.4. This follows because along this line $x_a=z_a\tan\theta_i$, and therefore $\bar{A}$ in the integrand is only a function of z_m. Thus, the integrand is degenerate and an exact solution can be found (the solution is found by differentiating (3.12) with respect to z_a and noting $\bar{A}(0)=\bar{E}_o$). The solution is given by (suppressing the subscript a on the independent variables x and z)

$$\bar{A}(z) = e^{\tau z\,[\cos\theta_i-1]}\, e^{\bar{\bar{g}}z} \cdot \left\{ \bar{I} + \tau\,(\cos\theta_i-1)\left[e^{-\bar{\bar{g}}z}\, e^{-\tau z[\cos\theta_i-1]} - \bar{I}\right] \cdot \right.$$

$$\left. \cdot \left[\bar{\bar{g}} + \tau\,(\cos\theta_i-1)\bar{I} \right]^{-1} \right\} \cdot \bar{E}_o$$

where the tensor $\bar{\bar{g}}$ is defined by

---

[6]Consider the scalar second kind Volterra integral equation $\varphi(z) = B(z) + \int_o^z dz'\ G(z,z')\ \varphi(z')$, where $G(z,z')$ denotes the kernel. The kernel is said to be degenerate, or separable, if $G(z,z') = G_1(z)\ G_2(z')$.

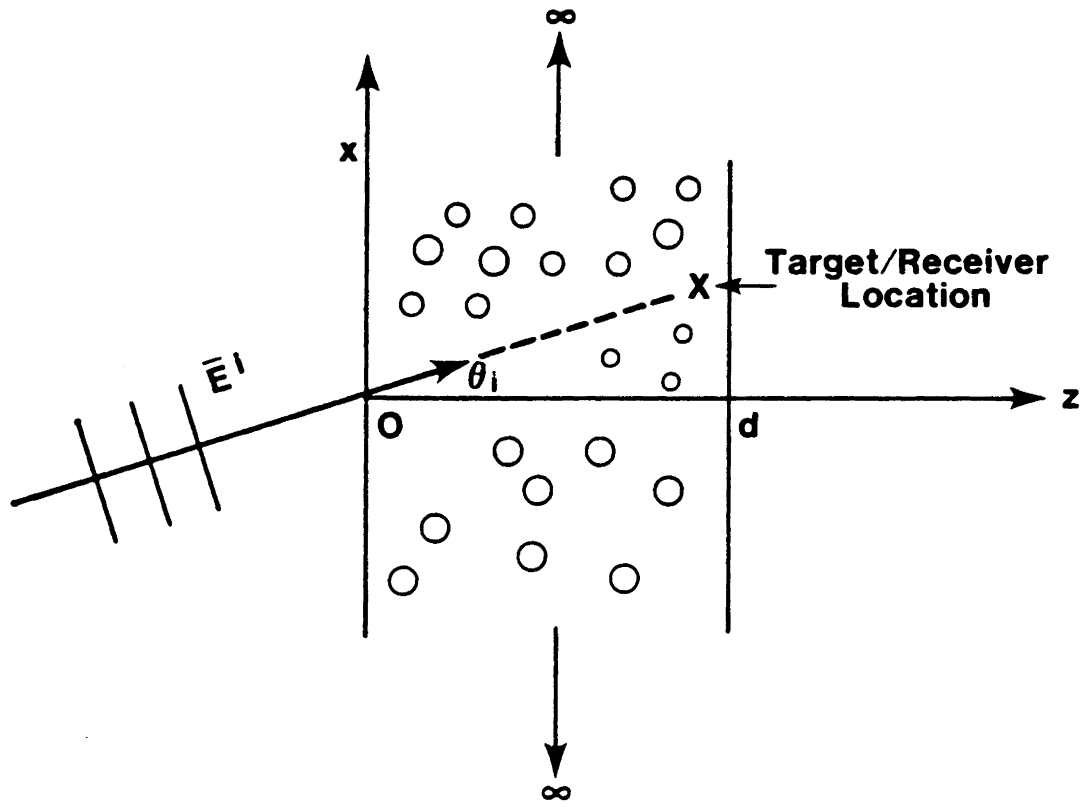

Figure 3.4: Slab geometry showing target/receiver location for exactly solving equation (3.12).

$$\bar{\bar{g}} \doteq \frac{\sec\theta_i}{2\tau}\,\rho_o\,\bar{\bar{f}}(\hat{k}_{im},\hat{k}_{im};s) \tag{3.13}$$

Therefore,

$$\langle\bar{E}^t(x,z;s)\rangle \simeq e^{\bar{\bar{g}}z}\cdot\left[\,\bar{\Gamma}_<(\theta_i;z)\cdot\bar{E}_o\,e^{-\tau z}\,\right]e^{-\tau x\,\sin\theta_i} \qquad (z<d) \tag{3.14}$$

where

$$\bar{\Gamma}_<(\theta_i;z) \doteq \bar{I} + \tau\,(\cos\theta_i-1)\left[e^{-\bar{\bar{g}}z}\,e^{-\tau z[\cos\theta_i-1]}-\bar{I}\right]\cdot\left[\,\bar{\bar{g}}+\tau\,(\cos\theta_i-1)\bar{I}\,\right]^{-1}$$

For $z\geq d$:

$$\langle\bar{E}^t(x,z;s)\rangle \simeq \left[\,\bar{\Gamma}_>(\theta_i;z)\cdot\bar{E}_o\,e^{-\tau z}\,\right]e^{-\tau x\,\sin\theta_i} \tag{3.15}$$

with

$$\bar{\Gamma}_>(\theta_i;z) \doteq e^{-\tau z[\cos\theta_i-1]}\,\bar{I} + \left[\,e^{\bar{\bar{g}}d}\cdot\bar{\Gamma}_<(\theta_i;z) - \bar{I}\,e^{-\tau d[\cos\theta_i-1]}\,\right]$$

The restriction for the validity of these solutions is that x is chosen such that $x=z\,\tan\theta_i$, and θ_i is at most a few degrees (less than, say, 10 degrees).

Equations (3.14) and (3.15) reduce to the following well-known solutions for the special case $\theta_i=0$:

$$\langle\bar{E}^t(z;s)\rangle \simeq e^{\bar{\bar{g}}z}\cdot\bar{E}_o\,e^{-\tau z} \qquad (z<d) \tag{3.16}$$

and

$$\langle\bar{E}^t(z;s)\rangle \simeq e^{\bar{\bar{g}}d}\cdot\bar{E}_o\,e^{-\tau z} \qquad (z\geq d) \tag{3.17}$$

with $\bar{\bar{f}}(\hat{k}_{im},\hat{k}_{im};s)=\bar{\bar{f}}(\hat{z},\hat{z};s)$. The exponential raised to a tensor terms

which appear in (3.14-3.17) are treated as exponential matrix operations.

Since the tensor $\bar{\bar{g}}$ represents a summation over the resonances of the scatterers, it is clear that each pole term contributes to attenuation and depolarization of the propagating wave. (Depolarization occurs only when the scattering tensor has non-zero off-diagonal elements.) When strong resonance characteristics of individual scatterers are present, attenuation and depolarization will be dominant in the neighborhood of these resonant frequencies.

3.3 Extension of the Results to the Case of Slight Radial Variations

Results of the previous section are now extended to permit slight radial variations to exist among the particles of the slab. The particles are otherwise identical. Even with this restriction, the concept of average resonances and average modal structures is difficult to rigorously develop. This is because modal variations must be modelled by a random function which is dependent on both frequency and spatial variations. To avoid the complexities of differing modal spatial distributions, the modal structure of each scatterer is assumed to spatially correspond to that of a reference scatterer, and therefore be only a varying function of frequency (which, in turn, is a varying function of radius). The function $\gamma_s(a_m)$ is introduced to relate the shift in resonance locations of the mth scatterer relative to the reference scatterer. Therefore, the αth resonance associated with the mth scatterer is given by $s_{\alpha m} = \gamma_s(a_m)s_\alpha$, where s_α is the reference resonant frequency. The tensor $\bar{\bar{g}}$ is then explicitly

$$\bar{\bar{g}}(s;a_m) = \frac{\sec\theta_i}{2\tau}\ \rho_o\left\{\sum_{\alpha=1}^{\infty}\left[\bar{\delta}_{\alpha f}(\hat{k}_{im},\hat{k}_{im},s,s_{\alpha m})\ \bar{R}_\alpha(s_{\alpha m})+\bar{\bar{\kappa}}'_{\alpha f}(s,s_{\alpha m})\right]\ (s-s_{\alpha m})^{-1}+\right.$$

$$\left.+\ \bar{\bar{\chi}}'_f(s)\right\}$$

The preceding solutions for $\langle\bar{E}^t\rangle$ (equations (3.13)-(3.16)) apply directly by replacing $\bar{\bar{g}}$ with

$$\int_{a_m} da_m\ \bar{\bar{g}}(s;a_m)\ \eta(a_m)$$

recalling $\eta(a_m)$ defines the density function for the radial distribution. The effect of the averaging procedure has been to spread the effective stopband regions associated with each resonance.

CHAPTER IV

SINGLE AND MULTIPLE SCATTERING BY LOSSY HOMOGENEOUS SPHERES FROM A RESONANCE PERSPECTIVE: AN EXAMPLE

The formal development presented in Chapters II and III is applied in this chapter using the canonical example of the sphere. Since the sphere is the simplest three-dimensional scatterer which has an exact solution, it has been the topic of numerous studies since the initial separation of variable solution presented by Mie in 1908. Mie's solution for the field scattered by a homogeneous sphere provides the starting point for the material in this chapter.

To clearly illustrate the theory developed in the first two chapters, spherical water droplets with strong resonance characteristics are studied. The radii of the spheres were chosen to range from a few centimeters to a few millimeters, and the frequency was restricted to be less than about 30 GHz. For these parameters, $k_o a$, a being the radius of the sphere, will generally be less than 10. Figure 4.1 illustrates the potentially strong resonance characteristics associated with the extinction coefficient (Van Bladel, 1964) for water droplets with varying radii. A frequency-dependent complex refractive index based on the Debye relaxation model for material polarization was used for the figure. The specific form of this index will be discussed later in the chapter.

The resonances of dielectric spheres have been studied to various degrees, and for various purposes, by others. Gastine, *et al.* (1967)

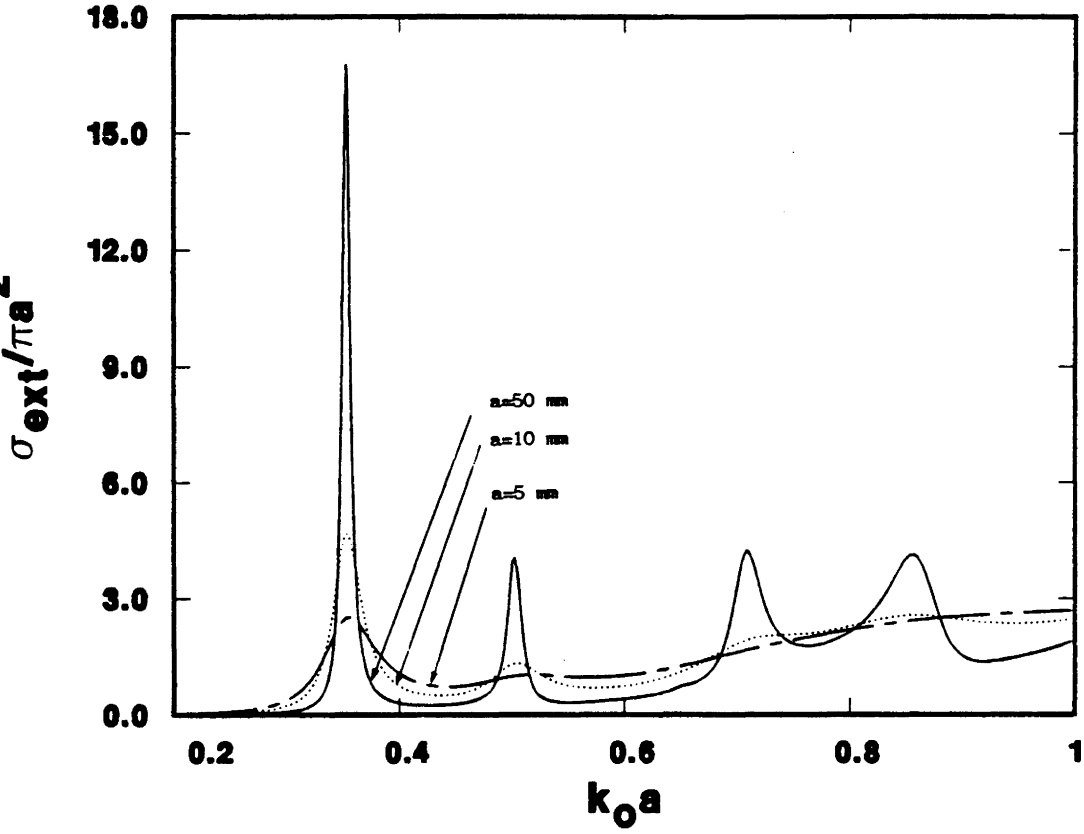

Figure 4.1: Normalized extinction cross-section for the dielectric sphere for a variety of radii.

apparently provided the first detailed investigation into resonances which varied with a frequency-independent, real refractive index. Studies by Nussenzveig (1969), and Inada and Plonus (1970), represent two excellent examples which sought specific resonances, also based on a frequency-independent real refractive index, for use with the Watson transformation (Watson, 1918) to construct an asymptotic high-frequency representation of the Mie series for the scattered field. Explanations for the natural phenomena of the rainbow and the more difficult problem of the glory have evolved from such works. These studies, and most others, have been interested in resonances of the dielectric sphere for purposes which differ from the one here. In addition, resonance trajectories based on a physically meaningful frequency-dependent complex refractive index, which have not previously appeared in the literature, are introduced in this chapter. Resonance trajectories for the case of a frequency-independent complex refractive index have recently been published (Riley, 1986).

The present chapter is divided into two parts. In the first part, the complex resonances of a spherical water droplet are studied in detail. The Mie series for the electric field scattered by the sphere is then reconstructed from the resonances using the Mittag-Leffler expansion Theorems 1 and 2 described in Section 2.1. The resonance expansions are subsequently used to characterize the resonance peaks previously noted for the extinction cross-section of the sphere. Part II uses the developed expansions to form appropriate resonance scattering tensors for use in the multiple scattering results for the slab geometry described in Chapter III. Results are presented which clearly depict the dominance of

slab resonances on attenuating the propagating wave. In addition, average ensemble resonances are discussed using the example of a slab containing an ensemble of dielectric spheres with varying radii.

I. RECONSTRUCTION OF THE FAR-ELECTRIC FIELD SCATTERED BY A LOSSY DIELECTRIC SPHERE FROM ITS NATURAL RESONANCES

4.1.1 Mathematical Development

The geometry of interest is shown in Figure 4.2. A plane-wave incident along a general radial vector $\hat{k}_i$ is assumed. Integral equations (2.1) and (2.13) completely characterize this geometry; however, since the geometry is separable, it is convenient to solve the problem using an eigenfunction approach. The sphere is assumed to be homogeneous, non-magnetic, non-conductive, and characterized by a frequency dependent complex refractive index, $m_2^2(\beta)=\epsilon'(\beta)-j\epsilon''(\beta)$. The scattered radiation-zone electric field is shown in Appendix B to be given by

$$E_\theta^{sc} = j\frac{E_o a}{(-j\beta)r} e^{-\beta r/a} \sum_{n=1}^{\infty} \tilde{a}_n \left[c_n \left[\frac{1}{\sin\theta\sin\theta_i} \frac{\partial^2}{\partial\varphi\partial\varphi_i} \chi_n \right] + b_n \left[\frac{\partial^2}{\partial\theta\partial\theta_i} \chi_n \right] \right] \tag{4.1a}$$

$$E_\varphi^{sc} = j\frac{E_o a}{(-j\beta)r} e^{-\beta r/a} \sum_{n=1}^{\infty} \tilde{a}_n \left[b_n \left[\frac{1}{\sin\theta} \frac{\partial^2}{\partial\varphi\partial\theta_i} \chi_n \right] + c_n \left[\frac{1}{\sin\theta_i} \frac{\partial^2}{\partial\theta\partial\varphi_i} \chi_n \right] \right] \tag{4.1b}$$

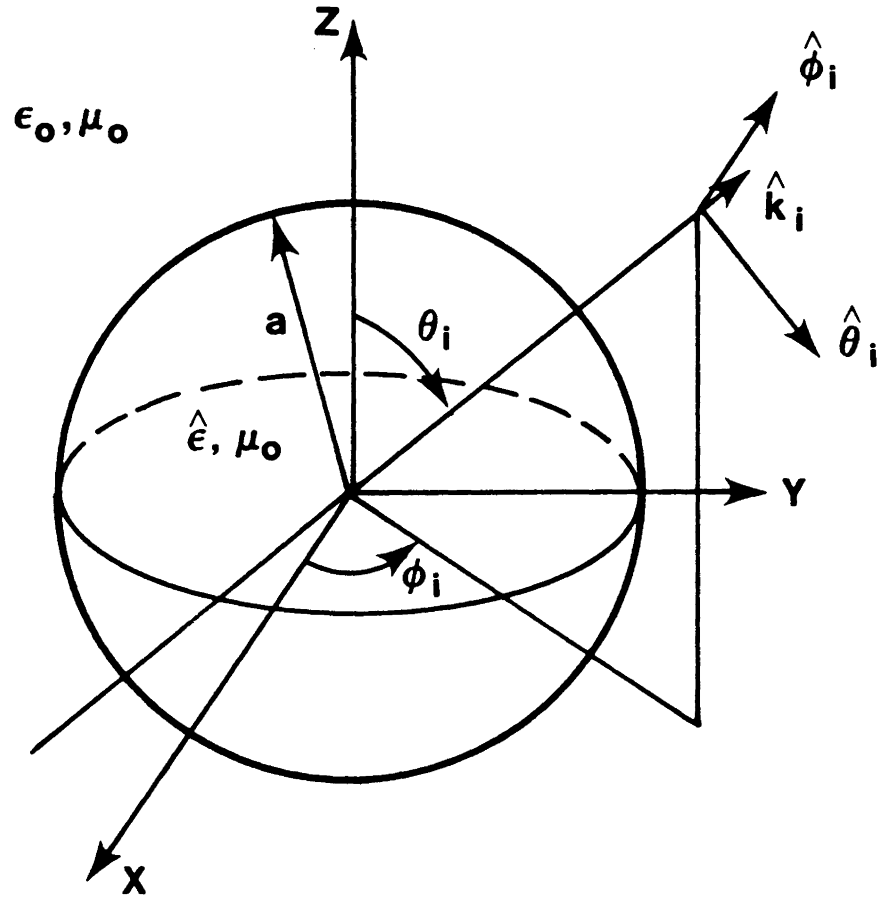

Figure 4.2: Sphere geometry for general incident angle $\hat{k}_i$.

where $\tilde{a}_n \triangleq \frac{(2n+1)}{n(n+1)}$, $\beta \triangleq \tau a$ (recalling $\tau = s/c$),

$$\chi_n \triangleq \sum_{m=0}^{n} \ell_m \frac{(n-m)!}{(n+m)!} P_n^m(\cos\theta) P_n^m(\cos\theta_i) \cos m(\varphi - \varphi_i),$$

with $\ell_0 = 1$, and $\ell_m = 2$ for $m \geq 1$, and

$$b_n \triangleq \frac{\left[(-jm_2\beta) j_n(-jm_2\beta)\right]' j_n(-j\beta) - m_2^2 \, j_n(-jm_2\beta)\left[(-j\beta) j_n(-j\beta)\right]'}{m_2^2 \, j_n(-jm_2\beta)\left[(-j\beta) h_n^{(2)}(-j\beta)\right]' - h_n^{(2)}(-j\beta)\left[(-jm_2\beta) j_n(-jm_2\beta)\right]'} \tag{4.2a}$$

$$c_n \triangleq \frac{\left[(-j\beta) j_n(-j\beta)\right]' j_n(-jm_2\beta) - j_n(-j\beta)\left[(-jm_2\beta) j_n(-jm_2\beta)\right]'}{h_n^{(2)}(-j\beta)\left[(-jm_2\beta) j_n(-jm_2\beta)\right]' - j_n(-jm_2\beta)\left[(-j\beta) h_n^{(2)}(-j\beta)\right]'} \tag{4.2b}$$

In (4.2), $h_n^{(2)}$ denotes the spherical Hankel function of the second kind, order n; j_n denotes the spherical Bessel function of the first kind, order n; and P_n^m denotes the associated Legendre polynomial of order n, degree m. The prime on the bracketed j_n and h_n terms denotes differentiation with respect to their argument. For notational convenience, the numerator of the b_n coefficient is defined to be $\Gamma_{bn}(-jm_2\beta)$, while the denominator will be denoted by $\Lambda_{bn}(-jm_2\beta)$; for the c_n term, the numerator will be represented by $\Gamma_{cn}(-jm_2\beta)$, and $\Lambda_{cn}(-jm_2\beta)$ will be used to denote the denominator.

To determine if Theorems 1 or 2 of Section 2.1 can be applied to the coefficients b_n and c_n, it is necessary to examine their asymptotic behavior as $|\beta|$ and $|m_2\beta|$ become large. Let N represent an arbitrarily

large finite integer. The following asymptotic relations, valid for $|\beta|>>n$, and $|m_2\beta|>>n$, with ($n\leq N$) are derived in Appendix C:

$$b_n \sim \begin{cases} -\frac{1}{2} & \left[\frac{\pi}{2} < \begin{matrix}\arg(m_2\beta)\\ \arg(\beta)\end{matrix} < 3\frac{\pi}{2}\right] \\ (-1)^n \frac{e^{2\beta}}{2}\frac{(1-m_2)}{(1+m_2)} & \left[-\frac{\pi}{2} < \begin{matrix}\arg(m_2\beta)\\ \arg(\beta)\end{matrix} < \frac{\pi}{2}\right], \end{cases} \tag{4.3a}$$

and

$$c_n \sim \begin{cases} -\frac{1}{2} & \left[\frac{\pi}{2} < \begin{matrix}\arg(m_2\beta)\\ \arg(\beta)\end{matrix} < 3\frac{\pi}{2}\right] \\ (-1)^{n+1} \frac{e^{2\beta}}{2}\frac{(1-m_2)}{(1+m_2)} & \left[-\frac{\pi}{2} < \begin{matrix}\arg(m_2\beta)\\ \arg(\beta)\end{matrix} < \frac{\pi}{2}\right] \end{cases} \tag{4.3b}$$

The restriction that N be finite is necessary for the asymptotic approximations to hold.

Asymptotic expansions (4.3) are sufficient to establish that neither b_n nor c_n can be expanded in their entirety. This is because if an effort is made to control the exponential growth in the right half of the complex plane, exponential growth will be introduced in the left half-plane (if one includes the exponential term $\exp(-\beta r/a)$ a similar conclusion is drawn). As a consequence, neither the numerators of the coefficients (Γ_{bn},Γ_{cn}) nor the $\exp(-\beta r/a)$ term will be included in the expansions; an attempt will be made to expand only the coefficient denominators (Λ_{bn}, Λ_{cn}). Note that this complication with expanding the entire coefficient was to be expected from the general conclusion drawn

in Section 2.2.

The denominator of the c_n term, including the $-j\beta$ multiplicative factor, is shown in Appendix C to possess the following asymptotic behavior for $-\frac{\pi}{2}\leq\arg(\beta)\leq\frac{\pi}{2}$, $\frac{\pi}{2}\leq\arg(\beta)\leq 3\frac{\pi}{2}$, $|\beta|>>n$, and $|m_2\beta|>>n$ $(n\leq N)$:

$$(-j\beta)\Lambda_{bn}(-jm_2\beta) \sim -j\, e^{-\beta} \begin{cases} (-1)^n \dfrac{e^{-m_2\beta}}{2}(1-m_2) & \left[\ \frac{\pi}{2} < \arg(m_2\beta) < 3\frac{\pi}{2}\ \right] \\ \dfrac{e^{m_2\beta}}{2}(1+m_2) & \left[\ -\frac{\pi}{2} < \arg(m_2\beta) < \frac{\pi}{2}\ \right] \end{cases} \tag{4.4}$$

The asymptotic behavior of the denominator of the c_n coefficient, also including the $-j\beta$ factor, is given by

$$(-j\beta)\Lambda_{cn}(-jm_2\beta) \sim -j\, e^{-\beta} \begin{cases} (-1)^n \dfrac{e^{-m_2\beta}}{2m_2}(1-m_2) & \left[\ \frac{\pi}{2} < \arg(m_2\beta) < 3\frac{\pi}{2}\ \right] \\ (-1)\dfrac{e^{m_2\beta}}{2m_2}(1+m_2) & \left[\ -\frac{\pi}{2} < \arg(m_2\beta) < \frac{\pi}{2}\ \right] \end{cases} \tag{4.5}$$

which is also valid for $-\frac{\pi}{2}\leq\arg(\beta)\leq\frac{\pi}{2}$, $\frac{\pi}{2}\leq\arg(\beta)\leq 3\frac{\pi}{2}$, $|\beta|>>n$, and $|m_2\beta|>>n$ $(n\leq N)$.

For $|\mathrm{Re}(m_2\beta)| > |\mathrm{Re}(\beta)|$, the reciprocals of both $(-j\beta)\Lambda_{bn}$ and $(-j\beta)\Lambda_{cn}$ exhibit exponential decay throughout both the left and right half-planes. If this condition is not satisfied, which is indeed possible for a complex refractive index, exponential growth can occur. Exponential growth can also occur when $\mathrm{Re}(m_2\beta) = 0$ (though not embodied by (4.4) and (4.5)). Thus, although the reciprocals of both $(-j\beta)\Lambda_{bn}$ and $(-j\beta)\Lambda_{cn}$ represent potential candidates for expansion, further analysis

based on the specific profile of m_2 is required to ensure their proper decay throughout the entire complex plane. In the sequel, specialization to the case of a dielectric water droplet in the microwave frequency region is made.

A refractive index for water based on the Debye relaxation model (Bohren and Huffman, 1983) is used for a numerical example. Debye relaxation characterizes the polarization mechanism of materials from statics to the lower end of the infrared spectrum. The following model for the refractive index of water has been confirmed experimentally through approximently 50 GHz (Bohren and Huffman, 1983):

$$m_2(\omega) = \sqrt{\epsilon_v}\,\frac{\sqrt{j\omega + (\epsilon_d/\upsilon\epsilon_v)}}{\sqrt{j\omega + (1/\upsilon)}}\,, \tag{4.6a}$$

where $\epsilon_d \doteq 77.5$, $\epsilon_v \doteq 5.27$, $\upsilon \doteq 0.8\cdot 10^{-11}$. This refractive profile is graphically illustrated in Figure 4.3. By direct integration, (4.6a) is found to satisfy the Kramers-Kronig relations as it must (Jackson, 1975). Note also that as $|\omega| \to \infty$, $m_2 \to \sqrt{\epsilon_v}$, confirming that (4.6a) is not globally valid over the entire electromagnetic spectrum (to be globally valid, a necessary condition is that $m_2 \to 1$ as $|\omega| \to \infty$ (Jackson, 1975)).

In the β plane, the representation becomes

$$m_2(\beta) = \sqrt{\epsilon_v}\,\frac{\sqrt{\beta + (\epsilon_d a/c\upsilon\epsilon_v)}}{\sqrt{\beta + (a/\upsilon c)}}\,, \tag{4.6b}$$

The branch cut in the β plane is taken to be a curved line segment

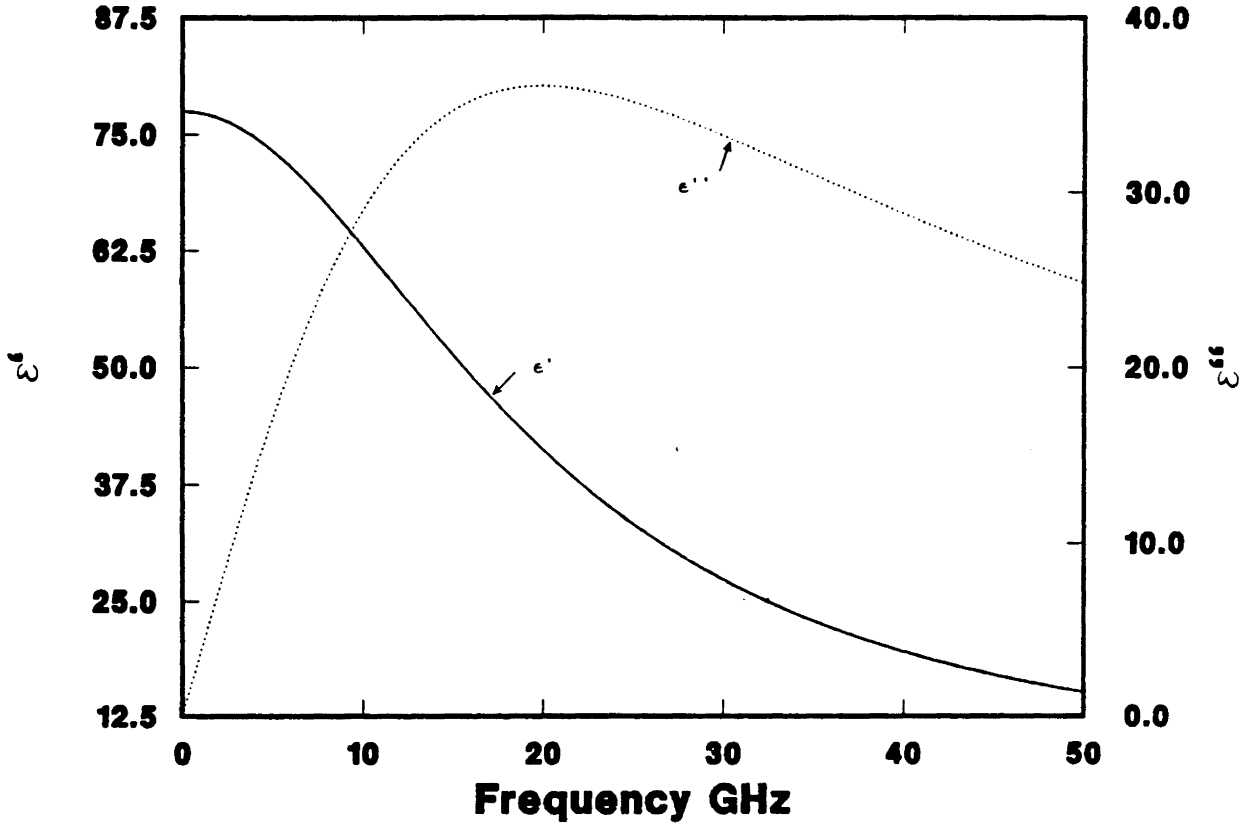

Figure 4.3: Square of the refractive index profile for water based on the Debye relaxation model for water at room temperature. $m_2^2 = \epsilon' - j\epsilon''$.

connecting $\beta = -(\epsilon_d a/c\upsilon\epsilon_v)$ to $\beta = -(a/\upsilon c)$ (a curved segment is chosen for reasons which will become clear in the sequel). Note that the branch cut moves toward the origin of the β plane as $a \to 0$. Also note that at the branch point $\beta = -(\epsilon_d a/c\upsilon\epsilon_v)$, m_2 vanishes; whereas at the branch point $\beta = -(a/\upsilon c)$, m_2 becomes infinite.

The electric (TM) oscillations are determined from $\Lambda_{bn}=0$. Since refractive index (4.6b) generally implies that $|m_2|^2 >> 1$, $\Lambda_{bn}=0$ approximately reduces to

$$j_n(-jm_2\beta)\left[(-j\beta)h_n^{(2)}(-j\beta)\right]' = 0 \tag{4.7}$$

The term $[(-j\beta)h_n^{(2)}(-j\beta)]'$ is of interest. As shown in Appendix B, in the limit as $|m_2| \to \infty$ the denominator of the b_n coefficient becomes this term. The zeros of this term correspond then to the natural electric resonances of the perfectly conducting sphere, with the corresponding modes typically referred to as surface modes (Nussenzveig, 1969). It is known that for each n this term has only a finite number of zeros (Stratton, 1941). Thus, for the dielectric sphere under the condition $|m_2|^2 >> 1$, the electric resonances for each order are approximately represented by the finite collection of electric oscillations for the perfectly conducting sphere, and an infinite collection of electric oscillations (due to j_n) which depend on m_2. Since (4.7) is only approximate, the true poles will be slightly displaced from the values obtained from this equation.

A further simplification for obtaining estimates of the poles is to use an asymptotic approximation for the zeros of the j_n term.

Specifically, the αth zero of $j_n(-jm_2\beta)$, with n fixed, is given approximately by (Abramowitz and Stegun, 1964)

$$-jm_2(\beta_{n\alpha})\beta_{n\alpha} \sim \pm \left\{ (\alpha + \tfrac{n}{2})\pi - \frac{n(n+1)}{(2\alpha+n)\pi} \right\} \doteq j_{n\alpha} \tag{4.8}$$

which is a good approximation when $\alpha>>n$, and is an adequate estimate when $\alpha\sim n$. Since m_2 is dependent on $\beta_{n\alpha}$, a simple explicit representation for $\beta_{n\alpha}$ is not directly possible. By using (4.6b) the following cubic equation is obtained:

$$\beta_{n\alpha}^3 + \frac{\epsilon_d a}{v c \epsilon_v} \beta_{n\alpha}^2 + \frac{1}{\epsilon_v} j_{n\alpha}^2 \left[\beta_{n\alpha} + \frac{a}{cv} \right] = 0 \tag{4.9}$$

Standard numerical techniques can be used for the full solution of (4.9). Alternatively, asymptotic approximations to the zeros can be readily made. For the case $|\beta_{n\alpha}|<<1$, neglecting the cubic term in (4.9) leads to the roots

$$\beta_{n\alpha} \simeq - j_{n\alpha}^2 \frac{v}{2\epsilon_d} \left(\frac{c}{a}\right) \left\{ 1 \pm \left[1 - 4 \frac{\epsilon_d}{j_{n\alpha}^2} \left(\frac{a}{vc}\right)^2 \right]^{1/2} \right\} \tag{4.9a}$$

If $4 (\epsilon_d/j_{n\alpha}^2) (a/vc)^2 >> 1$, (4.9a) further simplifies to

$$\beta_{n\alpha} \simeq - j_{n\alpha}^2 \frac{v}{2\epsilon_d} \left(\frac{c}{a}\right) \pm j\, j_{n\alpha} \frac{1}{\sqrt{\epsilon_d}} \left\{ 1 - j_{n\alpha}^2 \frac{v^2}{8\epsilon_d} \left(\frac{c}{a}\right)^2 \right\} \tag{4.9b}$$

If $4\,(\epsilon_d/j_{n\alpha}^2)\,(a/vc)^2 \ll 1$, (4.9a) approximately reduces to

$$\beta_{n\alpha} \simeq -\left(\frac{a}{vc}\right)\left\{1 + \frac{\epsilon_d}{j_{n\alpha}^2}\left(\frac{a}{vc}\right)^2\right\} \tag{4.9c}$$

Using the numerical values for v and ϵ_d, formula (4.9b) is valid as long as $j_{np}^2/a^2 \ll 1\cdot10^8$, whereas (4.9c) is valid for $a^2/j_{n\alpha}^2 \ll 1\cdot10^8$.

For the case $|\beta_{n\alpha}| \gg 1$, (4.9) leads to the approximate roots

$$\beta_{n\alpha} \simeq -\frac{1}{2}\frac{\epsilon_d a}{vc\epsilon_v} \pm \frac{1}{2}\left\{\left[\frac{\epsilon_d a}{vc\epsilon_v}\right]^2 - \frac{4}{\epsilon_v}\,j_{n\alpha}^2\right\}^{1/2} \tag{4.9d}$$

If $(\epsilon_d a/vc\epsilon_v)^2 \gg 4\,j_{n\alpha}^2/\epsilon_v$, then

$$\beta_{n\alpha} \simeq -\frac{\epsilon_d a}{vc\epsilon_v} + j_{n\alpha}^2\left(\frac{vc}{\epsilon_d a}\right) \tag{4.9e}$$

If $(\epsilon_d a/vc\epsilon_v)^2 \ll 4\,j_{n\alpha}^2/\epsilon_v$, an approximation to the roots is given by

$$\beta_{n\alpha} \simeq -\frac{1}{2}\frac{\epsilon_d a}{vc\epsilon_v} \pm j\,\frac{1}{\sqrt{\epsilon_v}}\,j_{n\alpha}\left\{1 - \left[\frac{\epsilon_d a}{vc\epsilon_v}\right]^2 \frac{\epsilon_v}{4\,j_{n\alpha}^2}\right\} \tag{4.9f}$$

In all cases the appropriate sign(s) has (have) been chosen to give the closest approximation to the actual roots of (4.9).

From (4.9b, c, e, and f) it is observed that the poles corresponding to j_n fall in three classes: 1. Conjugate pairs with relatively small real and imaginary portions which will be considered to

be the *dominant* poles (from (4.9b)); 2. Purely real poles between branch points (from (4.9c) and (4.9e)); and 3. conjugate pairs with relatively large real and imaginary portions (from (4.6f)). It is noted that the presence of the purely real poles between the branch points is the reason the branch cut was taken to be a parabolic line segment. It is also noted that when the radius of the sphere is several millimeters, the contributions due to the poles in classes 2 and 3 will be negligibly small due to the exponential decay of j_n (the residues will be approximately zero). Lastly it is observed that (4.9c) implies that an accumulation point for the roots exists at the branch point $\beta=-(a/vc)$; thus infinity fails to be the only accumulation point.

For the magnetic oscillations, the poles of the c_n coefficient are approximately given by

$$h_n^{(2)}(-j\beta)\ \left[(-jm\beta)\ j_n(-jm\beta)\right]' = 0$$

Standard recursion relationships (Abramowitz and Stegun, 1964) can be used to further simplify this to

$$h_n^{(2)}(-j\beta)\ j_{n-1}(-jm\beta) = 0$$

Thus, for the case $|m_2|^2>>1$, approximations for the magnetic oscillations of the lossy dielectric sphere are given by the magnetic oscillations of the perfectly conducting sphere, and expression (4.9) with $j_{n\alpha}$ replaced by $j_{(n-1)\alpha}$ (thus all approximations to the poles given by (4.9b,c,e and f) are also valid by making a similar replacement). A listing of the

electric and magnetic oscillations for the perfectly conducting sphere through n=8 is given in Table 4.1.

The approximations described above provide useful estimates for the natural oscillations of the dielectric sphere when $|m_2|^2>>1$. These estimates may subsequently be refined iteratively to the zeros of Λ_{bn} or Λ_{cn} by standard function iterative zero-searching techniques (e.g., Muller's method, Muller, 1956). Figures 4.4 and 4.5 depict, respectively, the radius dependence in the β plane of the n=1 and n=2 electric oscillations which satisfy $\Lambda_{bn}=0$. Figures 4.6 and 4.7 respectively depict the radius dependence of the n=1 and n=2 magnetic oscillations which satisfy $\Lambda_{cn}=0$.

Since $m_2 \rightarrow \sqrt{\epsilon_v}$ as $|\beta|\rightarrow\infty$, it follows that $|\mathrm{Re}(m_2\beta)|>|\mathrm{Re}(\beta)|$ as $|\beta|\rightarrow\infty$, and therefore $1/(-j\beta)\Lambda_{bn}$ and $1/(-j\beta)\Lambda_{cn}$ satisfy the decay requirements for application of either expansion (2.10) or (2.12) associated with Theorems 1 and 2, respectively, of Section 2.1. In addition, the requirements for simple poles and analyticity at $\beta=0$ are also satisfied. A requirement which is not satisfied is a single accumulation point of the poles at infinity. It has been found, however, that the residues corresponding to the poles which approach the accumulation point $\beta=-(a/vc)$ tend to zero, and, for this reason, the single accumulation point at infinity assumption will be taken as not being violated. Thus, all assumptions for application of either expansion (2.10) or (2.12) are taken to be satisfied and therefore either expansion can be used.

When high accuracy is required, expansion (2.10) is to be preferred. This is because in a practical situation it is only possible

Table 4.1a: Natural electric oscillations for the perfectly conducting sphere through order n=8. Conjugates exist for those poles with nonzero imaginary portions.

Order	Electric Oscillations
1	-0.5 + j 0.86602540
2	-0.70196418 + j 1.80733949
2	-1.59607164 + j 0.0
3	-0.84286219 + j 2.75785595
3	-2.15713781 + j 0.87056923
4	-0.95422989 + j 3.71478435
4	-2.57139919 + j 1.75230275
4	-2.94874185 + j 0.0
5	-1.04767344 + j 4.67641047
5	-2.90806183 + j 2.64431626
5	-3.54426473 + j 0.86892596
6	-1.12890552 + j 5.64163503
6	-3.19523637 + j 3.54488618
6	-4.03356055 + j 1.74303977
6	-4.28459513 + j 0.0
7	-1.20120343 + j 6.60971525
7	-3.44759209 + j 4.45256475
7	-4.45400803 + j 2.62330507
7	-4.89719646 + j 0.86839132
8	-1.26663874 + j 7.58012542
8	-3.67388939 + j 5.36622189
8	-4.82542445 + j 3.50950313
8	-5.42626873 + j 1.73981086
8	-5.61555738 + j 0.0

Table 4.1b: Natural magnetic oscillations for the perfectly conducting sphere through order n=8. Conjugates exist for those poles with nonzero imaginary portions.

Order	Magnetic Oscillations
1	-1.0 + j 0.0
2	-1.5 + j 0.86602540
3	-1.83890732 + j 1.75438096
3	-2.32218535 + j 0.0
4	-2.10378940 + j 2.65741804
4	-2.89621060 + j 0.86723413
5	-2.32467430 + j 3.57102292
5	-3.35195640 + j 1.74266142
5	-3.64673860 + j 0.0
6	-2.51593225 + j 4.49267295
6	-3.73570836 + j 2.62627231
6	-4.24835940 + j 0.86750967
7	-2.68567688 + j 5.42069413
7	-4.07013916 + j 3.51717405
7	-4.75829053 + j 1.73928606
7	-4.97178686 + j 0.0
8	-2.83898395 + j 6.35391130
8	-4.36828922 + j 4.41444250
8	-5.20484079 + j 2.61617515
8	-5.58788604 + j 0.86761445

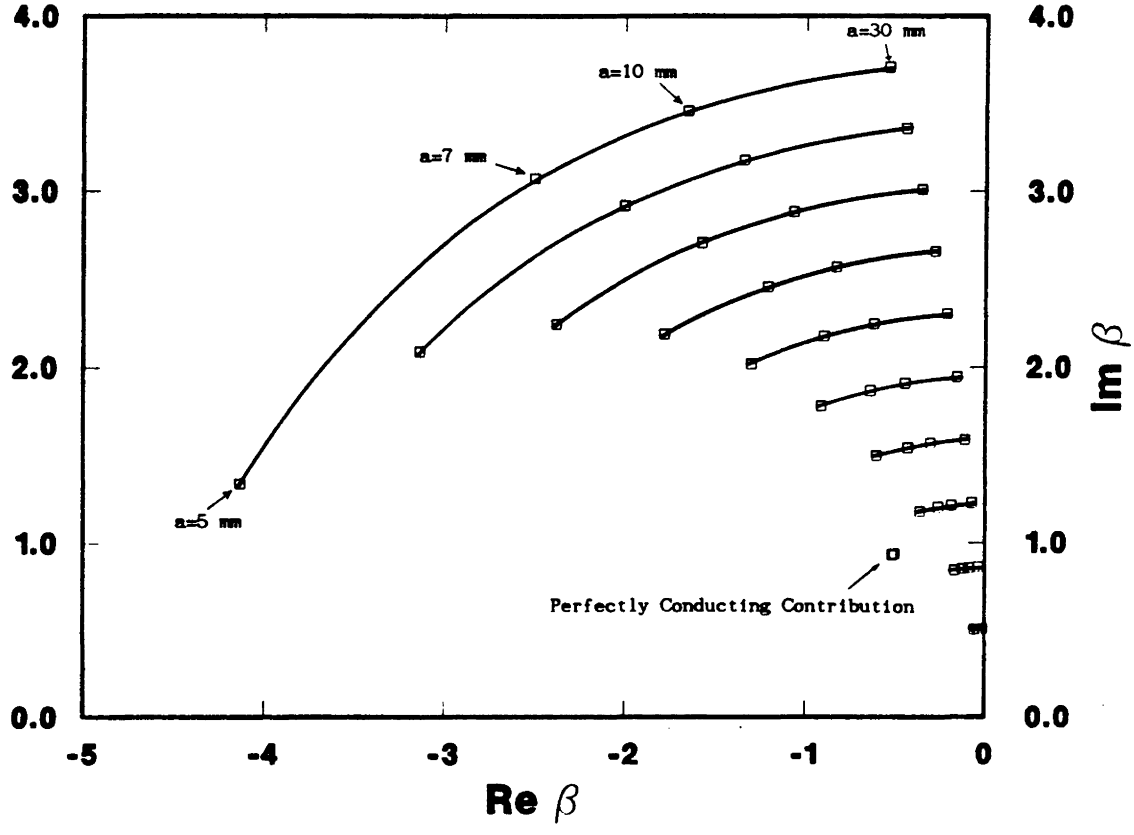

Figure 4.4: The n=1 dominant and perfectly conducting electric resonance trajectories as a function of radius.

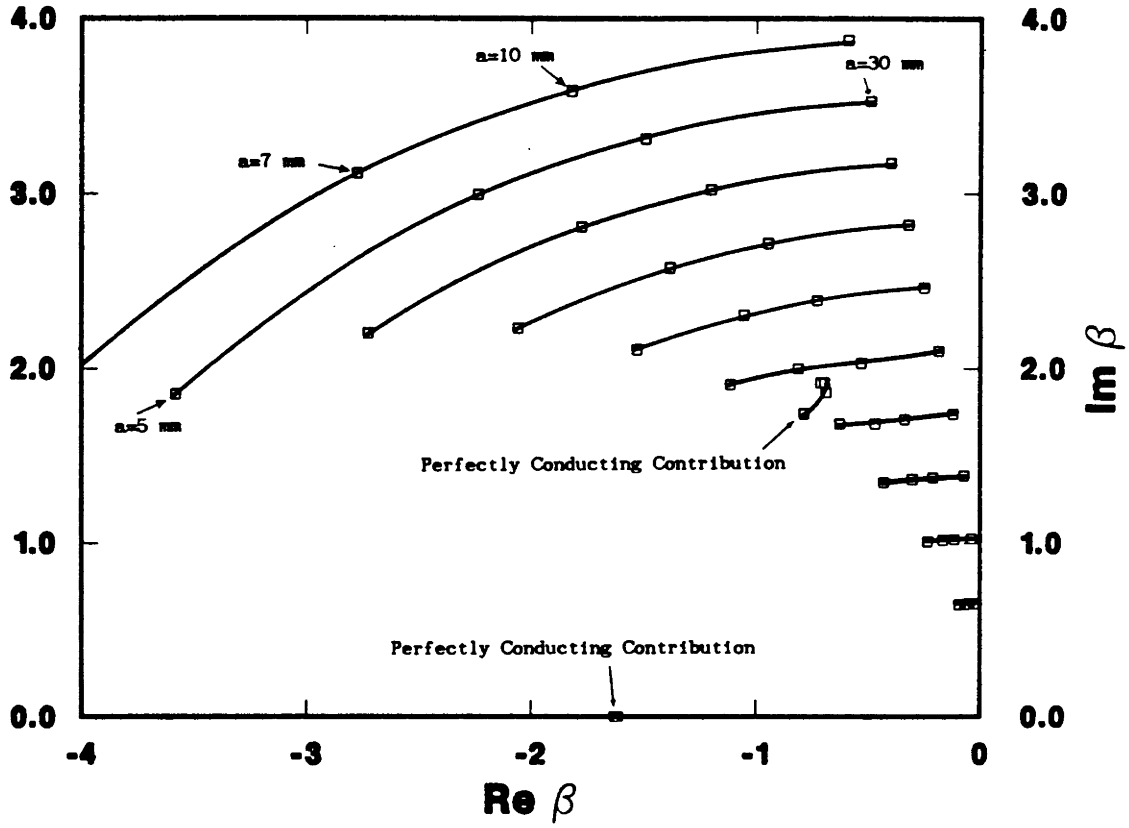

Figure 4.5: The n=2 dominant and perfectly conducting electric resonance trajectories as a function of radius.

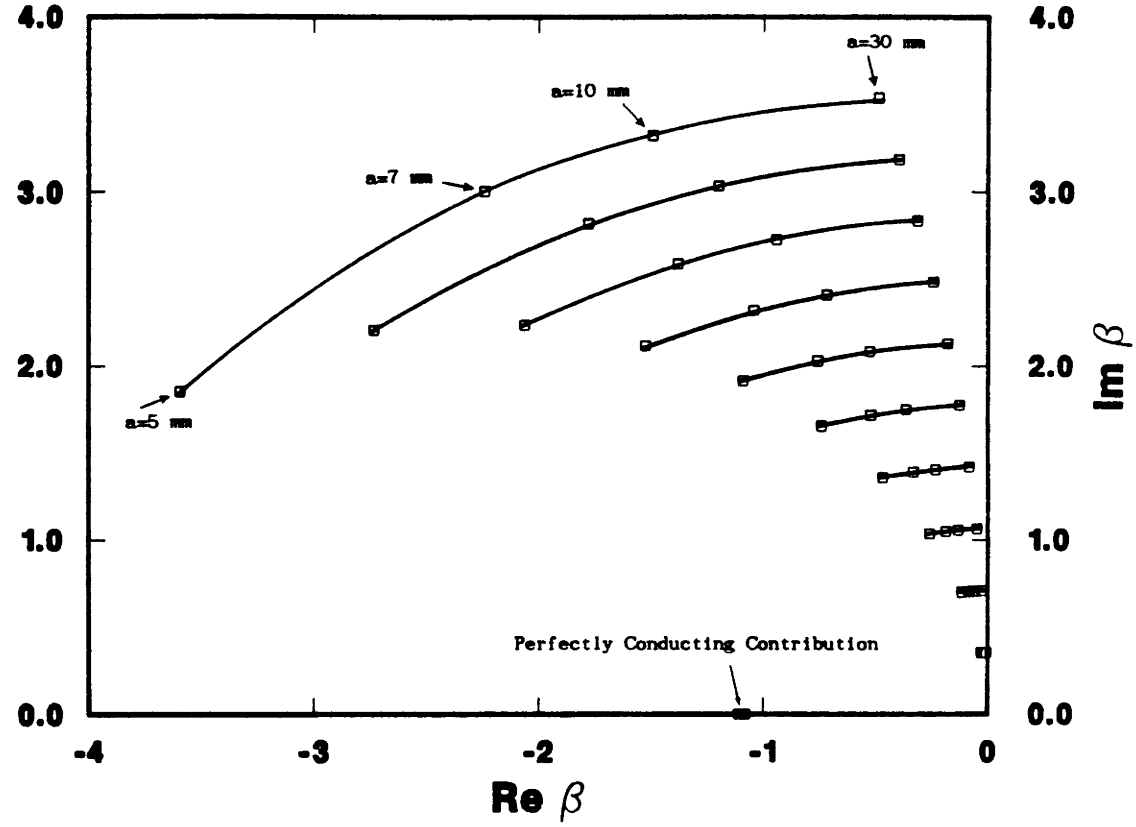

Figure 4.6: The n=1 dominant and perfectly conducting magnetic resonance trajectories as a function of radius.

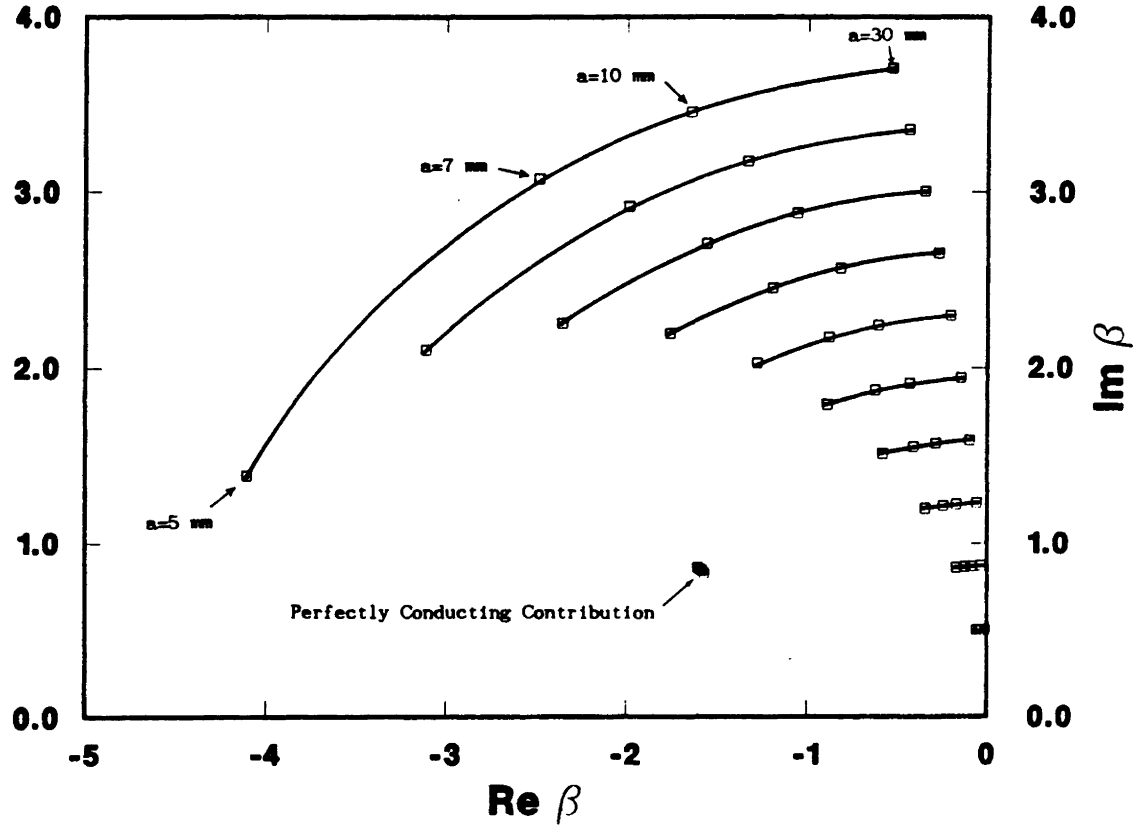

Figure 4.7: The n=2 dominant and perfectly conducting magnetic resonance trajectories as a function of radius.

to include a finite subset of the infinite set of resonances associated with each term being expanded, and therefore the contribution due to the great circle contour C shown in Figure 4.8 formally must be included in the expansion. Since this contour contribution is smaller for expansion (2.10) than for expansion (2.12), expansion (2.10) will yield higher accuracy when summing over the same number of poles. On the other hand, there may be applications where the simpler form of expansion (2.12) is desired.

Completely specified resonance expansions for the Mie series (4.1), truncated after N terms and neglecting the great circle contribution, may be given as follows:

$$E_\theta^{sc} \simeq ja \frac{E_o e^{-\beta r/a}}{r} \mathcal{F}_\theta \tag{4.10}$$

where

$$\mathcal{F}_\theta \doteq \sum_{n=1}^{N} \tilde{a}_n \left[\frac{\partial^2}{\partial\theta\partial\theta_i}\chi_n\right] \Gamma_{bn}(-jm_2\beta) \left[R_{bn}(0) + \sum_{\alpha} R_{\alpha_{bn}} \left\{ \frac{1}{(\beta-\beta_{\alpha_{bn}})} + \frac{1}{\beta_{\alpha_{bn}}} \right\} + I_{bn} \right]$$
$$+ \sum_{n=1}^{N} \tilde{a}_n \left[\frac{1}{\sin\theta\sin\theta_i}\frac{\partial^2}{\partial\varphi\partial\varphi_i}\chi_n\right] \Gamma_{cn}(-jm_2\beta) \left[R_{cn}(0) + \sum_{\alpha} R_{\alpha_{cn}} \left\{ \frac{1}{(\beta-\beta_{\alpha_{cn}})} + \frac{1}{\beta_{\alpha_{cn}}} \right\} + I_{cn} \right]$$

and

$$E_\varphi^{sc} \simeq ja \frac{E_o e^{-\beta r/a}}{r} \mathcal{F}_\varphi \tag{4.11}$$

where

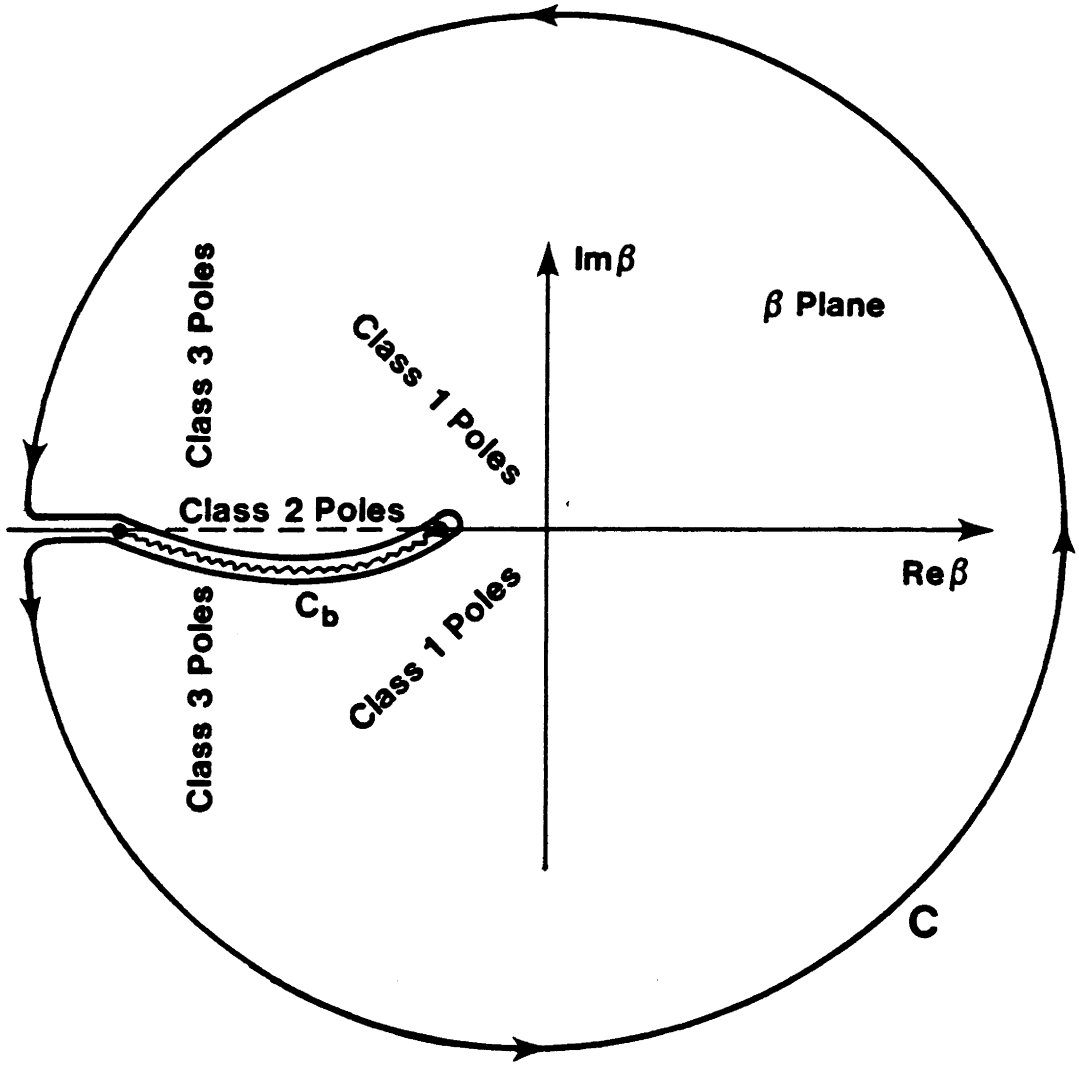

Figure 4.8: Contour used to construct the resonance expansion.

$$\mathcal{F}_{\varphi} \doteq \sum_{n=1}^{N} \tilde{a}_n \left[\frac{1}{\sin\theta} \frac{\partial^2}{\partial\varphi\partial\theta_i} \chi_n\right] \Gamma_{bn}(-jm_2\beta) \left[R_{bn}(0)+\sum_{\alpha} R_{\alpha_{bn}} \left\{\frac{1}{(\beta-\beta_{\alpha_{bn}})} + \frac{1}{\beta_{\alpha_{bn}}}\right\} + I_{bn}\right]$$

$$+ \sum_{n=1}^{N} \tilde{a}_n \left[\frac{1}{\sin\theta_i} \frac{\partial^2}{\partial\theta\partial\varphi_i} \chi_n\right] \Gamma_{cn}(-jm_2\beta) \left[R_{cn}(0)+\sum_{\alpha} R_{\alpha_{cn}} \left\{\frac{1}{(\beta-\beta_{\alpha_{cn}})} + \frac{1}{\beta_{\alpha_{cn}}}\right\} + I_{cn}\right]$$

The static contributions for the expanded terms are given by $R_{bn}(0)= j(2n+1)/\{(\sqrt{\epsilon_d})^n[n\ (\epsilon_d+1)\ +\ 1]\}$, and $R_{cn}(0)= -j/(\sqrt{\epsilon_d})^n$ (these are established in Appendix C). The branch cut contributions are represented by

$$I_{bn}(\beta) \doteq \frac{\beta}{2\pi j} \int_{C_b} d\xi \frac{1}{\xi\ (\xi-\beta)\ (-j\xi)\ \Lambda_{bn}(-jm\xi)}$$

and

$$I_{cn}(\beta) \doteq \frac{\beta}{2\pi j} \int_{C_b} d\xi \frac{1}{\xi\ (\xi-\beta)\ (-j\xi)\ \Lambda_{cn}(-jm\xi)}$$

Observe that because $j_n(-z)=(-1)^n\ j_n(z)$, Λ_{bn} and Λ_{cn} are even functions around the branch when n is even, and therefore the branch cut contributions are zero for this case. When n is odd however, a branch cut contribution will be present.

As noted, the contribution from the contour C has been neglected in expansions (4.10) and (4.11). Though it will not be demonstrated, when the branch cut contributions are also neglected, a direct analogy between terms of the general resonance expansion derived for the far-scattered field, given by (2.20), can be made with (4.10) and (4.11).

The residues $R_{\alpha_{bn}}$ and $R_{\alpha_{cn}}$ are determined by the formulas

$$R_{\alpha_{bn}} = \frac{1}{\frac{d}{d\beta}\left[(-j\beta)\Lambda_{bn}(-jm_2\beta)\right]_{\beta=\beta_{\alpha_{bn}}}} = \frac{1}{(-j\beta_{\alpha_{bn}})\ \frac{d}{d\beta}\left[\Lambda_{bn}(-jm_2\beta)\right]_{\beta=\beta_{\alpha_{bn}}}}$$

and

$$R_{\alpha_{cn}} = \frac{1}{\frac{d}{d\beta}\left[(-j\beta)\Lambda_{cn}(-jm_2\beta)\right]_{\beta=\beta_{\alpha_{cn}}}} = \frac{1}{(-j\beta_{\alpha_{cn}})\ \frac{d}{d\beta}\left[\Lambda_{cn}(-jm_2\beta)\right]_{\beta=\beta_{\alpha_{cn}}}}$$

The resonances $\beta_{\alpha_{bn}}$ and $\beta_{\alpha_{cn}}$ satisfy $\Lambda_{bn}(-jm_2\beta_{\alpha_{bn}})=0$ and $\Lambda_{cn}(-jm_2\beta_{\alpha_{cn}}) = 0$. Tables 4.2-4.7 list the dominant resonances and corresponding residues for the refractive index profile (4.6b) for a variety of radii.

As previously noted, it is not possible to numerically realize an exact termwise reconstruction of the Mie series since the number of poles is infinite for each order n. The reconstruction improves, of course, as more poles are added to the expansion since the further the surrounding contour is drawn into the complex plane, the smaller the error introduced by neglecting the contribution due to the contour. Tables 4.8a-e demonstrate the rate of convergence of equation (4.10) as more poles are included in the series. The branch cut contributions have been neglected. As seen Tables 4.8a-c, the branch cut contribution is indeed negligible. As the branch cut moves closer to the origin of the β plane ($a \to 0$), however, the contribution is no longer negligible. This is shown in Tables 4.8d and 4.8e. As a general conclusion, under the restriction $a \geq 4$mm with the frequency, f, less than 10 GHz, the branch cut

Table 4.2: Dominant natural oscillations and corresponding residues for the case a=0.03 meters, n=1. PEC denotes the perturbed pole corresponding to the perfectly conducting sphere. Conjugates exist for those poles with nonzero imaginary portions. The residues for the conjugates are obtained by negating the real portion of the residues given. (a) Electric; (b) Magnetic.

TABLE 4.2a

POLES	RESIDUES
-0.01005377+j0.50225489	0.00363676+j0.00006312
-0.03582515+j0.86146717	-0.01084414+j0.00234811
-0.07383546+j1.22554678	0.01327011-j0.00839176
-0.11238821+j1.58870016	-0.01229825+j0.00807566
-0.15882836+j1.94713241	0.01234913-j0.00501832
-0.21505243+j2.30306507	-0.01208990+j0.00130258
-0.35704395+j2.65733767	0.01088013+j0.00232299
-0.44274260+j3.01018339	-0.00866967-j0.00530367
-0.50338943+j0.93506443 (PEC)	0.00055236+j0.00131579

TABLE 4.2b

POLES	RESIDUES
-0.00598697+j0.35265385	-0.03776283-j0.00221040
-0.02278160+j0.70791488	0.06448852+j0.01105626
-0.04883890+j1.06243330	-0.07631193-j0.02790388
-0.08373043+j1.41824510	0.07373676+j0.04923295
-0.12759164+j1.77372341	-0.05881731-j0.06926196
-0.18063129+j2.12853673	0.03495400+j0.08278771
-0.24301343+j2.48248455	-0.00671428-j0.08655265
-0.31485841+j2.83541312	-0.02090634+j0.07971492
-1.10876603+j0.0 (PEC)	0.0 -j0.00003056

Table 4.3: Dominant natural oscillations and corresponding residues for the case a=0.03 meters, n=2. PEC denotes the perturbed poles corresponding to the perfectly conducting sphere. Conjugates exist for those poles with nonzero imaginary portions. The residues for the conjugates are obtained by negating the real portion of the residues given. (a) Electric; (b) Magnetic.

TABLE 4.3a

POLES	RESIDUES
-0.01554911+j0.65001503	0.00061261+j0.00008676
-0.03881615+j1.02429033	-0.00236806-j0.00047586
-0.07252456+j1.38422956	0.00609894+j0.00113708
-0.12114151+j1.73781878	-0.01241880-j0.00037952
-0.18534580+j2.09713578	0.01691650-j0.00489626
-0.25080302+j2.46153970	-0.01497269+j0.00718642
-0.32098254+j2.82063172	0.01330481-j0.00508995
-0.40059589+j3.17567558	-0.01215417-j0.00200820
-0.69463795+j1.91653075 (PEC)	-0.00074869+j0.00062747
-1.62871396+j0.0 (PEC)	0.0 +j1.22E-08

TABLE 4.3b

POLES	RESIDUES
-0.00961670+j0.50798252	-0.00958901-j0.00072035
-0.02876487+j0.87275934	0.02521805+j0.00334304
-0.05798571+j1.23114438	-0.04254499-j0.00875897
-0.09725541+j1.58752531	0.05635383-j0.01774521
-0.14625733+j1.94302187	-0.06298693-j0.03028026
-0.20471497+j2.29780692	0.06099294+j0.04476610
-0.27253174+j2.65173761	-0.05077031-j0.05835734
-0.34973881+j3.00461474	0.03412898+j0.06802390
-1.60683911+j0.86239061 (PEC)	0.00000023-j0.00000027

Table 4.4: Dominant natural oscillations and corresponding residues for the case a=0.015 meters, n=1. PEC denotes the perturbed pole corresponding to the perfectly conducting sphere. Conjugates exist for those poles with nonzero imaginary portions. The residues for the conjugates are obtained by negating the real portion of the residues given. (a) Electric; (b) Magnetic.

TABLE 4.4a

POLES	RESIDUES
-0.01911087+j0.50199510	0.00363349+j0.00040468
-0.06268408+j0.85884419	-0.01142197+j0.00071012
-0.13075083+j1.21965396	0.01495572-j0.00673948
-0.20786549+j1.57971514	-0.01318050+j0.00607123
-0.30229262+j1.93270427	0.01215177-j0.00251815
-0.41656021+j2.28069064	-0.01060751-j0.00115612
-0.55099665+j2.62411666	0.00820508+j0.00405092
-0.70583733+j2.96270066	-0.00526720-j0.00572147
-0.50614263+j0.93366553 (PEC)	0.00012330+j0.00178909

TABLE 4.4b

POLES	RESIDUES
-0.01052412+j0.35250897	-0.03763817-j0.00362384
-0.04118199+j0.70593517	0.06327151+j0.01543654
-0.09072924+j1.05962514	-0.07202474-j0.03444372
-0.15884258+j1.41234228	0.06471300+j0.05522458
-0.24574418+j1.76307500	-0.04520301-j0.07108253
-0.35178856+j2.11104183	0.01924648+j0.07731040
-0.47734636+j2.45555438	0.00683076-j0.07255452
-0.62280015+j2.79593499	-0.02768802+j0.05865649
-1.10370030+j0.0 (PEC)	0.0 -j0.00001931

Table 4.5: Dominant natural oscillations and corresponding residues for the case a=0.015 meters, n=2. PEC denotes the perturbed poles corresponding to the perfectly conducting sphere. Conjugates exist for those poles with nonzero imaginary portions. The residues for the conjugates are obtained by negating the real portion of the residues given. (a) Electric; (b) Magnetic.

TABLE 4.5a

POLES	RESIDUES
-0.03108780+*j*0.64965478	0.00059576+*j*0.00017446
-0.07727227+*j*1.02284366	-0.00222534-*j*0.00101505
-0.14211430+*j*1.37998653	0.00569200+*j*0.00308145
-0.23066596+*j*1.72498788	-0.01288316-*j*0.00540368
-0.35469352+*j*2.07225785	0.02204719-*j*0.00052380
-0.48571114+*j*2.43281864	-0.01665891+*j*0.00537238
-0.62816413+*j*2.78078048	0.01272623-*j*0.00254748
-0.79150572+*j*3.11985638	-0.01006021-*j*0.00045463
-0.70382094+*j*1.91572011 (PEC)	-0.00357752+*j*0.00041934
-1.62621723+*j*0.0 (PEC)	0.0 +*j*3.38E-09

TABLE 4.5b

POLES	RESIDUES
-0.01914981+*j*0.50779325	-0.00952273-*j*0.00142583
-0.05691883+*j*0.87172567	0.02471226+*j*0.00635636
-0.11415910+*j*1.22805244	-0.04075305-*j*0.01525086
-0.19113746+*j*1.58066700	0.05188461+*j*0.02722400
-0.28783664+*j*1.93035394	-0.05430242-*j*0.04042098
-0.40418735+*j*2.27694123	0.04743035+*j*0.05217756
-0.54028014+*j*2.61985396	-0.03344430-*j*0.05964410
-0.69638895+*j*2.95836338	0.01601692+*j*0.06093077
-1.59953672+*j*0.85765417 (PEC)	0.00000019+*j*0.00000009

Table 4.6: Dominant natural oscillations and corresponding residues for the case a=0.005 meters, n=1. PEC denotes the perturbed pole corresponding to the perfectly conducting sphere. Conjugates exist for those poles with nonzero imaginary portions. The residues for the conjugates are obtained by negating the real portion of the residues given. (a) Electric; (b) Magnetic.

TABLE 4.6a

POLES	RESIDUES
-0.05541431+j0.50011413	0.00333877+j0.00177092
-0.16791330+j0.84274971	-0.01157942-j0.00720257
-0.36416695+j1.17232455	0.02294060+j0.00005768
-0.60488404+j1.49688177	-0.01423916-j0.00031603
-0.91245755+j1.78146746	0.00895364+j0.00379283
-1.30057371+j2.01868247	-0.00452459-j0.00505271
-1.78307905+j2.18666225	0.00133483+j0.00443921
-2.38243687+j2.24221627	0.00032284-j0.00304247
-0.51722562+j0.92868064 (PEC)	-0.00568043+j0.00440512

TABLE 4.6b

POLES	RESIDUES
-0.02867018+j0.35156660	-0.03677538-j0.00923331
-0.11498376+j0.69876553	0.05665807+j0.03210854
-0.26025511+j1.03631844	-0.05300309-j0.05665831
-0.46742777+j1.35761392	0.03158457+j0.07065093
-0.74148181+j1.65412307	-0.00504493-j0.06867718
-1.09001591+j1.91398055	-0.01512498+j0.05406712
-1.52446915+j2.11898798	0.02390156-j0.03505192
-2.06262671+j2.23777203	-0.02296841+j0.01911299
-1.08024786+j0.0 (PEC)	0.0 -j0.00000109

Table 4.7: Dominant natural oscillations and corresponding residues for the case a=0.005 meters, n=2. PEC denotes the perturbed poles corresponding to the perfectly conducting sphere. Conjugates exist for those poles with nonzero imaginary portions. The residues for the conjugates are obtained by negating the real portion of the residues given. (a) Electric; (b) Magnetic.

TABLE 4.7a

POLES	RESIDUES
-0.09377618+j0.64579030	0.00041557+j0.00048921
-0.23454935+j1.00798960	-0.00052792-j0.00265882
-0.43097426+j1.34615567	-0.00261771+j0.00845272
-0.62708220+j1.68144856	0.00178495-j0.03556039
-1.11369433+j1.90636011	0.01097438-j0.01403138
-1.52891435+j2.10720177	-0.00949167+j0.00272680
-2.05924427+j2.22871056	0.00590480+j0.00098788
-2.27586477+j2.20149496	-0.00327557-j0.00176312
-0.78576757+j1.73928346 (PEC)	-0.00424980+j0.04049634
-1.61278942+j0.0 (PEC)	0.0 +j0.0

TABLE 4.7b

POLES	RESIDUES
-0.05745800+j0.50583480	-0.00882835-j0.00420458
-0.17096091+j0.86140048	0.01982335+j0.01796184
-0.34415617+j1.19743382	-0.02652212-j0.03956706
-0.58122984+j1.51050799	0.02592011+j0.06098445
-0.88883418+j1.79172770	-0.01985972-j0.07272650
-1.27681666+j2.02751779	0.01196759+j0.07024889
-1.75932035+j2.19559942	-0.00537229-j0.05696024
-2.35838124+j2.25357053	0.00229499+j0.04033781
-1.57035619+j0.82815935 (PEC)	-0.00000298+j0.00000130

Table 4.8: Comparison of Eq. (4.1a) and (4.10). The branch cut and great circle contour contributions have been neglected. For Tables 4.8a-d, only the dominant, or class 1 poles have been included in the series. In Table 4.8e, poles in classes 1-3 have been included. The error between the "exact" and the resonance solutions for Table 4.8e is primarily due to the neglected branch cut contribution required for the n=1 term. For all presented results, $\theta_i=\varphi_i=\varphi=\theta=0$, and $E_o=1$ V/m.

(a) a=0.03 m, $\beta=j$ 1.0, r=10 a

Exact (2 term) Solution for Electric Field: -0.0080244 + j 0.0672074

Total Number of Dominant Poles	Resonance Solution for Electric Field
28	-0.0317117 + j 0.0451669
60	-0.0076482 + j 0.0662221
172	-0.0080430 + j 0.0671935
252	-0.0080241 + j 0.0672079

(b) a=0.01 m, $\beta=j$ 1.0, r=10 a

Exact (2 term) Solution for Electric Field: 0.0057172 + j 0.0697791

Total Number of Dominant Poles	Resonance Solution for Electric Field
28	-0.0456345 + j 0.0652409
60	0.0059494 + j 0.0683411
174	0.0057172 + j 0.0697794

(c) a=0.005 m, $\beta=j$ 1.0, r=10 a

Exact (2 term) Solution for Electric Field: 0.0099211 + j 0.0736589

Total Number of Dominant Poles	Resonance Solution for Electric Field
28	-0.0493293 + j 0.1423078
60	0.0089034 + j 0.0723570
86	0.0098083 + j 0.0736492

(d) a=0.003 m, $\beta=j$ 1.0, r=10 a

Exact (2 term) Solution for Electric Field: 0.0101280 + j 0.0768886

Total Number of Dominant Poles	Resonance Solution for Electric Field
29	0.0658467 + j 0.2295799
54	0.0157024 + j 0.0889637

(e) a=0.003 m, $\beta=j$ 1.0, r=10 a

Exact (2 term) Solution for Electric Field: 0.0101280 + j 0.0768886

Total Number of Class 1 - 3 Poles	Resonance Solution for Electric Field
50	0.0651779 + j 0.2305129
110	0.0124536 + j 0.0908458

contribution can be neglected for the refractive index profile (4.6b), and, in fact, the class 1 poles are sufficient. A broadband comparison of the resonance series (4.10) with the standard Mie series (4.1a) is shown in Figures 4.9a and 4.9b (the branch cut contribution was neglected).

In the following section, single poles are used to capture the response locally to a resonance.

4.1.2 Extinction, Scattering, and Absorption Cross-Sections

The extinction, scattering, and absorption cross-sections for the sphere can be derived from (4.1) and energy considerations. Since the cross-sections are defined relative to the forward scattering direction, it is convenient to take $\theta_i=\varphi_i=\theta=\varphi=0$ in (4.1). Because the actual derivation of these cross-sections is somewhat lengthy and is adequately given elsewhere (Van Bladel, 1964), only the results are provided here. The extinction, scattering, and absorption cross-sections are stated, respectively, as

$$\sigma_{ext} = \frac{2\pi}{\tau^2} \sum_{n=1}^{\infty} (2n+1)\ \mathrm{Re}(b_n + c_n) \tag{4.12}$$

$$\sigma_{sca} = -\frac{2\pi}{\tau^2} \sum_{n=1}^{\infty} (2n+1)\ (|b_n|^2 + |c_n|^2) \tag{4.13}$$

$$\sigma_{abs} = \sigma_{ext} - \sigma_{sca} \tag{4.14}$$

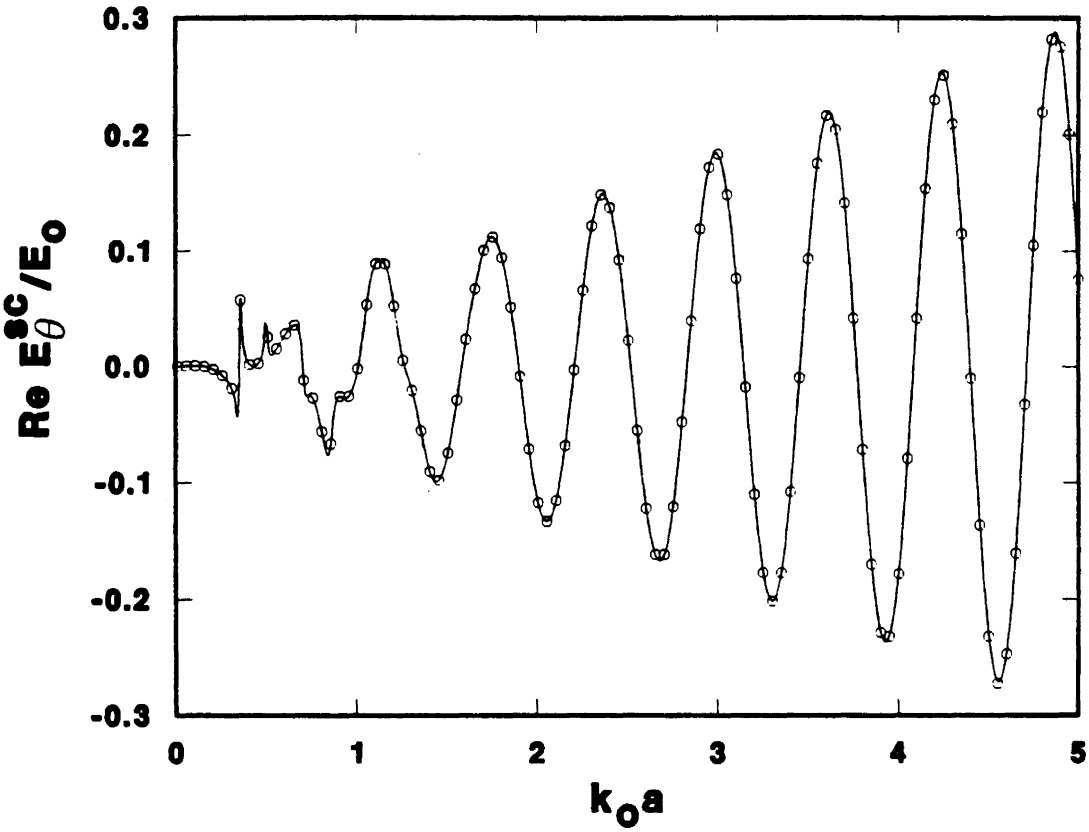

Figure 4.9a: Broadband comparison of the real portion of the resonance expansion with the real portion of the standard Mie series. The continuous line denotes the Mie solution. The circles denote the resonance solution which is an overlay. a=30 mm and a total of 1280 resonances were used to generate the resonance solution. r/a=10.0, $\varphi_i=\varphi=0.0$, and $\theta_i=\theta=0.0$.

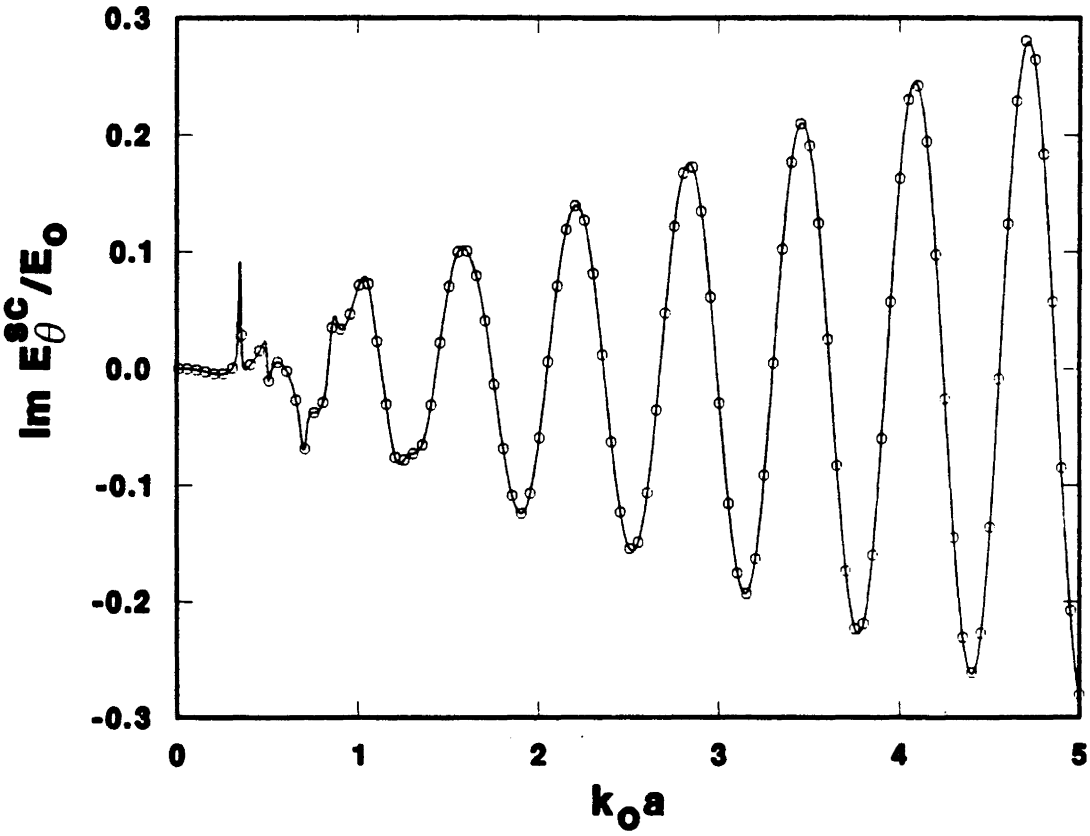

Figure 4.9b: Broadband comparison of the imaginary portion of the resonance expansion with the imaginary portion of the standard Mie series. The continuous line denotes the Mie solution. The circles denote the resonance solution which is an overlay. a=30 mm and a total of 1280 resonances were used to generate the resonance solution. r/a=10.0, $\varphi_i=\varphi=0.0$, and $\theta_i=\theta=0.0$.

Depending on the particular problem, extinction can be dominated by either scattering or absorption. When the refractive index is purely real, the absorption is zero.

As previously noted, Figure 4.1 depicts the resonant, or ripple, structure associated with the extinction coefficient. Note that the ripple structure generally becomes less pronounced as $a \to 0$, which is a consequence of the class 1 poles moving deeper into the left half-plane.

In Figure 4.10, it is shown how individual pole terms characterize specific resonance peaks in the extinction cross-section for the case a=0.03 m. Note that the first two peaks are due, respectively, to the first magnetic and the first electric oscillations as given in Table 4.2. The use of these two resonances (and their complex conjugates) is seen to be sufficient to describe the scattered field through approximately $k_o a=0.6$. It is also seen that by including the next higher electric and magnetic resonances from Table 4.2, the peaks around $k_o a=0.7$ and 0.85 are beginning to be characterized. Including the first three electric and magnetic resonances improves the convergence and is seen to give a fairly accurate fit of the "exact" solution through $k_o a=1.0$. Figure 4.11 depicts similar results for the case a=5 mm. Observe that the accuracy of the leading order pole approximation deteriorates as $a \to 0$, because of the dampening of strong resonance characteristics and also the breakdown of the simple pole approximation.

4.1.3 Observations on the Developed Expansions

The resonance expansions presented for the scattered field

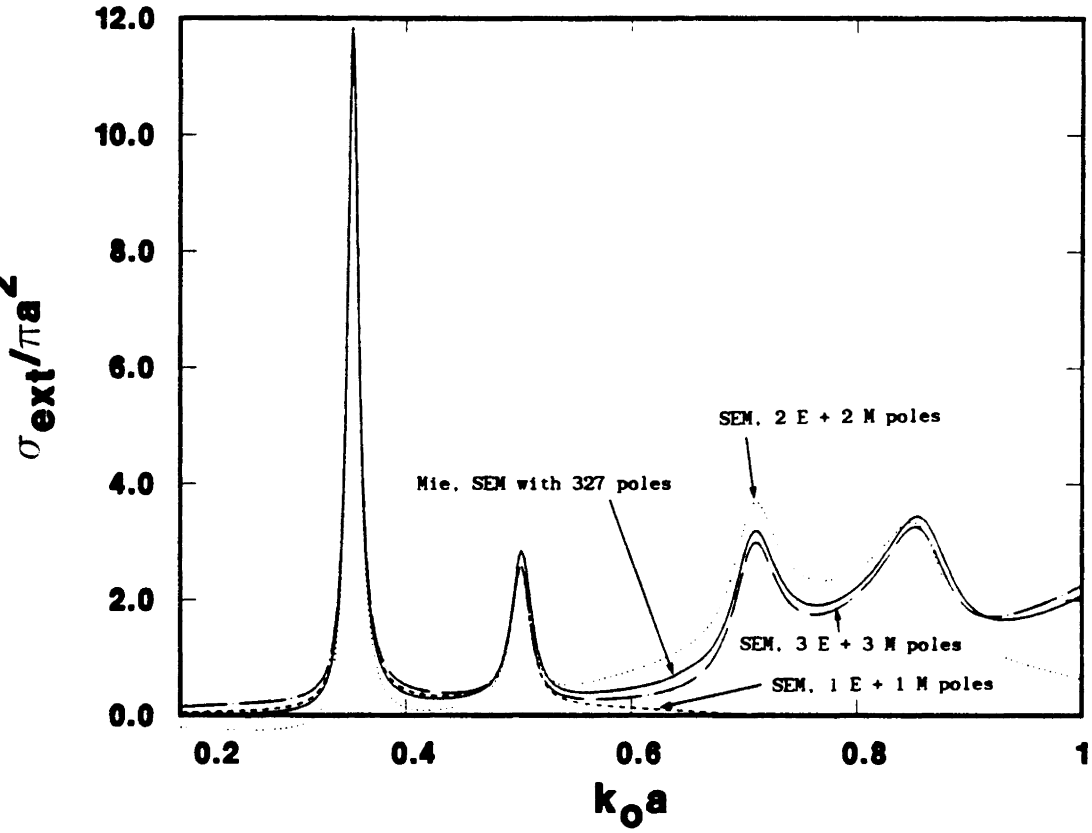

Figure 4.10: Extent to which the dominant SEM poles can be used to describe the extinction cross-section for the case a=30 mm. 1 E + 1 M is interpreted as the dominant n=1 electric pole and the dominant n=1 magnetic pole. The others are interpreted similarly.

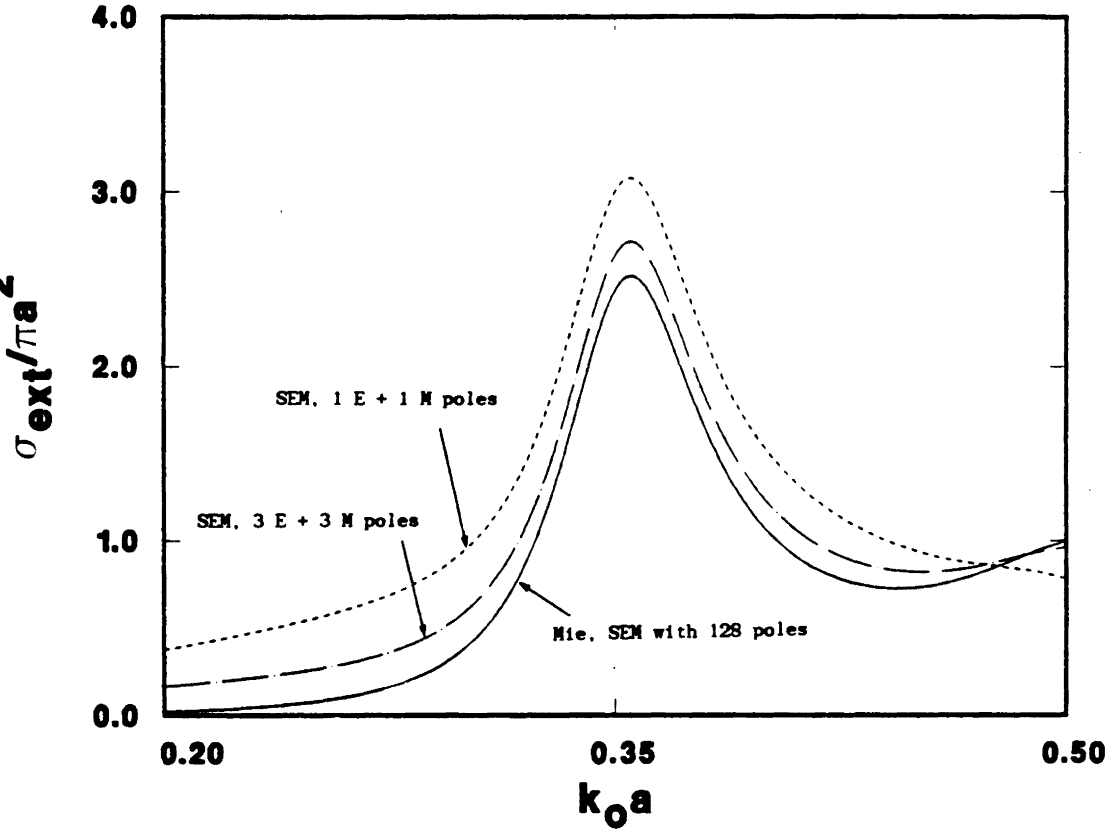

Figure 4.11: Extent to which the dominant SEM poles can be used to describe the extinction cross-section for the case a=5 mm. 1 E + 1 M is interpreted as the dominant n=1 electric pole and the dominant n=1 magnetic pole. 3 E + 3 M is interpreted similarly.

represent the most simple expansions possible in that they are simple in structure and are independent of an unknown additive entire function. However, use of Theorems 1 and 2 of Section 2.1 was possible only after a detailed analysis of the asymptotic behavior of potential candidates for expansion. Generally, unless one can cast the problem into a form such that the hypotheses of Theorems 1 or 2 are satisfied, one must be content with a resonance expansion which includes an unknown entire function as described in Section 2.2. An unfortunate consequence of recasting the problem, however, is that complicated functions which depend on s must generally be excluded from the expansion (this was conjectured to be the case from the general expansions of Section 2.2). Although this is somewhat unsatisfying, it is important to note that the obtained expansion is completely specified, valid for an arbitrary scattering angle, and characterizes the response in terms of the scatterer's resonances. In addition, an important feature of the presented expansions is that they do not seem to possess convergence problems with increasing frequency (previous attempts to reconstruct the scalar spherical scatterer using alternative expansions to the one used here have been found to possess convergence problems as $k_o a$ increases (Eftimiu and Huddleston, 1984)).

Theoretically, expansions (2.10) and (2.12) termwise exactly reconstruct a finite number of terms of the original separation of variables solution. Whether or not the exact reconstruction can be realized numerically depends on whether a finite or infinite collection of resonances are associated with each term to be expanded. As shown in Section 4.1.1, only an approximate numerical reconstruction for the

truncated Mie series for the electric field scattered by a dielectric sphere is possible. As also shown, the branch cut contribution associated with a frequency dependent refractive index is often negligible.

The resonance expansion form is useful for the extinction cross-section discussed in Section 4.1.2. This case is of particular importance for the multiple scattering application to be studied in Part II of this chapter. The reason for this can be summarized as follows. The extinction cross-section is dependent on the real portion of the scattering coefficients. The attenuation which results from propagation through a slab containing a discrete distribution of scatterers exhibits a decaying exponential behavior, with the argument of the exponential being related to the forward scattering coefficients of the obstacles in the ensemble. Thus, the real portion of this cross-section for a single sphere has direct implications on the attenuation of a wave propagating through the ensemble. In particular, the resonances of a single sphere will characterize attenuation due to the ensemble. When the spheres possess varying radii, the resonances will be decreased in amplitude and broadened in their frequency spectrum.

II. APPLICATION OF THE RESONANCE EXPANSIONS TO A SLAB CONTAINING A RANDOM DISTRIBUTION OF DIELECTRIC SPHERES

4.2.1 Resonance Scattering Tensor and Average Electric Field Expressions

In the far-scattering zone, the electric field scattered by a

single sphere is written as

$$\bar{E}^{sc} = \frac{e^{-\beta r/a}}{4\pi\, r} E_o \left\{ \hat{\theta}\, \tilde{E}_\theta^{sc} + \hat{\varphi}\, \tilde{E}_\varphi^{sc} \right\} \tag{4.15}$$

where, from (4.8) and (4.9),

$$\tilde{E}_\theta^{sc} \doteq j\, 4\pi a\, \mathcal{F}_\theta \tag{4.16}$$

and

$$\tilde{E}_\varphi^{sc} = j\, 4\pi a\, \mathcal{F}_\varphi \tag{4.17}$$

For application to a slab containing an ensemble of spheres, it is convenient to represent $\bar{E}^{sc}$ in terms of cartesian coordinates $(\hat{x},\hat{y},\hat{z})$. In addition, from Chapter III only the forward scattering direction is of interest; namely, $\theta=\theta_i$ and $\varphi=\varphi_i$. In terms of the cartesian coordinate system and the forward scattering restriction, $\bar{E}^{sc}$ has the following matrix representation:

$$\bar{E}^{sc} = \frac{e^{-\beta r/a}}{4\pi\, r} \begin{bmatrix} \hat{x}\hat{x}\, \tilde{E}_\theta^{sc} & 0 & 0 \\ 0 & \hat{y}\hat{y}\, \tilde{E}_\theta^{sc} & 0 \\ 0 & 0 & \hat{z}\hat{z}\, \tilde{E}_\theta^{sc} \end{bmatrix} \cdot \begin{bmatrix} \hat{x}\, E_x^i \\ \hat{y}\, E_y^i \\ \hat{z}\, E_z^i \end{bmatrix}$$

where $\bar{E}^i = \hat{\theta}_i\, E_o$ (cf. Section 4.1.1). The unit vectors generally will not appear in the matrix representation, they are included for emphasis.

Analogous to (2.20) and (2.21), the resonance scattering tensor is then

$$\bar{\bar{T}} = \begin{bmatrix} \hat{x}\hat{x}\,\tilde{E}_{\theta}^{sc} & 0 & 0 \\ 0 & \hat{y}\hat{y}\,\tilde{E}_{\theta}^{sc} & 0 \\ 0 & 0 & \hat{z}\hat{z}\,\tilde{E}_{\theta}^{sc} \end{bmatrix} \tag{4.18a}$$

Under the forward scattering restriction, $\tilde{E}_{\theta}^{sc}$ can be written in resonance form as

$$\tilde{E}_{\theta}^{sc} \doteq j\,2\pi a \sum_{n=1}^{N} (2n+1) \left[\Gamma_{bn}(-jm_2\beta) \left[R_{bn}(0) + \sum_{\alpha} R_{\alpha_{bn}} \left\{ \frac{1}{(\beta-\beta_{\alpha_{bn}})} + \frac{1}{\beta_{\alpha_{bn}}} \right\} \right] + \right.$$
$$\left. + \Gamma_{cn}(-jm_2\beta) \left[R_{cn}(0) + \sum_{\alpha} R_{\alpha_{cn}} \left\{ \frac{1}{(\beta-\beta_{\alpha_{cn}})} + \frac{1}{\beta_{\alpha_{cn}}} \right\} \right] \right] \tag{4.18b}$$

The reduction of the angular dependence follows from relations given in Appendix B. Although convergence is not quite as fast, the alternative form

$$\tilde{E}_{\theta}^{sc} = j\,2\pi a \sum_{n=1}^{N} (2n+1) \left[\Gamma_{bn}(-jm_2\beta) \sum_{\alpha} R_{\alpha_{bn}} \frac{1}{(\beta-\beta_{\alpha_{bn}})} + \Gamma_{cn}(-jm_2\beta) \sum_{\alpha} R_{\alpha_{cn}} \frac{1}{(\beta-\beta_{\alpha_{cn}})} \right] \tag{4.18c}$$

is valid, and, in fact, may be preferred because of its simpler structure. In both representations, the branch cut contribution has been neglected as discussed in Section 4.1.1.

For the case of normal incidence, $\theta=\theta_i=0$ with $\varphi=\varphi_i$, the scattering tensor can be written as

$$\bar{\bar{f}} = \begin{bmatrix} \hat{x}\hat{x}\,\tilde{E}_{\theta}^{sc} & 0 \\ 0 & \hat{y}\hat{y}\,\tilde{E}_{\theta}^{sc} \end{bmatrix} \tag{4.19}$$

It is not necessary to include a $\hat{z}\hat{z}$ term because this term will ultimately vanish due to the fact that $E_z^i \doteq 0$.

For the case $\varphi_i=\varphi=0$, but $\theta_i=\theta \neq 0$, the scattering tensor (4.18a) can similarly be written as

$$\bar{\bar{f}} = \begin{bmatrix} \hat{x}\hat{x}\,\tilde{E}_{\theta}^{sc} & 0 \\ 0 & \hat{z}\hat{z}\,\tilde{E}_{\theta}^{sc} \end{bmatrix} \tag{4.20}$$

In this case, it is not necessary to include a $\hat{y}\hat{y}$ term because this term will ultimately vanish since $E_y^i \doteq 0$.

Consider now multiple scattering by a slab with a uniform spatial distribution of identical spheres. The scattering tensor of interest is given by (3.13). For convenience, (3.13) is reproduced here

$$\bar{\bar{g}} = \frac{\sec\theta_i}{2\tau}\,\rho_o\,\bar{\bar{f}}(\hat{k}_{im},\hat{k}_{im};s)$$

It is important to note that since the scattering tensor for the sphere is a diagonal matrix, terms of the form $\exp(\bar{\bar{g}}z)$ which appear in (3.14)-(3.17) simply become matrices with exponentials on the diagonal. Specifically, for the case $\theta_i=\theta=0$, $0<z<d$, and a collection of identical spheres, $\langle\bar{E}^t(z)\rangle$ is given by

$$\langle \bar{E}^t(z) \rangle = \begin{bmatrix} \hat{x}\hat{x} \exp\left[\frac{\rho_o}{2\tau} \tilde{E}_\theta^{sc} z \right] & 0 \\ 0 & \hat{y}\hat{y} \exp\left[\frac{\rho_o}{2\tau} \tilde{E}_\theta^{sc} z \right] \end{bmatrix} \cdot \begin{bmatrix} \hat{x} \cos\varphi_i \\ \hat{y} \sin\varphi_i \end{bmatrix} E_o e^{-\beta z/a} \tag{4.21a}$$

In terms of the extinction cross-section, the representation becomes

$$\langle \bar{E}^t(z) \rangle = \begin{bmatrix} \hat{x}\hat{x} \exp\left[\frac{\rho_o}{2} [-\sigma_{ext} + j\mathrm{Im}(\tilde{E}_\theta^{sc}/\tau)] z \right] & 0 \\ 0 & \hat{y}\hat{y} \exp\left[\frac{\rho_o}{2} [-\sigma_{ext} + j\mathrm{Im}(\tilde{E}_\theta^{sc}/\tau)] z \right] \end{bmatrix} \cdot \begin{bmatrix} \hat{x} \cos\varphi_i \\ \hat{y} \sin\varphi_i \end{bmatrix} E_o e^{-\beta z/a} \tag{4.21b}$$

Equation (4.21b) shows clearly that the extinction cross-section determines the attenuation through the slab.

For the case $\varphi_i = \varphi = 0$, but $\theta_i = \theta \neq 0$, the average scattered field within the slab is given by (3.14) with $\bar{\bar{F}}$ given by (4.20).

For the case when the distribution of the spheres is spatially uniform, but the radius of the spheres is slightly varying, it is necessary to integrate over the radial variations of $\bar{\bar{g}}$ as given by (3.18). Only the dominant (class 1) natural oscillations will be considered here, and approximation (4.9b) is sufficient for characterizing these resonance locations. Approximations to the dominant natural electric oscillations of the mth scatterer are given directly by (4.9b). Approximations to the magnetic oscillations are also given by (4.9b), but with $j_{n\alpha}$ replaced by $j_{(n-1)\alpha}$.

The radii of the spheres are assumed to be uniformly distributed between a_ℓ and a_u, with a_ℓ and a_u conforming to the constraint governing

the validity of (4.9b) and are not widely separated as implied by Section 3.3. For each n and each α of interest, "average" dominant electric resonances of the ensemble are given approximately by the closed form expression

$$\langle \beta_{\alpha_{bn_m}}(a_m) \rangle \doteq \frac{1}{(a_u - a_\ell)} \int_{a_\ell}^{a_u} da_m \, \beta_{\alpha_{bn_m}}(a_m) =$$

$$\frac{1}{(a_u - a_\ell)} \left\{ -j_{n\alpha}^2 \frac{\upsilon}{2\epsilon_d} c \ln(a_u/a_\ell) \pm j \, j_{n\alpha} \frac{1}{\sqrt{\epsilon_d}} \left[(a_u - a_\ell) - j_{n\alpha}^2 \frac{\upsilon^2}{8\epsilon_d} c^2 \left(\frac{1}{a_\ell} - \frac{1}{a_u} \right) \right] \right\} \tag{4.22}$$

Approximations to the average dominant magnetic resonances are obtained by replacing $j_{n\alpha}$ by $j_{(n-1)\alpha}$. The values for ϵ_d and υ are recalled to be 77.5 and $0.8 \cdot 10^{-11}$, respectively. The region of validity of (4.22) is restated to be $j_{n\alpha}^2/a^2 \ll 1 \cdot 10^8$.

To average $\bar{\bar{g}}$ over the radial variations, the following integrals, corresponding to resonance expansion form (4.18c), must be evaluated for each n and each α of interest:

$$\frac{1}{(a_u - a_\ell)} \int_{a_\ell}^{a_u} da_m \, a_m^2 \, \Gamma_{bn}(-jm_2(a_m)\,\beta) \, R_{\alpha_{bn_m}}(a_m; \beta_{\alpha_{bn_m}}(a_m)) \frac{1}{(\beta - \beta_{\alpha_{bn_m}}(a_m))}$$

$$\frac{1}{(a_u - a_\ell)} \int_{a_\ell}^{a_u} da_m \, a_m^2 \, \Gamma_{cn}(-jm_2(a_m)\,\beta) \, R_{\alpha_{cn_m}}(a_m; \beta_{\alpha_{cn_m}}(a_m)) \frac{1}{(\beta - \beta_{\alpha_{cn_m}}(a_m))}$$

Similar integrals must be evaluated if resonance form (4.18b) is used.

The integrands are sufficiently complicated that numerical evaluation is required to obtain high accuracy. However, a suitable approximation can be obtained by performing the following: (1) Use the average resonances described by (4.22) to calculate corresponding average residues, and (2) Set $a_m=(a_u+a_\ell)/2$ and evaluate $a_m^2\,\Gamma_{bn}(-jm_2(a_m)\,\beta)$ and $a_m^2\,\Gamma_{cn}(-jm_2(a_m)\beta)$.

4.2.2 Attenuation Expressions for the Coherent Intensity and Numerical Results

Expressions and results are presented in this section which depict the following for the coherent intensity: (1) Attenuation of a normally incident due to dominant slab resonances for the case of a distribution of identical spheres, and also for a distribution of spheres with varying radii, and (2) Incident angle dependence associated with (1).

(1) Normal Incidence.

Let $\theta_i=\varphi_i=\theta=\varphi=0$, and restrict n=1 and $\alpha=1$. Using resonance form (4.18c), the attenuation of the average electric field within a slab containing a distribution of identical spheres of radius a is found from (4.21a) to be given by

$$-20\,\log_{10}\left\{\exp\left[\rho_o\, z\,\mathrm{Re}\left\{ j\,\frac{3\pi a^2}{\beta}\left[\Gamma_{b1}(-jm_2\beta)\left[R_{1_{b1}}\,\frac{1}{(\beta-\beta_{1_{b1}})}-R^*_{1_{b1}}\,\frac{1}{(\beta-\beta^*_{1_{b1}})}\right]+\Gamma_{c1}(-jm_2\beta)\left[R_{1_{c1}}\,\frac{1}{(\beta-\beta_{1_{c1}})}-R^*_{1_{c1}}\,\frac{1}{(\beta-\beta^*_{1_{c1}})}\right]\right]\right\}\right]\right\} \quad (4.23)$$

Expression (4.23) is valid for $z \leq d$, $a \geq 5mm$, and $k_o a < 0.6$.

Now let the radii of the spheres within the slab be uniformly distributed between a_ℓ and a_u. The attenuation attributed to the average leading order resonances of the ensemble is given by

$$-20 \log_{10} \left\{ \exp \left[\frac{\rho_o z}{(a_u - a_\ell)} \operatorname{Re} \left\{ \int_{a_\ell}^{a_u} da_m \, j \frac{3\pi a_m^2}{\beta} \left[\Gamma_{b1}(-jm_2\beta) \left[R_{1_{b1}}(a_m) \frac{1}{(\beta - \beta_{1_{b1}})} - R^*_{1_{b1}}(a_m) \frac{1}{(\beta - \beta^*_{1_{b1}})} \right] + \Gamma_{c1}(-jm_2\beta) \left[R_{1_{c1}}(a_m) \frac{1}{(\beta - \beta_{1_{c1}})} - R^*_{1_{c1}}(a_m) \frac{1}{(\beta - \beta^*_{1_{c1}})} \right] \right] \right\} \right] \right\} \tag{4.24}$$

which is valid for $z \leq d$, $(a_u + a_\ell)/2 \geq 5mm$, and $k_o(a_u + a_\ell)/2 < 0.6$. To simplify the integral evaluation, approximations discussed in Section 4.2.1 can be used.

(2) Oblique Incidence.

For $\varphi_i = \varphi = 0$, $\theta_i = \theta \neq 0$, and $z \leq d$, the solution for $\langle \bar{E}^t \rangle$ is given by (3.14). From (3.14), it follows that the attenuation is given by

$$-20 \log_{10} \left\{ \left| \exp \left[\frac{\sec\theta_i}{2\tau} \rho_o z \tilde{E}^{sc}_\theta \right] + \frac{\tau (\cos\theta_i - 1)}{\frac{\sec\theta_i}{2\tau} \rho_o \tilde{E}^{sc}_\theta + \tau(\cos\theta_i - 1)} * \right. \right.$$
$$\left. \left. * \left\{ \exp \left[-\tau z (\cos\theta_i - 1) \right] - \exp \left[\frac{\sec\theta_i}{2\tau} \rho_o z \tilde{E}^{sc}_\theta \right] \right\} \right| \right\} \tag{4.25}$$

For n=1 and $\alpha=1$, $\tilde{E}^{sc}_\theta$ can be written in leading order resonance form as

$$\tilde{E}_{\theta}^{sc} = j\,6\pi a \left\{ \Gamma_{b1}(-jm_2\beta) \left[R_{1_{b1}} \frac{\beta}{\beta_{1_{b1}}(\beta-\beta_{1_{b1}})} - R^{*}_{1_{b1}} \frac{\beta}{\beta^{*}_{1_{b1}}(\beta-\beta^{*}_{1_{b1}})} + R_{bn}(0) \right] + \right.$$

$$\left. + \Gamma_{cn}(-jm_2\beta) \left[R_{1_{c1}} \frac{\beta}{\beta_{1_{c1}}(\beta-\beta_{1_{c1}})} - R^{*}_{1_{c1}} \frac{\beta}{\beta^{*}_{1_{c1}}(\beta-\beta^{*}_{1_{c1}})} + R_{cn}(0) \right] \right\} \tag{4.26}$$

Expressions (4.25) and (4.26) are valid for $z \lesssim d$, $a \gtrsim 5mm$, $k_o a < 0.6$, and θ_i less than, say, 10 degrees.

For the case of an ensemble of spheres with varying radii, (4.25) is also valid, but with $\tilde{E}_{\theta}^{sc}$ replaced by

$$\frac{1}{(a_u - a_\ell)} \int_{a_\ell}^{a_u} da_m \, \tilde{E}_{\theta}^{sc}(a_m)$$

Figures 4.12–4.15 compare the accuracy of these resonance form solutions for the attenuation of the coherent intensity with the exact Mie series solution.

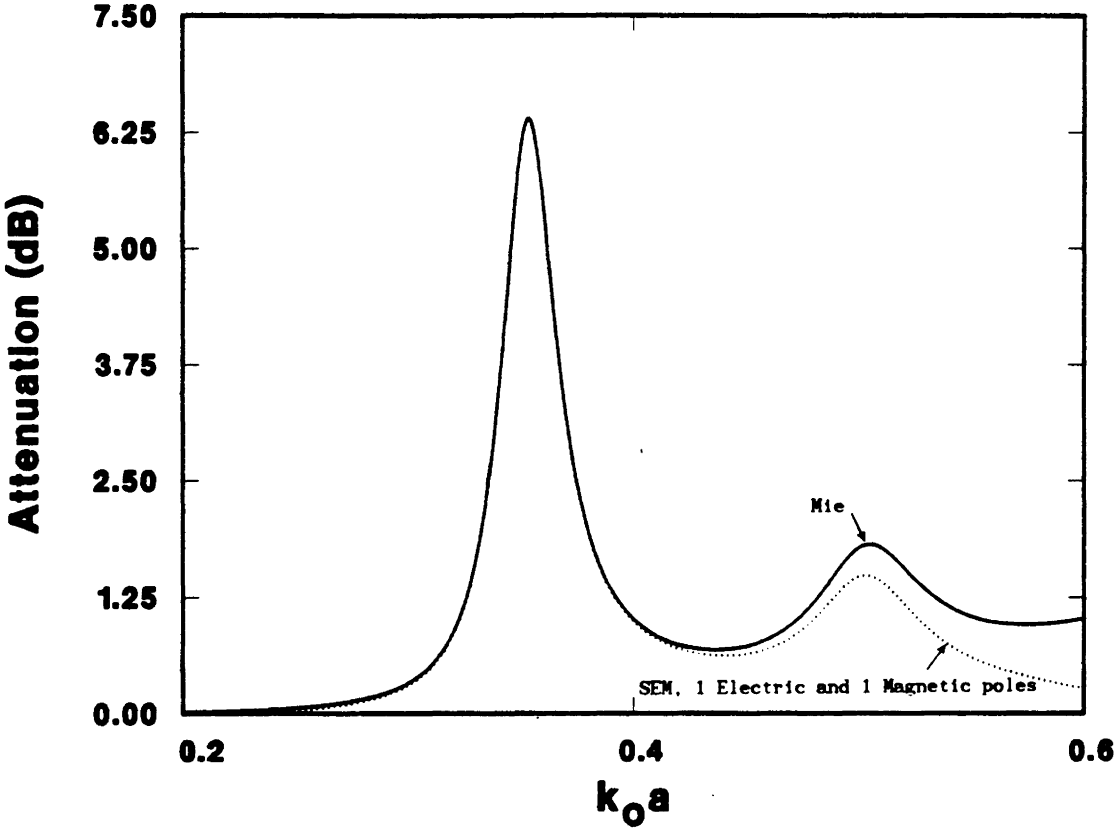

Figure 4.12: Extent to which dominant SEM poles can be used to describe the attenuation through a slab of identical spherical water droplets of radius a=10 mm for the case of normal incidence. ρ_o=1000/m^3, z=1 meter.

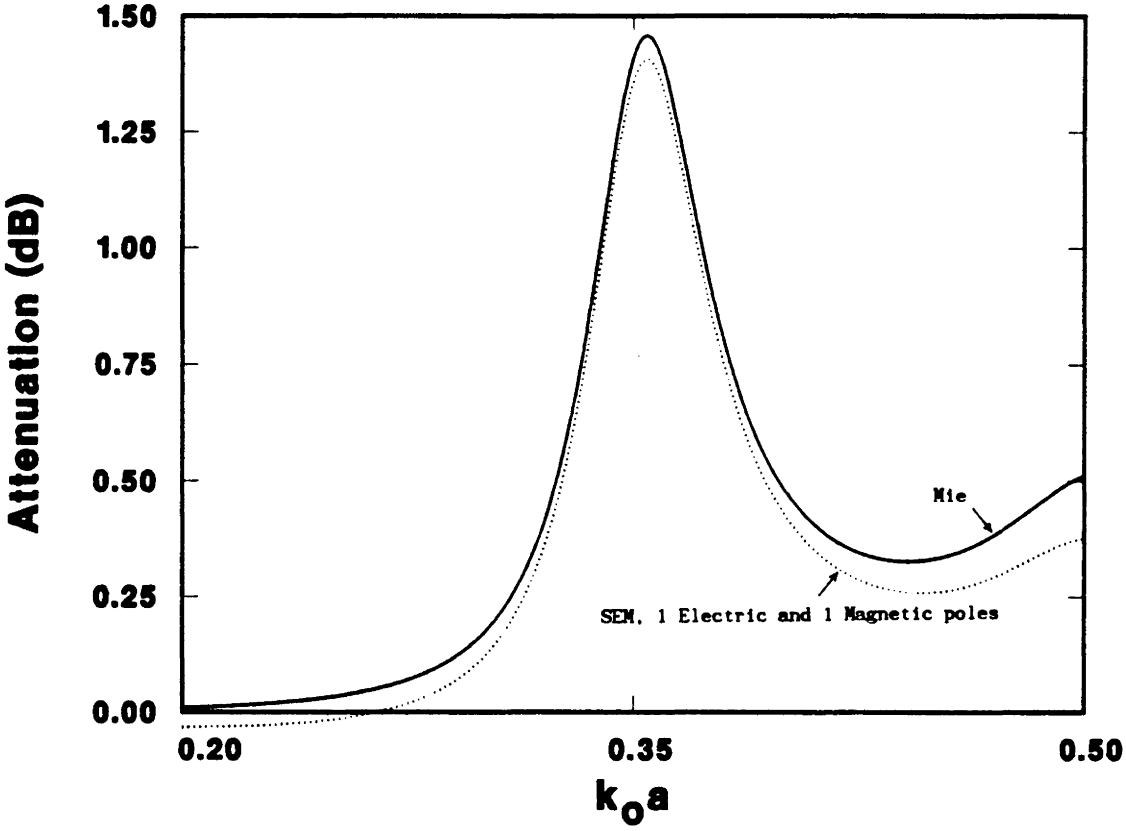

Figure 4.13: Extent to which dominant SEM poles can be used to describe the attenuation through a slab of spherical water droplets with radii which vary between 4 mm and 8 mm for the case of normal incidence. $\rho_o=1000/m^3$, z=1 meter.

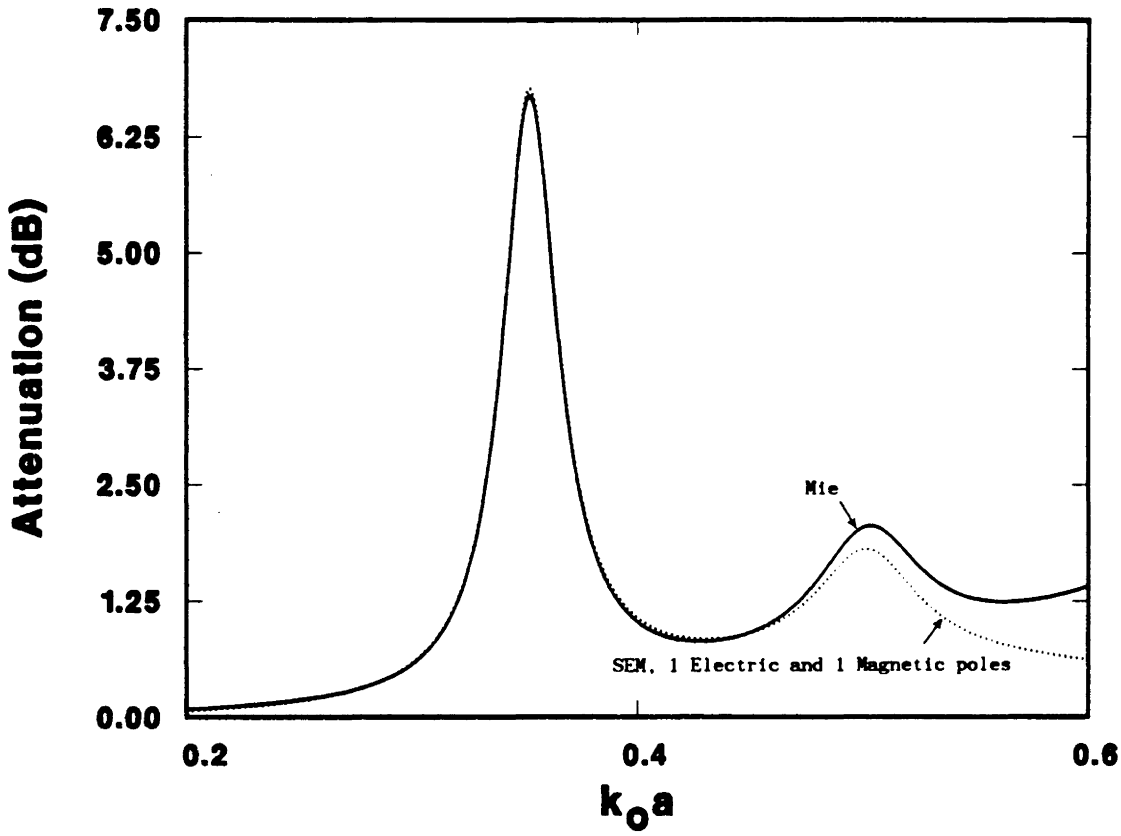

Figure 4.14: Extent to which dominant SEM poles can be used to describe the attenuation through a slab of identical spherical water droplets of radius a=10 mm for the case of oblique incidence at θ_i=6 degrees. ρ_o=1000/m^3, z=1 meter.

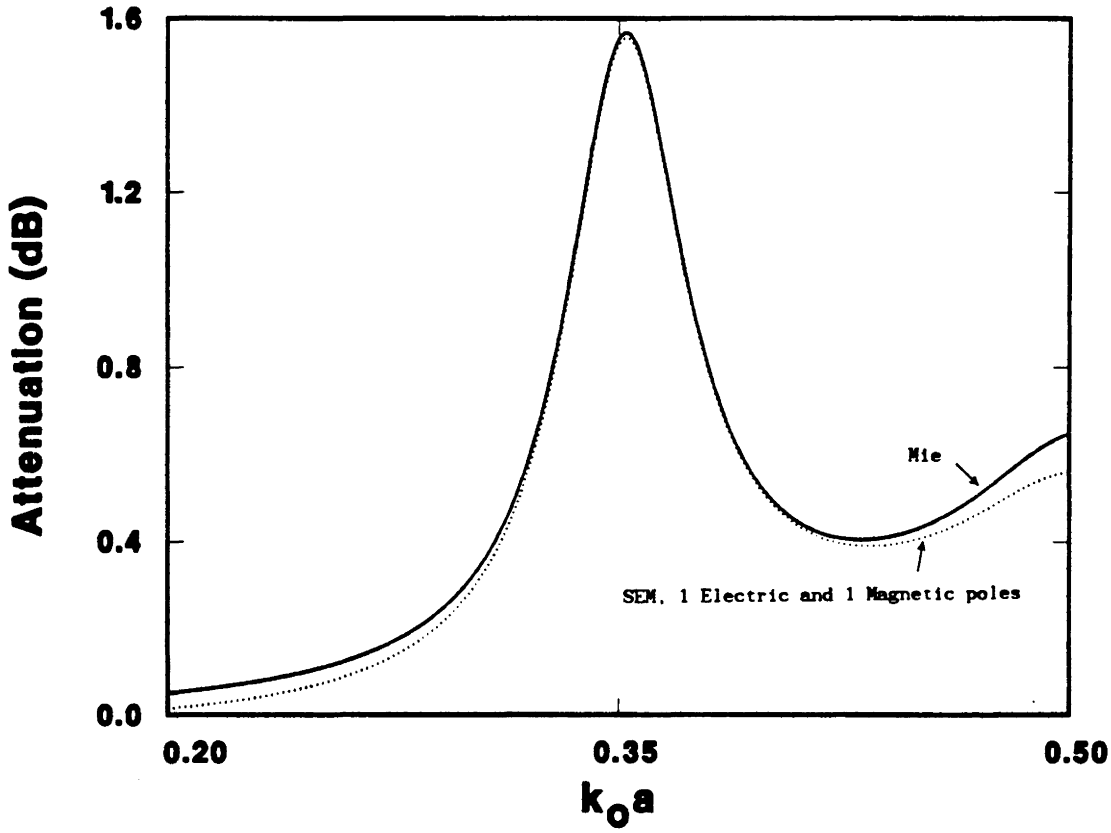

Figure 4.15: Extent to which dominant SEM poles can be used to describe the attenuation through a slab of spherical water droplets with radii which vary between 4 mm and 8 mm for the case of oblique incidence at θ_i=6 degrees. ρ_o=1000/m^3, z=1 meter.

CHAPTER V

CONCLUDING REMARKS, LIMITATIONS, AND RECOMMENDATIONS FOR FUTURE STUDIES

A general summary of major results and contributions contained within this thesis follows. The classical theory of multiple scattering and the singularity expansion method were merged to introduce a general theory for modeling resonance phenomena associated with a discrete distribution of scatterers. General resonance expansions for the field scattered by a single dielectric obstacle were derived under a simple pole assumption (an assumption which is not necessarily valid for arbitrary dielectric scatterers). A resonance scattering tensor for the far-scattered field was subsequently introduced. The resonance scattering tensor was then used within the framework of Twersky's multiple scattering theory and an integral equation was derived for the coherent electric field intensity. Application of this integral equation to the case of a plane-wave obliquely incident on a slab containing a random distribution of dielectric obstacles was then made for two cases: (1) an identical collection of particles, and (2) a collection of particles with varying radii. A modified resonance scattering tensor was generated to accommodate the case of varying radii due to the dependence of resonance locations on particulate radii; the concept of "average" resonances was subsequently introduced. From the solution of the multiple scattering integral equation specialized to the slab geometry,

the influence of slab resonances on attenuating and depolarizing the incident wave was clearly indicated. A specific numerical application was finally made to the case of a slab geometry filled with a random distribution of lossy dielectric spheres. Resonance trajectories as a function of a frequency-dependent complex refractive index, as well as an accurate resonance expansion for the scattered field, and a resonance scattering tensor were introduced. The resonance scattering tensor was finally used in conjunction with the multiple scattering results to graphically demonstrate attenuation locally to slab resonances.

The proposed theory provides an alternative representation of a discrete multiple scattering problem and is of computational utility when strong resonance features of a multiple scattering environment are clearly visible. For resonances to be visible it is generally required that the particles in the ensemble are very similar in size and composition. As was demonstrated for the case of an ensemble of homogeneous dielectric spheres with a refractive index based on the Debye relaxation model, strong resonances can indeed be visible, and concise approximate expressions for the attenuation based on the dominant resonances were shown to be valid over a reasonably broad frequency spectrum. Unfortunately, such idealized ensembles which only contain perfect spheres are generally not observed in practice. Most realistic ensembles, for example rain or atmospheric aerosols, are composed of diversified particles which tend to obscure, if not obliterate, resonance features. Thus, the practical utility of the method is limited.

A further limitation with the applicability of the method is that it is very difficult, in general, to accurately determine the location of

the resonances for general dielectric obstacles. When a series solution for the obstacle exists, it is possible to find these locations; however, even in this case it can be quite difficult to track them. One is generally limited to the frequency spectrum define by $k_o \ell < 10$, where ℓ represents a characteristic length associated with an obstacle. In this thesis, the resonances of the homogeneous dielectric sphere were studied in detail. Further separable problems which would be of interest for application of the theory would be a layered dielectric sphere, and prolate and oblate dielectric spheroids.

From a theoretical mathematical viewpoint, a great deal of research needs to be done to provide a sound basis for much of the material discussed in Chapter II. Significant progress has been made along this direction for perfectly conducting scatterers, but little is available for the more complicated dielectric problem.

REFERENCES

Abramowitz, M., and Stegun, I. A., *Handbook of Mathematical Functions*, Ninth Printing, Dover, New York, 1964.

Arfken, G., *Mathematical Methods for Physicists*, pp.366-369, Academic Press, New York, 1970.

Baum, C. E., "On the singularity expansion method for the solution of electromagnetic interaction problems," *AFWL Interaction Notes*, Note 88, Dec. 1971.

Baum, C. E.,"The singularity expansion method," in *Transient Electromagnetic Fields*, Ed. Felsen, L. B., Springer-Verlag, New York, 1976.

Bleistein, N., and Handelsman, R. A., *Asymptotic Expansion of Integrals*, pp.340-347, Holt, Rinehart and Winston, 1975.

Bohren, C. F., and Huffman, D. R., *Absorption and Scattering of Light by Small Particles*, Wiley, New York, 1983.

Cordaro, J. T., and Davis, W. A., "Time-domain techniques in the singularity expansion method," *IEEE Trans. Ant. Prop.*, AP-29, p. 543, May, 1981.

Davis, W. A., and Riley, D. J., "Time domain techniques in the singularity expansion method," Air Force Weapons Lab, AFWL-TR-82-156, 1983.

de Wolf, D. A., "Electromagnetic reflection from an extended turbulent medium: cumulative forward-scatter single-backscatter approximation," *IEEE Trans. Ant. Prop.*, AP-19, pp.254-262, 1971.

Eftimiu, C., and Huddleston, P. L., "Reconstruction of a spherical scatterer from its natural frequencies," *IEEE Trans. Ant. Prop.*, AP-32, pp.694-698, July 1984.

Felsen, L. B., "Comments on early time SEM," *IEEE Trans. Ant. Prop.*, AP-33, pp.118-119, Jan., 1985.

Foldy, L. L., "The multiple scattering of waves," *Physics Rev.*, 67, pp. 107-121, 1945.

Gastine, M., Courtois, L., Dormann, J. L., "Electromagnetic Resonances of Free Dielectric Spheres," *IEEE Trans. Microwave Theory and Tech.*, MTT-15, pp.694-700, Dec. 1967.

Harrington, R. F., *Time-Harmonic Electromagnetic Fields*, McGraw-Hill, 1961.

Hochstadt, H., *Integral Equations*, pp.37-43, Wiley, New York, 1973.

Inada, H., and Plonus, M. A., "The diffracted field contribution to the scattering from a large dense dielectric sphere," *IEEE Trans. Ant. Prop.*, AP-18, pp.649-660, Sept. 1970.

Ishimaru, A., *Wave Propagation and Scattering in Random Media*, Vol. 2, pp.253-294, Academic Press, 1978.

Jackson, J. D., *Classical Electrodynamics*, 2nd Edition, Wiley, New York, pp. 314-316, 1975.

Landau, E., *Worlesungen uber Zahlentheorie*, Vol. 2, Leipzig, 1927.

Lax, M., "Multiple scattering of waves," *Rev. Mod. Physics*, 23, pp.287-310, 1951.

Liebe, H. J., and Gimmestead, G. G., "Calculation of clear air refractivity," *Radio Science*, 13, pp.245-251, 1978.

Marin, L., "Natural-mode representation of transient scattered fields," *IEEE Trans. Ant. Prop.*, AP-21, pp.809-818, Nov. 1973.

Marin, L., "Natural-mode representation of transient scattering from rotationally symmetric bodies," *IEEE Trans. Ant. Prop.*, AP-22, pp. 266-274, March 1974.

Markushevich, A. I., *Theory of Functions of a Complex Variable, Vol. II*, pp. 297-304, Prentice-Hall, New Jersey, 1965.

Mie, G., "Beitrage zur Optik truber Medien speziell kolloidaler Metallosungen," *Ann. Phys.*, 25, pp.377-445, 1908.

Morgan, M. A., "Singularity expansion representations of fields and currents in transient scattering," *IEEE Trans. Ant. Prop.*, AP-32, pp.466-473, May, 1984.

Morse, P. M., and Feshbach, H., *Methods of Theoretical Physics*, McGraw-Hill, New York, 1953.

Muller, D. E., "A method for solving algebraic equations using an automatic computer," *MTAC*, 10, pg.208, 1956.

Nussenzveig, H. M., "High-frequency scattering by a transparent sphere. I. Direct reflection and transmission," *J. Math. Phys.*, 10, pp.82-124, Jan., 1969.

Pearson, L. W., and Mittra, R., "The singularity expansion representation of the transient electromagnetic coupling through a rectangular aperture," *AFWL Interaction Notes*, Note 296, June 1976.

Pearson, L. W., "Evidence that bears on the left half plane asymptotic behavior of the SEM expansion of surface currents," *Electromagnetics*, 1, pp.395-402, Dec. 1981.

Pearson, L. W., Wilton, D. R., and Mittra, R., "Some implications of Laplace transform inversion on SEM coupling coefficients in the time domain," *Electromagnetics*, 2, pp.181-200, 1982.

Poggio, A. J., and Miller, E. K., "Integral equation solutions for three-dimensional scattering problems," in *Computer Techniques for Electromagnetics*, Ed. Mittra, R., Pergamon Press, New York, 1973.

Ramm, A. G., "On the basis property for the root vectors of some Nonselfadjoint operators," *J. Math. Anal. Appl.*, 80, pp.57-66, 1981.

Ramm, A. G., "Mathematical foundations of the singularity and eigenmode expansion methods (SEM and EEM)," *J. Math. Anal. Appl.*, 86, pp.562-591, 1982.

Riley, D. J., "A simple and accurate resonance expansion for the electromagnetic field scattering by a lossy dielectric sphere," *IEEE Trans. Ant. Prop.*, AP-34, pp. 737-741, May, 1986.

Stakgold, I., *Green's Functions and Boundary Value Problems*, Wiley, New York, 1979.

Spiegel, M. R., *Complex Variables*, Schaum's Outline Series, McGraw-Hill, New York, pp. 191-192, 1964.

Straiton, A. W., "The absorption and reradiation of radio waves by oxygen and water vapor in the atmosphere," *IEEE Trans. Ant. Prop.*, pp.595-597, July, 1975.

Stratton, J. A., *Electromagnetic Theory*, McGraw-Hill, New York, 1941.

Tesche, F. M., "On the singularity expansion method as applied to electromagnetic scattering from thin-wires," *IEEE Trans. Ant. Prop.*, AP-21, Jan. 1973.

Tsang, L., and Kong, J. A., "Scattering of electromagnetic waves from a half space of densely distributed dielectric scatterers," *Radio Science*, 18, pp.1260-1272, Nov. 1983.

Tsolakis, A., and Stutzman, W. L., "Multiple scattering of electromagnetic waves by rain," *Radio Science*, 17, pp.1495-1502, Nov. 1982.

Tsolakis, A. I., *Multiple scattering of electromagnetic waves by distributions of particles with applications to radio wave propagation through precipitation*, Ph.D. thesis under I. M. Besieris, Virginia Polytechnic Institute and State University, Blacksburg, Virginia, 1982.

Tsolakis, A. I., Besieris, I. M., and Kohler, W. E., "Two-frequency radiative transfer equation for scalar waves in a random distribution of discrete scatterers with pair correlations," *Radio Science*, 20, pp. 1037-1052, Sept. 1985.

Twersky, V., "Transparency of pair-correlated, random distributions of small scatterers, with applications to the cornea," *J. Opt. Soc. Am.*, 75, pp.524-530, 1975.

Twersky, V., "Multiple scattering of waves by periodic and by random distributions," in *Electromagnetic Scattering*, Ed. Uslenghi, P.L.E., pp.221-251, Academic Press, New York, 1978.

Van Bladel, J., "Some remarks on Green's dyadic for infinite space," *IRE Trans. Ant. Prop.*, 9, pp.563-566, Nov. 1961.

Van Bladel, J., *Electromagnetic Fields*, McGraw-Hill, New York, 1964.

Varadan, V. K., Ma, Y., and Varadan, V. V., "Coherent electromagnetic wave propagation through randomly distributed and oriented pair-correlated dielectric scatterers," *Radio Science*, 19, pp.1445-1449, Nov. 1984.

Watson, G. N., "The diffraction of electric waves by the earth," *Proc. Roy. Soc. London*, 95, pp.83-99, 1918.

APPENDIX A

STATIONARY PHASE EVALUATION

Equation (3.10) is derived in this appendix using the method of stationary phase for multiple integrals. It has been shown (see, for example, Bleistein and Handelsman, 1975, or Ishimaru, 1978) that an integral of the form

$$I = \int_{-\infty}^{\infty} dx_m \int_{-\infty}^{\infty} dy_m \; C(x_m, y_m) \; e^{-j\alpha \; f(x_m, y_m)}$$

has the first-order stationary phase evaluation given by

$$I = \frac{2\pi}{\alpha} e^{-j\pi/2} \; C(x_{ms}, y_{ms}) \; e^{-j\alpha \; f(x_{ms}, y_{ms})} \left\{ \frac{\partial^2}{\partial x_m^2} f(x_{ms}, y_{ms}) \; \frac{\partial^2}{\partial y_m^2} f(x_{ms}, y_{ms}) - \left[\frac{\partial^2}{\partial x_m \partial y_m} f(x_{ms}, y_{ms}) \right]^2 \right\} + o(1/\alpha) \qquad \text{(A1)}$$

where x_{ms}, y_{ms} denote the stationary phase points which satisfy the following:

$$x_{ms}: \; \frac{\partial}{\partial x_m} f(x_m, y_m) = 0 \; ; \quad y_{ms}: \; \frac{\partial}{\partial y_m} f(x_m, y_m) = 0$$

Formula (A1) is now applied to the integral

$$I = \int_{-\infty}^{\infty} dx_m \int_{-\infty}^{\infty} dy_m \; \bar{f}(\hat{R}_{am}, \hat{k}_{im}; s) \cdot \bar{A}(x_m, z_m; s) \; \frac{e^{-jk[\,|\bar{r}_a - \bar{r}_m| + x_m \sin\theta_i\,]}}{4\pi\,|\bar{r}_a - \bar{r}_m|}$$

For this case, $f(x_m, y_m) = |\bar{r}_a - \bar{r}_m| + x_m \sin\theta_i$.

The stationary phase points are determined from

$$\frac{\partial}{\partial y_m}\left[\,|\bar{r}_a - \bar{r}_m| + x_m \sin\theta_i\,\right] = -\frac{(y_a - y_m)}{|\bar{r}_a - \bar{r}_m|} = 0 \qquad \text{(A2)}$$

$$\frac{\partial}{\partial x_m}\left[\,|\bar{r}_a - \bar{r}_m| + x_m \sin\theta_i\,\right] = \sin\theta_i - \frac{(x_a - x_m)}{|\bar{r}_a - \bar{r}_m|} = 0 \qquad \text{(A3)}$$

Equation (A2) implies $y_{ms} = y_a$. (A3) implies $x_{ms} = x_a - [(y_a - y_m)^2 + (z_a - z_m)^2]^{1/2} \tan\theta_i$.

The various derivatives of f are given by

$$\frac{\partial^2}{\partial x_m^2} f(x_{ms}, y_{ms}) = \frac{1}{|z_a - z_m| \sec\theta_i} \cos^2\theta_i$$

$$\frac{\partial^2}{\partial y_m^2} f(x_{ms}, y_{ms}) = \frac{1}{|z_a - z_m| \sec\theta_i}$$

$$\frac{\partial^2}{\partial x_m \partial y_m} f(x_{ms}, y_{ms}) = 0$$

Therefore,

$$\frac{\partial^2}{\partial x_m^2} f(x_{ms},y_{ms}) \frac{\partial^2}{\partial y_m^2} f(x_{ms},y_{ms}) - \left[\frac{\partial^2}{\partial x_m \partial y_m} f(x_{ms},y_{ms}) \right]^2 = |z_a - z_m| \sec^2\theta_i$$

Since

$$f(x_{ms},y_{ms}) = x_a \sin\theta_i + |z_a - z_m|$$

and

$$\hat{R}_{am}\Big|_{\text{Stationary Phase Points}} = \frac{\hat{x}\,|z_a-z_m|\,\tan\theta_i + \hat{z}\,(z_a-z_m)}{|z_a-z_m|\,\sec\theta_i} = \hat{x}\,\sin\theta_i + \hat{z}\,\text{sgn}(z_a-z_m)\,\cos\theta_i$$

it follows that

$$I = \frac{\sec\theta_i}{2k} e^{-j\pi/2} e^{-jk[x_a\sin\theta_i + |z_a-z_m|]} \bar{f}(\hat{x}\,\sin\theta_i + \hat{z}\,\text{sgn}(z_a-z_m)\cos\theta_i, \hat{k}_{im}; s) \cdot$$

$$\cdot\, \bar{A}(x_a - |z_a-z_m|\tan\theta_i, z_m; s) + o(1/k)$$

Letting $jk=s/c=\tau$ yields (3.10).

APPENDIX B

MIE SERIES SOLUTION FOR THE FIELD SCATTERED BY PERFECTLY CONDUCTING AND DIELECTRIC SPHERES

A brief derivation of the Mie series (4.1) is presented in this appendix since it is somewhat non-standard. An incident plane-wave propagating in the $\hat{r}_i \doteq \hat{k}_i$ direction relative to a standard polar coordinate system is assumed. The geometry is shown in Figure 4.2.

The incident electric field is given by

$$\bar{E}^i = \hat{\theta}_i \, E_o \, e^{-jk_o r \cos\gamma} \tag{B1}$$

where $\cos\gamma = \cos\theta\cos\theta_i + \sin\theta\sin\theta_i\cos(\varphi-\varphi_i)$, and

$$\begin{aligned}\hat{\theta}_i = {} & \hat{r}\,(\sin\theta\cos\theta_i\cos(\varphi-\varphi_i) - \cos\theta\sin\theta_i) + \\ & \hat{\theta}\,(\cos\theta\cos\theta_i\cos(\varphi-\varphi_i) + \sin\theta\sin\theta_i) - \\ & \hat{\varphi}\,\cos\theta_i\sin(\varphi-\varphi_i)\end{aligned}$$

A spherical decomposition of (B1) is given by (Stratton, 1941)

$$\bar{E}^i = \hat{\theta}_i \, E_o \sum_{n=0}^{\infty} (-j)^n \, (2n+1) \, j_n(kr) \, \chi_n(\theta,\varphi;\theta_i,\varphi_i) \tag{B2}$$

where

$$\chi_n \doteq \sum_{m=0}^{n} \varepsilon_m \frac{(n-m)!}{(n+m)!} P_n^m(\cos\theta) P_n^m(\cos\theta_i) \cos m(\varphi-\varphi_i),$$

with $\ell_0 = 1$, and $\ell_m = 2$ for $m \geq 1$. In (B2), j_n denotes the spherical Bessel function of the first kind, and P_n^m represents the associated Legendre polynomials defined by

$$P_n^m(x) = (-1)^m \, (1-x^2)^{m/2} \, \frac{d^m}{dx^m} \, P_n^o(x)$$

A useful differential identity is the following (Stratton, 1941)

$$\frac{\partial}{\partial\theta} P_n^m(\cos\theta) = -\frac{1}{2} \left[(n-m+1)(n+m) \, P_n^{m-1} - P_n^{m+1} \right] \tag{B3}$$

Additional properties can be found in Abramowitz and Stegun, (1964).

The incident magnetic field is given by

$$\bar{H}^i = \hat{\varphi}_i \, \frac{E_o}{\eta_o} \, e^{-jk_o r \cos\gamma}$$

where $\hat{\varphi}_i = \hat{r} \, \sin\theta\sin(\varphi-\varphi_i) + \hat{\theta} \, \cos\theta\sin(\varphi-\varphi_i) + \hat{\varphi} \, \cos(\varphi-\varphi_i)$, and η_o denotes the impedance of free-space. The spherical decompostion of $\bar{H}^i$ is similar to (B2).

To derive an expression for the scattered field, it is convenient to follow the standard technique of decomposing the fields into TM and TE components relative to $\hat{r}$ magnetic and electric potentials (Debye potentials) (see, for example, Harrington, 1961). Let $\hat{r} \, A_r$ represent the magnetic vector potential, and $\hat{r} \, F_r$ represent the electric vector potential. Relative to these potentials, all field components are found from (Harrington, 1961)

$$E_r = \frac{1}{j\omega\epsilon}\left[\frac{\partial^2}{\partial r^2} + k^2\right] A_r$$

$$E_\theta = -\frac{1}{r\sin\theta}\frac{\partial}{\partial\varphi}F_r + \frac{1}{j\omega\epsilon}\frac{\partial^2}{\partial r\partial\theta}A_r$$

$$E_\varphi = \frac{1}{r}\frac{\partial}{\partial\theta}F_r + \frac{1}{j\omega\epsilon}\frac{1}{r\sin\theta}\frac{\partial^2}{\partial r\partial\varphi}A_r \qquad \text{(B4)}$$

$$H_r = \frac{1}{j\omega\mu_o}\left[\frac{\partial^2}{\partial r^2} + k^2\right] F_r$$

$$H_\theta = -\frac{1}{r\sin\theta}\frac{\partial}{\partial\varphi}A_r + \frac{1}{j\omega\mu_o}\frac{\partial^2}{\partial r\partial\theta}F_r$$

$$H_\varphi = \frac{1}{r}\frac{\partial}{\partial\theta}A_r + \frac{1}{j\omega\mu}\frac{1}{r\sin\theta}\frac{\partial^2}{\partial r\partial\varphi}F_r$$

Noting that

$$E_r^i = \hat{r}\cdot\hat{\theta}_i\, E_o\, e^{-jk_o r\cos\gamma} = -\frac{E_o}{jk_o r}\frac{\partial}{\partial\theta_i}e^{-jk_o r\cos\gamma},$$

$$H_r^i = -\frac{1}{jk_o r}\frac{E_o}{\eta_o}\frac{1}{\sin\theta_i}\frac{\partial}{\partial\varphi_i}e^{-jk_o r\cos\gamma}$$

and $\hat{J}_n(kr) \doteq (kr)j_n(kr)$ satisfies the differential equation

$$\left[\frac{\partial^2}{\partial r^2} + k^2\right]\hat{J}_n(kr) = \frac{n(n+1)}{r}\hat{J}_n(kr)$$

it follows from (B4) that

$$A_r^i = \frac{E_o}{\omega\mu_o} \sum_{n=0}^{\infty} \hat{a}_n \hat{J}_n(k_o r) \left[- \frac{\partial}{\partial\theta_i} \chi_n(\theta,\varphi;\theta_i,\varphi_i) \right]$$

$$F_r^i = \frac{E_o}{k_o} \sum_{n=0}^{\infty} \hat{a}_n \hat{J}_n(k_o r) \left[- \frac{1}{\sin\theta_i} \frac{\partial}{\partial\varphi_i} \chi_n(\theta,\varphi;\theta_i,\varphi_i) \right] \qquad \text{(B5)}$$

where $\hat{a}_n \doteq \frac{(2n+1)}{n(n+1)} (-j)^n$.

External to the sphere, the scattered potentials must be of the form given by (B5), but possess the proper behavior at infinity; namely

$$A_r^{sc} = \frac{E_o}{\omega\mu_o} \sum_{n=0}^{\infty} \hat{b}_n \hat{H}_n^{(2)}(k_o r) \left[- \frac{\partial}{\partial\theta_i} \chi_n(\theta,\varphi;\theta_i,\varphi_i) \right]$$

$$F_r^{sc} = \frac{E_o}{k_o} \sum_{n=0}^{\infty} \hat{c}_n \hat{H}_n^{(2)}(k_o r) \left[- \frac{1}{\sin\theta_i} \frac{\partial}{\partial\varphi_i} \chi_n(\theta,\varphi;\theta_i,\varphi_i) \right] \qquad \text{(B6)}$$

where $\hat{H}_n^{(2)}(k_o r) \doteq (k_o r) h_n^{(2)}(k_o r)$, with $h_n^{(2)}$ denoting the spherical Hankel function of the second kind.

The potentials associated with the total fields external to the sphere are given by

$$A_r^t = A_r^i + A_r^{sc} \; ; \qquad F_r^t = F_r^i + F_r^{sc}$$

In the case of a penetrable sphere, the internal potentials are of the form given by expansions (B6) with $\hat{b}_n \hat{H}_n^{(2)}(k_o r)$ replaced by $\hat{d}_n \hat{J}_n(m_2 k_o r)$, and $\hat{c}_n \hat{H}_n^{(2)}(k_o r)$ replaced by $\hat{e}_n \hat{J}_n(m_2 k_o r)$. All internal and external fields are found by using (B4). In particular, the total

electric field external to the sphere is given by

$$E_r^t = -j \frac{E_o}{(k_o r)^2} \sum_{n=1}^{\infty} n(n+1) \left[\hat{a}_n \hat{J}_n(k_o r) + \hat{b}_n \hat{H}_n^{(2)}(k_o r) \right] \left[- \frac{\partial}{\partial \theta_i} \chi_n \right]$$

$$E_\theta^t = - \frac{E_o}{(k_o r)} \sum_{n=1}^{\infty} \left\{ \left[\hat{a}_n \hat{J}_n(k_o r) + \hat{c}_n \hat{H}_n^{(2)}(k_o r) \right] \left[- \frac{1}{\sin\theta \sin\theta_i} \frac{\partial^2}{\partial \varphi \partial \varphi_i} \chi_n \right] \right.$$
$$\left. + j \left[\hat{a}_n \hat{J}_n'(k_o r) + \hat{b}_n \hat{H}_n^{(2)\prime}(k_o r) \right] \left[- \frac{\partial^2}{\partial \theta \partial \theta_i} \chi_n \right] \right\}$$

$$E_\varphi^t = - \frac{E_o}{(k_o r)} \sum_{n=1}^{\infty} \left\{ \left[\hat{a}_n \hat{J}_n(k_o r) + \hat{c}_n \hat{H}_n^{(2)}(k_o r) \right] \left[- \frac{1}{\sin\theta_i} \frac{\partial^2}{\partial \theta \partial \varphi_i} \chi_n \right] \right.$$
$$\left. + j \left[\hat{a}_n \hat{J}_n'(k_o r) + \hat{b}_n \hat{H}_n^{(2)\prime}(k_o r) \right] \left[- \frac{1}{\sin\theta} \frac{\partial^2}{\partial \theta \partial \varphi_i} \chi_n \right] \right\}$$

The primes on $\hat{J}_n$ and $\hat{H}_n^{(2)}$ represent differentiation with respect to $k_o r$.

The unknown coefficients are found as follows. In the case of a penetrable sphere, continuity of the tangential components of $\bar{E}^t$ and $\bar{H}^t$ across the interface lead to four equations for determining $\hat{b}_n$, $\hat{c}_n$, $\hat{d}_n$, $\hat{e}_n$. It is convenient to take $\varphi_i = \theta_i = 0$ for this purpose. Only the external fields are of interest here. Introduce the coefficients b_n and c_n such that $\hat{b}_n = b_n \hat{a}_n$, $\hat{c}_n = c_n \hat{a}_n$. The coefficients b_n, and c_n are found to be (Van Bladel, 1964)

$$b_n = \frac{\hat{J}_n(k_o a)\hat{J}_n'(m_2 k_o a) - m_2 \hat{J}_n'(k_o a)\hat{J}_n(m_2 k_o a)}{m_2 \hat{H}_n^{(2)\prime}(k_o a)\hat{J}_n(m_2 k_o a) - \hat{H}_n^{(2)}(k_o a)\hat{J}_n'(m_2 k_o a)}$$

and

$$c_n = \frac{\hat{J}_n'(k_o a)\hat{J}_n(m_2 k_o a) - m_2 \hat{J}_n(k_o a)\hat{J}_n'(m_2 k_o a)}{m_2 \hat{H}_n^{(2)}(k_o a)\hat{J}_n'(m_2 k_o a) - \hat{H}_n^{(2)\cdot}(k_o a)\hat{J}_n(m_2 k_o a)}$$

It is noted that the minus sign discrepancy with the results in Van Bladel is due to a different definition for the Legendre polynomials which is used here.

In the far-scattering zone, $\hat{H}_n^{(2)}(k_o r) \rightarrow j^{(n+1)} e^{-jk_o r}$, and $\hat{H}_n^{(2)\cdot}(k_o r) \rightarrow -j(j)^{(n+1)} e^{-jk_o r}$. The far-scattered electric field is then

$$E_\theta^{sc} \rightarrow j \frac{E_o}{k_o r} e^{-jk_o r} \sum_{n=1}^{\infty} (j)^n \hat{a}_n \left[c_n \left[\frac{1}{\sin\theta \sin\theta_i} \frac{\partial^2}{\partial\varphi \partial\varphi_i} \chi_n \right] + b_n \left[\frac{\partial^2}{\partial\theta \partial\theta_i} \chi_n \right] \right]$$

$$E_\varphi^{sc} \rightarrow j \frac{E_o}{k_o r} e^{-jk_o r} \sum_{n=1}^{\infty} (j)^n \hat{a}_n \left[b_n \left[\frac{1}{\sin\theta} \frac{\partial^2}{\partial\varphi \partial\theta_i} \chi_n \right] + c_n \left[\frac{1}{\sin\theta_i} \frac{\partial^2}{\partial\theta \partial\varphi_i} \chi_n \right] \right]$$

Replacing $\hat{H}_n^{(2)}(\cdot)$ by $(\cdot)h_n^{(2)}(\cdot)$, $\hat{J}_n(\cdot)$ by $(\cdot)j_n(\cdot)$, and then setting $k_o = -j(s/c) = -j\tau$ yields (4.1).

In the case of a perfectly conducting sphere, the internal field is zero, and the tangential total electric field must vanish on the surface. Alternatively, letting $m \rightarrow \infty$ in the above solutions for b_n and c_n yields

$$b_n = -\frac{\hat{J}_n'(k_o a)}{\hat{H}_n^{(2)\cdot}(k_o a)}; \qquad c_n = -\frac{\hat{J}_n(k_o a)}{\hat{H}_n^{(2)}(k_o a)}$$

All previous expressions for the external electric field apply by using

these coefficients.

Special Cases for the Angular Dependence

Three special cases are of interest: (1) $\theta_i = 0$ with φ_i, θ, and φ arbitrary, (2) $\theta_i = \theta = 0$ with φ and φ_i arbitrary, and (3) $\theta_i=\theta$ with $\varphi=\varphi_i$. Cases (1) and (2) follow from (B3) and other standard identities for the associated Legendre polynomials. Case (3) is most easily confirmed numerically.

Case (1):

$$\frac{\partial^2}{\partial\theta\partial\theta_i}\chi_n = \sin\theta\, P_n^{1\prime}(\cos\theta)\cos(\varphi-\varphi_i)$$

$$\frac{1}{\sin\theta\sin\theta_i}\frac{\partial^2}{\partial\varphi\partial\varphi_i}\chi_n = -\frac{P_n^1(\cos\theta)}{\sin\theta}\cos(\varphi-\varphi_i)$$

$$\frac{1}{\sin\theta_i}\frac{\partial^2}{\partial\theta\partial\varphi_i}\chi_n = -\sin\theta\, P_n^{1\prime}(\cos\theta)\sin(\varphi-\varphi_i)$$

$$\frac{1}{\sin\theta}\frac{\partial^2}{\partial\varphi\partial\theta_i}\chi_n = \frac{P_n^1(\cos\theta)}{\sin\theta}\sin(\varphi-\varphi_i)$$

Case (2):

$$\frac{\partial^2}{\partial\theta\partial\theta_i}\chi_n = \frac{1}{2}n(n+1)\cos(\varphi-\varphi_i)$$

$$\frac{1}{\sin\theta\sin\theta_i}\frac{\partial^2}{\partial\varphi\partial\varphi_i}\chi_n = \frac{1}{2}n(n+1)\cos(\varphi-\varphi_i)$$

$$\frac{1}{\sin\theta_i}\frac{\partial^2}{\partial\theta\partial\varphi_i}\chi_n = -\frac{1}{2}n(n+1)\sin(\varphi-\varphi_i)$$

$$\frac{1}{\sin\theta}\frac{\partial^2}{\partial\varphi\partial\theta_i}\chi_n = -\frac{1}{2}n(n+1)\sin(\varphi-\varphi_i)$$

Case (3):

$$\frac{\partial^2}{\partial\theta\partial\theta_i} \chi_n = \frac{1}{2} n(n+1)$$

$$\frac{1}{\sin\theta\sin\theta_i} \frac{\partial^2}{\partial\varphi\partial\varphi_i} \chi_n = \frac{1}{2} n(n+1)$$

$$\frac{1}{\sin\theta_i} \frac{\partial^2}{\partial\theta\partial\varphi_i} \chi_n = 0$$

$$\frac{1}{\sin\theta} \frac{\partial^2}{\partial\varphi\partial\theta_i} \chi_n = 0$$

APPENDIX C

ASYMPTOTIC RELATIONS FOR SPHERICAL BESSEL FUNCTIONS

Large Argument Relations

The following asymptotic relationships for spherical Bessel functions follow from results in Abramowitz and Stegun (1964):

$$j_n(-j\alpha) \sim \begin{cases} -(j)^n \dfrac{e^{-\alpha}}{2\alpha} & \dfrac{\pi}{2} < \arg(\alpha) < \dfrac{3\pi}{2} \\ (-j)^n \dfrac{e^{\alpha}}{2\alpha} & -\dfrac{\pi}{2} < \arg(\alpha) < \dfrac{\pi}{2} \end{cases}$$

$$[(-j\alpha)\ j_n(-j\alpha)]' \sim \begin{cases} (j)^n \dfrac{e^{\alpha}}{2} & \dfrac{\pi}{2} < \arg(\alpha) < \dfrac{3\pi}{2} \\ (-j)^n \dfrac{e^{\alpha}}{2} & -\dfrac{\pi}{2} < \arg(\alpha) < \dfrac{\pi}{2} \end{cases}$$

$$h_n^{(2)}(-j\alpha) \sim \left\{ -(j)^n \frac{e^{-\alpha}}{\alpha} \qquad \frac{\pi}{2} \le \arg(\alpha) \le \frac{3\pi}{2},\ -\frac{\pi}{2} \le \arg(\alpha) \le \frac{\pi}{2} \right.$$

$$[(-j\alpha)\ h_n^{(2)}(-j\alpha)]' \sim \left\{ (j)^n\, e^{-\alpha} \quad \frac{\pi}{2} \le \arg(\alpha) \le \frac{3\pi}{2},\ -\frac{\pi}{2} \le \arg(\alpha) \le \frac{\pi}{2} \right.$$

Thus,

$$\Gamma_{bn}(-jm_2\beta) \sim \begin{cases} -(-)^n \dfrac{e^{-m_2\beta}\ e^{-\beta}}{4\beta}(1 - m_2) & \dfrac{\pi}{2} < \dfrac{\arg(m_2\beta)}{\arg(\beta)} < \dfrac{3\pi}{2} \\ (-)^n \dfrac{e^{m_2\beta}\ e^{\beta}}{4\beta}(1 - m_2) & -\dfrac{\pi}{2} < \dfrac{\arg(m_2\beta)}{\arg(\beta)} < \dfrac{\pi}{2} \end{cases}$$

$$\Gamma_{cn}(-jm_2\beta) \sim \begin{cases} -(-)^n \dfrac{e^{-m_2\beta}\, e^{-\beta}}{4m_2\beta}(1 - m_2) & \dfrac{\pi}{2} < \dfrac{\arg(m_2\beta)}{\arg(\beta)} < \dfrac{3\pi}{2} \\ (-)^n \dfrac{e^{m_2\beta}\, e^{\beta}}{4m_2\beta}(1 - m_2) & -\dfrac{\pi}{2} < \dfrac{\arg(m_2\beta)}{\arg(\beta)} < \dfrac{\pi}{2} \end{cases}$$

$$\Lambda_{bn}(-jm_2\beta) \sim \begin{cases} (-)^n \dfrac{e^{-m_2\beta}\, e^{-\beta}}{2\beta}(1 - m_2); & \dfrac{\pi}{2} < \dfrac{\arg(m_2\beta)}{\arg(\beta)} < \dfrac{3\pi}{2},\ -\dfrac{\pi}{2} \le \arg(\beta) \le \dfrac{\pi}{2} \\ \dfrac{e^{m_2\beta}\, e^{-\beta}}{2\beta}(1 + m_2); & -\dfrac{\pi}{2} < \dfrac{\arg(m_2\beta)}{\arg(\beta)} < \dfrac{\pi}{2},\ \dfrac{\pi}{2} \le \arg(\beta) \le \dfrac{3\pi}{2} \end{cases}$$

$$\Lambda_{cn}(-jm_2\beta) \sim \begin{cases} (-)^n \dfrac{e^{-m_2\beta}\, e^{-\beta}}{2m_2\beta}(1 - m_2); & \dfrac{\pi}{2} < \dfrac{\arg(m_2\beta)}{\arg(\beta)} < \dfrac{3\pi}{2},\ -\dfrac{\pi}{2} \le \arg(\beta) \le \dfrac{\pi}{2} \\ -\dfrac{e^{m_2\beta}\, e^{-\beta}}{2m_2\beta}(1 + m_2); & -\dfrac{\pi}{2} < \dfrac{\arg(m_2\beta)}{\arg(\beta)} < \dfrac{\pi}{2},\ \dfrac{\pi}{2} \le \arg(\beta) \le \dfrac{3\pi}{2} \end{cases}$$

Relations (4.3), (4.4), and (4.5) follow immediately.

Small Argument Expansions

The following relationships for the spherical Bessel functions follow from results in Abramowitz and Stegun (1964):

$$j_n(-j\alpha) \sim \frac{(-j\alpha)^n}{(2n+1)!!} \qquad |\alpha| \to 0,\ n \ge 0$$

$$h_n^{(2)}(-j\alpha) \sim j\,\frac{(2n-1)!!}{(-j\alpha)^{n+1}} \qquad |\alpha| \to 0,\ n \ge 1$$

$$[(-j\alpha)\ j_n(-j\alpha)]' \sim (n+1)\ \frac{(-j\alpha)^n}{(2n+1)!!} \qquad |\alpha| \to 0,\ n \geq 0$$

$$[(-j\alpha)\ h_n^{(2)}(-j\alpha)]' \sim -j\ n\ \frac{(2n-1)!!}{(-j\alpha)^{n+1}} \qquad |\alpha| \to 0,\ n \geq 1$$

Using these results, it is found that

$$\frac{e^{-\beta}}{(-j\beta)\ A_{bn}(-jm_2\beta)} \to\ j\ \frac{(2n+1)}{m_r^n\ [n(m_r^2 + 1) + 1]} \qquad |\beta| \to 0,\ n \geq 1$$

$$\frac{e^{-\beta}}{(-j\beta)\ A_{cn}(-jm_2\beta)} \to\ -j\ \frac{1}{m_r^n} \qquad |\beta| \to 0,\ n \geq 1$$

Here, m_r represents the real part of the refractive index; this follows because the imaginary portion of the refractive index tends to zero as $|\beta| \to 0$.

The vita has been removed from the scanned document